PROVENANCE, DEPOSITIONAL ENVIRONMENT AND DIAGENETIC HISTORY OF BARAIL SEDIMENTS IN PARTS OF BELT OF SCHUPPEN, NAGALAND

THESIS SUBMITTED IN PARTIAL FULFILLMENT OF THE REQUIREMENTS FOR THE DEGREE OF DOCTOR OF PHILOSOPHY

BY

HIEVINU OLIVIA RICHA

Ph.D/GEL/00089 of 2017

DEPARTMENT OF GEOLOGY, SCHOOL OF SCIENCES

NAGALAND UNIVERSITY, KOHIMA CAMPUS

MERIEMA - 797004

NAGALAND, INDIA

JUNE 2025

NAGALAND UNIVERSITY

JUNE 2025

DECLARATION

I, Hievinu Olivia Richa, hereby declare that the subject matter of this thesis is the record of work done by me, during the period August 2017 to June 2025. That the contents of this thesis did not form basis of the award of any previous degree to me or to the best of my knowledge to anybody else, and that the thesis has not been submitted by me for any research degree in any other University/Institute.

This thesis is being submitted to the Nagaland University for the degree of Doctor in Philosophy in Geology.

Date:

Place: Scholar

Head

Prof. Vikoleno Rino

Department of Geology

Nagaland University

Kohima Campus, Meriema

Supervisor

Prof. S.K. Srivastava

Department of Geology

Nagaland University

Kohima Campus, Meriema

NAGALAND UNIVERSITY

Prof. S.K. Srivastava
Department of Geology
Email: *sanjaikohima@yahoo.co.in*
sksrivastava@nagalanduniversity.ac.in

CERTIFICATE

The thesis presented by Miss Hievinu Olivia Richa, M.Sc., bearing Registration No Ph.D/GEL/00089 of 29th August 2017 embodies the results of investigations carried by her under my supervision and guidance.

I certify that this work has not been presented for any degree elsewhere and that the candidate has fulfilled all conditions laid down by the University.

Date:

(S.K. SRIVASTAVA)

Supervisor

नागालैण्ड विश्वविद्यालय
NAGALAND UNIVERSITY

(संसद द्वारा पाररत अविवनयम 1989, क्रमांक 35 के अंतगगत स्थावपत कें द्रीय विश्वविद्यालय)

(A Central University established by the Act of Parliament No.35 of 1989) मुख्यालय: तुमामी, जुन्हेबोटो (नागालैण्ड), वपन कोड- 798627

Headquarters: Lumami, Dist: Zunheboto, (Nagaland), Pin Code-798 627

PLAGIARISM-FREE UNDERTAKING

Name of Scholar	Hievinu Olivia Richa
Registration Number	Ph.D/GEL/00089 of 29th August 2017
Title of PhD Thesis	Provenance, Depositional Environment and Diagenetic History of Barail Sediments in parts of Belt of Schuppen, Nagaland
Name &Institutional Address of the Supervisor/Co-Supervisor	Prof. S. K. Srivastava, Department of Geology, Nagaland University, Kohima Campus, Meriema
Name of the Department and School	Department of Geology/ School of Sciences
Date of submission	
Date of plagiarism check	02/06/2025
Name of the software used	DrillBit

I hereby declare/certify that the Ph.D. Thesis submitted by me is complete in all respect, as per the guidelines of the UGC/NU for this purpose. I also certify that the Thesis (soft copy and print version) has been checked for plagiarism using DrillBit similarity check software. Copy of the Report generated by the software is also enclosed.

Place :
Date :

(Name & Signature of the Scholar)

Name & Signature of the Supervisor with seal

DrillBit

The Report is Generated by DrillBit Plagiarism Detection Software

Submission Information

Author Name	Olivia
Title	Provenance, Depositional Environment and Diagenetic history of the Barail Sediments in parts of Belt of Schuppen, Nagaland
Paper/Submission ID	3716275
Submitted by	sksrivastava@nagalanduniversity.ac.in
Submission Date	2025-06-02 14:59:07
Total Pages, Total Words	51, 20068
Document type	Thesis

Result Information

Similarity **9 %**

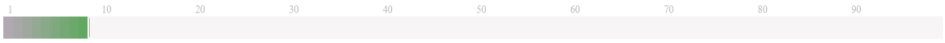

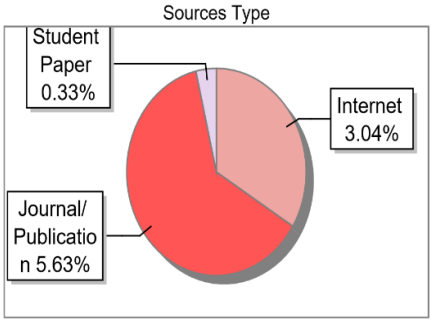

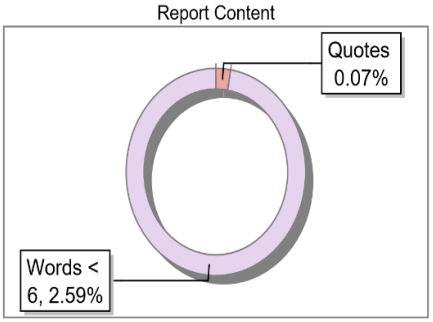

Exclude Information

Quotes	Excluded
References/Bibliography	Excluded
Source: Excluded < 6 Words	Excluded
Excluded Source	**23 %**
Excluded Phrases	Not Excluded

Database Selection

Language	English
Student Papers	Yes
Journals & publishers	Yes
Internet or Web	Yes
Institution Repository	Yes

A Unique QR Code use to View/Download/Share Pdf File

ACKNOWLEDGEMENT

At the very outset, all glory and praise to the Almighty Father for His bountiful blessings during the entire course of my research work. It has been quite a long journey and He has been ever merciful in all the works I have undertaken.

My profound gratitude goes to my Supervisor Prof. Sanjai. K. Srivastava, who has gone way beyond his capacity to see this research to completion. Not only rendering his deep knowledge in the matter, but also being a guide, teacher, friend but most of all, being a parent like figure, continuously encouraging and pushing me to do my best. Sir, words are truly inadequate to express my appreciation. I would also like to say thank you to Madam Srivastava for constantly upholding me in her thoughts and for being so supportive thus far.

I would like to express my sincere gratitude to the Head, Department of Geology and all the respected faculty and staff for providing the necessary provisions in carrying out the research work.

I also take this time to thank my fellow research scholars, Dr. Keneisazo Nagi and Dr. Vilavonuo Keditsu for their selfless involvement during fieldwork and assistance till the completion of this thesis. My sincere thanks to Dr. Akhrulu Vero, Miss Diezeneino Meyase, Dr. Mademshila Jamir, and Dr. Mehilo Apon for their unending support and guidance throughout the journey.

Special thanks to senior researchers Dr. Alono Thorie and Dr. A. Moalong Kichu for being so patient with me and guiding me through all the trifling matters of research. Your scientific input and involvement in this research is truly appreciated.

I would like to acknowledge Sophisticated Analytical Instrument Facility (SAIF), Dept of Instrumentation and USIC, Gauhati University, Guwahati, Assam and

Central Research Facility (CRF), Indian Institute of Technology (IIT), Kolkata for permitting the geochemical analyses.

I have been blessed to have had accompaniments in my father and brothers, who had forgone their schedules to aid me in carrying out all necessary fieldwork and trips required during the course of research. I take this time to thank my family for their unceasing prayers and encouragement for this research to come to a finish.

To my in-laws, who have been most enthusiastic in my research endeavor, I thank you for your unending prayers and the love and care you have showered upon me all this while.

Last, but not in the very least, my dear husband, Mr. Khruvo Vadeo, who has been a constant source of encouragement and a light to my world. Through all the testing times, he has been the one who kept me standing strong and moving on to see this work to accomplishment. I dedicate this research work to you.

To all the individuals, organizations, and facilities involved in the making of this research thesis, though I am unable to name each one, I would like to acknowledge your support and service in the completion of the same. Thank you.

(Hievinu Olivia Richa)

PARTICULARS OF THE CANDIDATE

NAME OF THE CANDIDATE	: Hievinu Olivia Richa
DEGREE	: Ph.D.
DEPARTMENT	: Geology
TITLE OF THE THESIS	: Provenance, Depositional Environment and Diagenetic History of Barail Sediments in parts of Belt of Schuppen, Nagaland
DATE OF ADMISSION	: 29th August 2017
APPROVAL OF RESEARCH PROPOSAL	: 16th August 2018
REGISTRATION NUMBER AND DATE	: Ph.D/GEL/00089 of 29/08/2017

Head of the Department

BIODATA OF THE CANDIDATE

I. PAPERS PUBLISHED

1. Richa, H. and Srivastava, S.K. (2024). Petrography and tectono-provenance of the Barail Group of rocks, Belt of Schuppen, India. *Journal of Sedimentary Environments*, 9, 1-17. 10.1007/s43217-024-00190-w

2. Srivastava, S.K., Humtsoe, Z., Laskar, J., and Richa, H (2024). Provenance of the Oligocene Barail Sandstones exposed in and around Longsa Village, Wokha District, Nagaland: Reflections from Petrography and Heavy Minerals. *Journal of Geosciences Research*, 9, 23-29. 10.56153/g19088-023-0156-43

3. Luirei, K., Lokho, K., Zimik, H., Rino, V., Chahong, N., Tiwari, S., Angkang, M., Khangrah, N., Richa, H., Neikha, K and Thong, G (2023). Stable hydrogen and oxygen isotope investigation of the saline and hyperalkaline springs in parts of the Inner Fold Belt and Ophiolite Complex of Manipur and Nagaland, India, *Himalayan Geology*, 44, 6

II. ABSTRACT PUBLISHED/ORAL PRESENTATION

1. Presentation entitled "Diagenetic Environment of Oligocene Laisong sandstones exposed along Kohima-Dimapur road, Nagaland, India" at the National Conference on Current Understanding from the Indian Sedimentary Basins and road ahead cum 38th Convention of Indian Association of Sedimentologists (IAS) at Delhi University, New Delhi from 9th to 11th December 2022

2. Presentation entitled "Provenance of the Jenam sandstones exposed along Kohima-Dimapur road, Belt of Schuppen, Nagaland" at the Virtual National Seminar on Sedimentation, Tectonics and Metallogeny of North-East India jointly organized by North-Eastern Hill University, Shillong (NEHU) and Geological Society of India (GSI), Bengaluru during 21st to 23rd September 2020

III. AWARDS/ RECOGNITION

1. Project Junior Research Fellow (JRF) at the Industry Academia Collaborative Project titled "Depositional environment and its implication on the Cenozoic sediment of the Schuppen Belt of Nagaland: A Sedimentologic and Remote Sensing Approach" between CoEES, Oil India Limited (OIL) Guwahati and Department of Geology, Nagaland University, Kohima Campus, Meriema during May 2018 to May 2020

2. Special Recognition Award for Outstanding Performance in the Debate Competition on topic "Application of Geosciences for sustainable growth is utopian dream for country like India" organized by Association of Petroleum Geologists (APG), Duliajan Chapter held on 21st July, 2018 at Duliajan, Assam, India

IV. UGC-NET - (126/0119 Rank) 2013

V. WORKSHOPS AND SEMINARS/WEBINARS ATTENDED

1. 3rd International Virtual Workshop on Global Seismology & Tectonics (IVWGST) organized by Geoscience & Technology Division, North East Institute of Science & Technology (CSIR), Jorhat, Assam, India from 20th to 30th September 2022

2. One Week Training Program on "Frontiers of Earth Science" under DST-STUTI Program of Department of Applied Geology, Indian Institute of Technology (ISM) Dhanbad funded by Department of Science and Technology (DST), Govt of India organized by the Department of Geological Sciences, Jadavpur University, Kolkata from 12th to 18th July 2022

3. Online Tier III Training course on "Local Groundwater related issues and Participatory Groundwater Management" held at the Department of Geology, Nagaland University, Kohima Campus, Meriema, Nagaland organized by the Central Ground Water Board, NER, Guwahati and Department of Water Resources, River Development & Ganga Rejuvenation, Ministry of Jal Shakti on 28th February 2022

4. Online International Conference On “Recent Developments in Earth Environmental Sciences, Natural Resource Management and Climate Change with Special Focus on Eastern Himalayas” organized by Department of Geology, Sikkim University, Gangtok from 8th to 9th October 2020

5. E-Training on “Fundamentals of Sedimentary Petrology” exclusively for SC and ST category conducted by Petrology Division of Geological Survey of India (GSI) Training Institute, Hyderabad from 2nd to 4th September 2020

6. E-Training on “Fundamentals of Mapping in Tertiary Terrain” exclusively for SC and ST conducted by RTD, NER, GSITI, Shillong from 24th to 26th August 2020

7. National workshop on “Sequence Stratigraphy and Basin Analysis” organized by Nagaland University and Oil India Limited (OIL) at Department of Geology, Nagaland University, Kohima Campus, Meriema from 26th to 30th November 2018

PREFACE

With the objective of reconstructing the depositional environment, understanding the diagenetic history and tectonic provenance of the Oligocene Barail Group of rocks in the Belt of Schuppen within Chumukedima district of Nagaland, facies analysis technique, petrographic, heavy minerals and geochemical attributes of the sediments have been studied in detail to pursue the said objectives. The results and inferences of the study have been presented in 8 chapters.

The **first chapter** gives a general preview of Nagaland followed by the study area, previous work done, objectives and scope of the present study and the hypothesis. The **second chapter** discusses the geologic setting, stratigraphy and tectonic framework of the region. This chapter includes the detail geology of the study area. The **third chapter** describes the detail methodology involved i.e. field and laboratory techniques applied in the study. The **fourth chapter** covers the parameters for lithofacies analysis and the various aspects of vertical profile sections, and the interrelationship between field observations and facies parameters which is used to deduce a facies scheme for the sediments in the study area. Herein, different sedimentary structures, trace fossils observed in the area are also described. The **fifth chapter** is grain size analysis, which brings about an understanding of the varied sedimentary environments. Various grain size parameters have been applied to understand the environment of deposition as well as textural maturity of the sediments. The **sixth chapter** is dedicated to petrography, heavy mineral studies, diagenetic features, major oxide geochemistry, and clay mineralogy. The analytical results from various geochemical analysis aid in provenance studies. Depositional environment and tectonic provenance is described in detail in **Chapter 7**. Here, reconstruction of palaeoenvironment, depositional history and evidences from trace fossils are discussed. This chapter also discusses the tectonic provenance of the area with evidences inferred from the preceding chapters. **Chapter 8** summarizes the thesis followed by conclusions.

Each of the chapters are arranged with all texts appearing first and the relevant tables, plates and figures following in that order. It is with great hope that this thesis will be a good source of information and provide new and complementary data for future research works.

List of Figures

List of Plates

List of Tables

CONTENTS

CHAPTER 1
INTRODUCTION

1.1 GENERAL

North eastern Indian state of Nagaland lies within latitudes and longitudes of 25°11'46.5" / 93°19'26.8" and 27°2'10" / 95°14'39.8" respectively. It shares its borders with the state of Assam, Arunachal Pradesh and Manipur international border with Myanmar to the east. Hills of Nagaland is represented by an immature, young mountainous terrain and is a part of mobile belt. The geological evolution of the Naga Hills is the result of interaction between the Indian plate and the Myanmar plate in the east. The Assam-Arakan orogenic belt of Mesozoic and Cenozoic periods is an ideal setting for understanding the geodynamic processes responsible for their evolution. Kumar and Naik suggested that this is a classic example of transformation of a passive margin into an active margin setup owing to changing plate interactions and evolution of north-east south-west trending foreland basin in response to the regional tectonics of through time. Nagaland represents a structurally and tectonically complicated region and morphotectonically it is divided into three NE-SW trending linear units viz., Belt of Schuppen, Inner Fold Belt and Naga Hills Ophiolite from west to east (Goswami, 1960; Mathur and Evans, 1964; DGM, 1978).

The Barail Group of rocks consisting of the oldest Laisong, middle Jenam and youngest Renji Formations and are confined within the Piphema and Sanis-Chongliyimsen Thrusts respectively. The Barail sedimentary wedge is deposited within the subduction-accretion complex in the active margin of Indo-Myanmar plate convergence (Nandy, 1976; Dasgupta *et al*., 1991; Nandy and Dasgupta, 1989). Naogaon, Baragoloi and Tikak Parbat Formations of Upper Assam has been homotaxially correlated with Laisong, Jenam and Renji Formations of the Belt of Schuppen of Nagaland (GSI, 2011).

1.2 GEOMORPHIC FEATURES

Mount Saramati (3,841.00 meters) is the state's highest peak; this is where the Naga Hills merge with the Patkai Range in which it forms the boundary with Myanmar. Rivers such as Doyang and Diphu to the north, the Barak River in the southwest, dissect the entire state. Twenty per cent (20%) of the total land area of the state is covered with forest, a haven for flora and fauna. Blythe Tragopan, a vulnerable species of Galliform, is the state bird while a semi-domesticated gaur Mithun is the state animal of Nagaland. The forests of Nagaland are home to more than 300 orchid species.

Nagaland has a largely monsoon climate with high humidity levels. Annual rainfall averages around 1,800-2,500 millimetres, spread between May to September. Temperature ranges from between 21° C to 40°C and drops to 4° C in winter. The climate is sub-tropical

with very high humidity ranging from 74 to 87%. In the Chumukedima district, the Dzumha River flows NW-SE and runs almost parallel to the national highway. The Jharnapani River, Chathe River flow in Medziphema with a number of tributaries which later converge into the Dhansiri River and flow into Assam.

1.3 STUDY AREA

The study area forms a part of the Survey of India Toposheet No. 83 G/13 and G/14 and is bounded between N 25°44′50" and N 25°47′00" latitudes and E 93°53′00" and E 93°58′00" longitudes. It falls in the southern extension of the Belt of Schuppen. The study area is part of Chumukedima district and lies between Piphema village and Medziphema town. The location map of the study area is shown in Figure 1.1.

1.4 REVIEW OF PREVIOUS LITERATURES

The work of Oldham (1883) describing the geology of Kohima and Manipur may be regarded as an early outlook into the complex geology of Nagaland. Mallet (1876) was one of the first to actually describe the regional geology of the Naga Hills and surrounding regions. Hayden (1910) studied the coal deposits in Nagaland and Borjan area. Pascoe's (1912) extensive expeditions in Naga Hills and Surma Valley of Assam region threw light on the broad geology of the area and adjoining regions.

Systematic descriptions of the geology of the region have been provided by Geological Survey of India (1981), Oil and Natural Gas Corporation (Ganju *et al*., 1986) and the Directorate of Geology and Mining, Government of Nagaland (1978). Based on lithological variations, Evans (1932) and Mathur and Evans (1964) have given the Cenozoic stratigraphic succession providing further insight to the complex region. Other prominent workers such as Brunnschweiler (1966), Desikachar (1974), Rangarao (1983), Ganju and Khar (1985), Chakravarti and Banerjee (1988), Acharyya (2007), Nandy (2017), have contributed immeasurably to the framework of the region. Bastia *et al*., (1993) discussed the tectonic evolution and structural complexity of the Belt of Schuppen.

Recent contribution on the Belt of Schuppen have been made by Aier *et al*., (2011), Vadlamani *et al*., (2015), Singh *et al*., (2016), Bezbaruah *et al*., (2016), Nandy (2017), Srivastava and Kesen (2018), Borgohain *et al*., (2021), Srivastava and Kikon (2021). Srivastava *et al*., (2018) and Srivastava and Kesen (2018) have worked on the Palaeogene sediments, south of Kohima town and Laisong sandstones in and around Pherima, Dimapur using lithofacies and petrographic properties for depositional environment and provenance interpretations respectively. Moiya *et al*., (2019) deciphered the tectonic history of part of the Belt of Schuppen through Chronological studies (optically stimulated luminescence).

Borgohain *et al*., (2021) have performed comprehensive petrographic and diagenetic studies of the Barail sandstones of Naga Schuppen Belt and their implication on reservoir quality of the region.

1.5 OBJECTIVES AND SCOPE OF THE PRESENT STUDY

The proposed study is an attempt to understand the provenance of the Barail sediments of the study area using petrographic characteristics and petrological markers which can be correlated to the geodynamics and subsequent sedimentation history of the region. In the present work attempts have also been made to develop a lithofacies scheme for palaeo-environmental reconstruction of the Oligocene sediments of the study area. The outcome of the present investigation would add some new information which would enhance our understanding of the tectonics and the depositional history of the region. While doing the literature review it was observed that a significant amount of published data is available on the Barail sediments from the northern part of the Belt of Schuppen. However not much published data is available with respect to the depositional environment and provenance studies of the Barail Group of rocks from the southern part of Belt of Schuppen.

Keeping that in mind, in the present work, attempts have been made to generate data on the depositional environment and also the probable source which would enhance our understanding of the Barail sedimentation in this part of the Belt of Schuppen.

The study has been carried out with the following objectives:

1. To reconstruct the depositional environment applying facies analysis technique.
2. To search for the provenance of Oligocene sediments using petrographic, heavy minerals and geochemical attributes.

1.6 HYPOTHESIS

The available literatures on the geology of the region suggest that the thick sedimentary deposits are the result of un-interrupted sedimentation within a northeast-southwest trending linear trough resulted from the subduction of the Indian plate below the Myanmar plate. Sedimentation, during the period, kept pace with subsidence; however, there were periods of slight emergence also facilitating the formation of coal. The highly folded and faulted Naga Hills are the result of the continuous subduction of the Indian plate eastward below Myanmar plate. The study area, a part of the Belt of Schuppen, is comprised of Barail Group of rocks exposed between Piphema Thrust and the Sanis-Chongliyimsen Thrust. So far no comprehensive work has been carried out on these sediments.

1.7 BRIEF METHODOLOGY

Detailed field work and laboratory analysis has been carried out to fulfill the aforementioned objectives. Fieldwork involves the detail study of lithological and facies variations, measurement of bed attributes, recording of sedimentary structures, sampling and GPS (Global Positioning System) coordinates.

FIELD INVESTIGATIONS

a. Collection of both random and oriented samples from suitable rock exposures in time and space.
b. Construction of Vertical Profile Sections.
c. Recording of Sedimentary structures including biogenic.
d. Identification of lithofacies.

LABORATORY ANALYSIS

Laboratory analysis of the collected samples include rock thin section, diagenetic study, grain size analysis, heavy mineral separation, X-ray Diffraction (XRD), Scanning Electron Microscope (SEM) Energy Dispersive X-ray (EDX/EDS) Analysis and X-ray Fluorescence Spectroscopy (XRFS) analysis.

a. Grain size analysis
b. Petrographic and Modal analysis
c. Clay mineral analysis using XRD
d. Scanning Electron Microscopic studies
e. Geochemical (Major Oxides) analysis

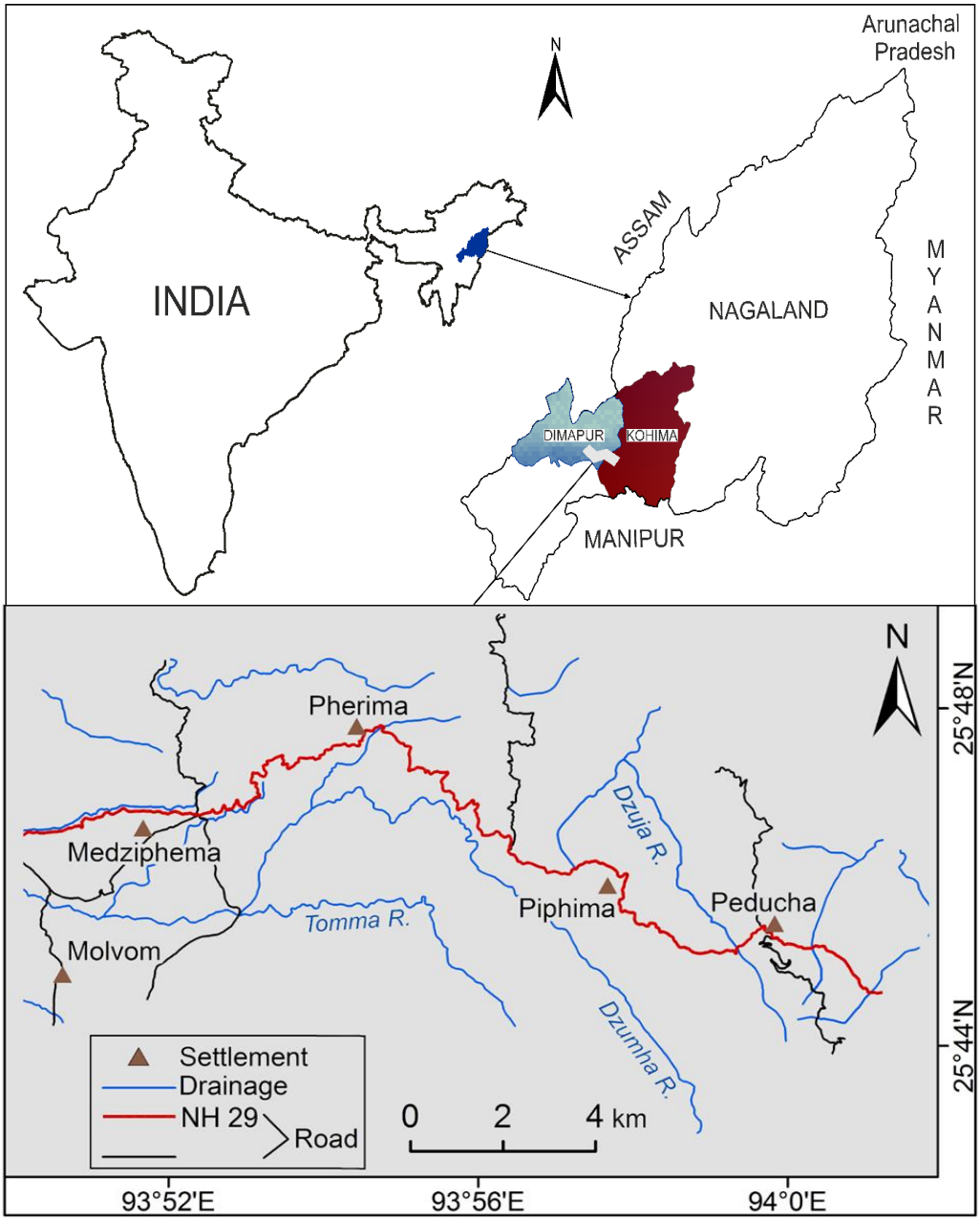

Figure 1.1: Location Map of the Study Area

CHAPTER 2

GEOLOGICAL SETTING AND TECTONIC FRAMEWORK

2.1 REGIONAL GEOLOGIC SETTING

Tectonically, Nagaland which is a part of the Arakan-Yoma Range, forms one of the most significant parts of the Indo-Myanmar-Andaman mobile belt trending in NE-SW direction. It extends northward into the eastern syntaxial bend of the Himalayas and southward through the Andaman and Nicobar Islands. The Naga Hills are bounded on the western side by the Precambrian Karbi Anglong Massif (earlier known as Mikir Massif) and Tertiary shelf sediments of Assam; and in the eastern side by the Central Lowlands of Myanmar. The collision between the Indian plate and the Eurasian plate around 70 Ma (Valdiya, 1998; Yin and Harrison, 2000) formed the present topographic complexity represented by the Himalayas. Orogenic upheavals from the Mesozoic up to Cenozoic periods produced complex geodynamic and varying litho-tectonic units in the region. The region is tectonically active and is considered a very high risk seismic zone.

2.2 MAJOR STRUCTURAL FEATURES

The collision of the Indian plate and the Myanmar plate, with the subduction of the former under the latter, had resulted in the formation of three distinct morphotectonic units in the Naga Hills *viz.*, Belt of Schuppen (BoS), Inner Fold Belt (IFB) and Naga Hills Ophiolite (NHO) (Goswami, 1960; Mathur and Evans, 1964; DGM, 1978) as shown in Figure 2.1.

2.2.1 BELT OF SCHUPPEN

The term ‘Schuppen Belt’ was first described by Suess in 1904 as imbricate thrust systems. The Belt of Schuppen of Nagaland is a narrow linear belt of NNE-SSW trending imbricate thrust slices running along the western flank of Nagaland (Mathur and Evans, 1964). The BoS is marked by the Halflong-Disang thrust in the southeast and Naga Thrust in the northeast (Ranga Rao, 1983). Evans (1932) gave the dimension of this linear unit as ~200 km strike length and width range from 20-25 km. Sediments ranging in age from Oligocene to Quaternary are encountered in this belt with complete absence of Eocene Disang sediments. Six (6) major thrusts *viz.*, Disang, Khari, Kongan, Lakhuni, Sanis-Chongliyimsen and Naga Thrusts (Figure 2.2) have been mapped by the Geological Survey of India (GSI, 1983), Oil and Natural Gas Corporation Limited (ONGC, 1987), and other early workers (Corps, 1949; Ganju and Khar, 1985; Ranga Rao and Samanta, 1987; Kunte, 1988; and Kent *et al*., 2002).

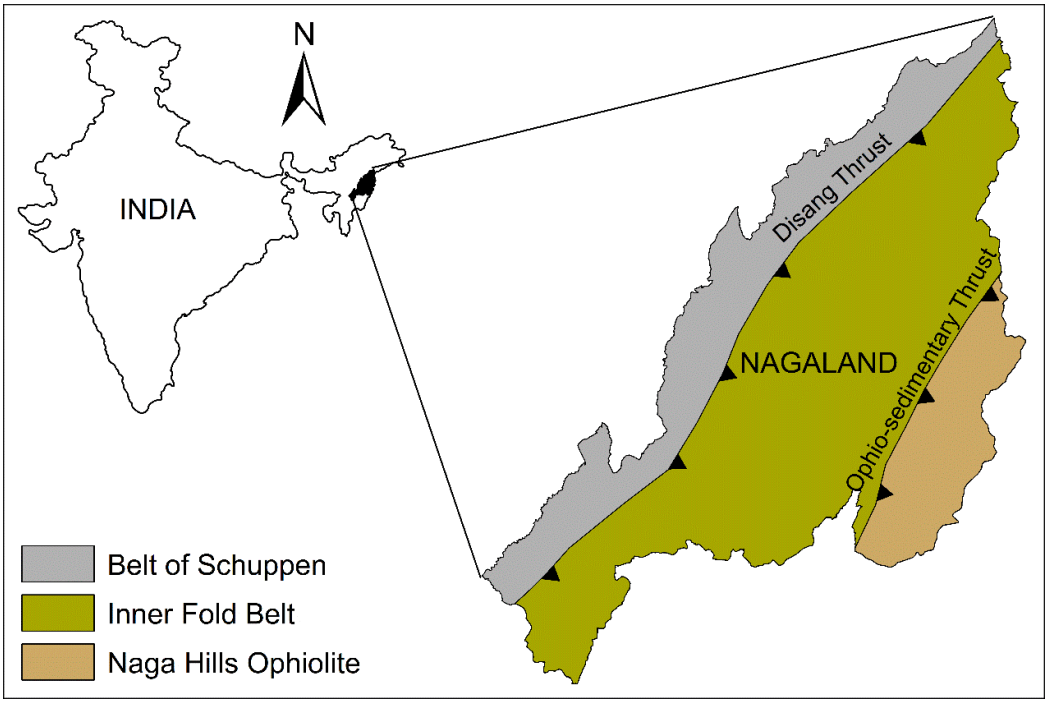

Figure 2.1: Morphotectonic units of Nagaland (after Goswami, 1960; Mathur and Evans, 1964; DGM, 1978)

2.2.2 INNER FOLD BELT

The Inner Fold Belt occupies the central part of the Naga Hills. It is represented by a series of anticlines and synclines which are confined within two major tectonic features *viz.* Halflong-Disang Thrust in the west and the Ophio-Disang/Ophio-Sedimentary Thrust in the east. This belt is occupied by the Patkai Synclinorium in the north and Kohima Synclinorium in the south. Thick folded and thrusted piles of splintery shaly sequences of Upper Cretaceous-Middle Eocene rocks of the Disang Group dominate this unit (GSI, 2011). Within the Inner Fold Belt, the dominantly argillaceous Disang sediments grades into an arenaceous Barail unit through a mixed Disang-Barail Transition (Srivastava, 2002). The Barails forms the core of the synclines which are further overlain by the undifferentiated Surma Group (Singh and Adiga, 1977; Verma and Yadekar, 1983; Devdas and Gandhi, 1985; Sarma, 1985). The Miocene Surma sediments uncomfortably over lie the Barail sediments.

2.2.3 NAGA HILLS OPHIOLITE

The NNE-SSW trending Naga Hills Opholite/Naga Ophiolite Belt is an obducted block of the continental crust formed due to the collision of the Indian plate and Myanmar microplate. It runs nearly 90 Km along the Myanmar border, occurring as steeply dipping,

dismembered tectonic slices which are juxtaposed against the Disang Group of sediments of the Eocene (GSI, 2011). This belt constitutes a complex composition of Mesozoic and Cenozoic magmatic, metamorphic and sedimentary rocks, represented by tectonic slices of serpentines, volcanics and cumulates. Chert and limestone are the associated pelagic sediments (Dilek, 2015) where the bedded chert contain siliceous microfossil *radiolaria* and are often associated with the volcanics. These Ophiolite suites of rocks are unconformably overlain by an Ophiolite derived volcanoclastic with an open marine to pelagic sedimentary cover which has been designated as the Phokphur Formation by the Geological Survey of India (GSI, 1975).

2.3 STRATIGRAPHY OF NAGALAND

A generalised stratigraphy of Nagaland (Table 2.1) is presented after the works of Mathur and Evans (1964); DGM (1978) Ghose *et al*., (2010); GSI (2011); Imchen *et al*., (2014); GSI (2017) which are briefly described below.

2.3.1 NAGA METAMORPHICS

The Naga Metamorphics were christened by Brunnschweiler (1966) mainly for the meso-grade metamorphic rocks which occurs towards the Myanmar side of the Indo-Myanmar Ranges. It mostly consists of unfossiliferous Proterozoic crystalline rocks represented by quartzite, marble/limestone, mica schist, gneisses, sheared granite, etc. (Brunnschweiler, 1966). The base of this formation is not exposed but it is tectonically juxtaposed against or even overlay the Ophiolites as well as the Phokphur Formation.

2.3.2 NIMI FORMATION

Nimi Formation lies on the eastern fringe of Nagaland and is considered a detached part of the Pre-Tertiary Myanmar continental crust (Agarwal and Ghose, 1986). It stretches over 216 km, and is assumed to be of Pre-Mesozoic age. This formation consists of crystalline quartzite, phyllite, carbonaceous phyllite, quartzite-sericite schist and granites (Agarwal and Ghose, 1986).

2.3.3 ZEPUHU FORMATION

Zepuhu Formation occupies the eastern fringe of Nagaland trending in NE-SW direction with a length of about 90km and 5-10 km in width. It consists of crystalline limestone, schist and schistose granite, and is considered to be of Pre-Mesozoic age (Agrawal and Kacker, 1979).

2.3.4 JOPI/PHOKPHUR FORMATION

The Phokphur Formation of Oligocene age consists of volcanoclastics, marine to paralic sediments, shales, tuffaceous greywacke, carbonaceous shale, polymictic conglomerates with lithic-feldspathic arenite and occasional coal streaks (GSI, 2011). Gastropod and plant fossils suggest a shallow marine to fluvial environment with hot and tropical type climate (GSI, 2011).

2.3.5 DISANG GROUP

The Disang Group was first described by Mallet in 1876 as dark grey shales with minor intercalations of sandstone. The Disang Group of rocks are the oldest exposed sedimentary rock of central Naga Hills comprising the Lower and Upper Disang Formations. The Lower Disang Formation consist of monotonous and dominantly thick successions of splintery grey shales and dark to black carbonaceous shales, shales-siltstone with thinly bedded fine grained sandstones. The Upper Disang Formation is characterized by fine grained flaggy sandstones that alternate with shales and subordinate siltstone. The thickness and occurrence of siltstone-sandstone increases towards the upper part of the sequence. The Lower Disang Formation yielded Cretaceous foraminifera, and Late Eocene Nummulites from the Upper Disang Formation (Mishra, 1983). The Disang Group of rocks conformably grades upward onto the Barail Group through the Disang-Barail Transitional Sequences (DBTS) (Pandey and Srivastava, 1998; Srivastava *et al*., 2004; Srivastava and Pandey, 2005).

2.3.6 DISANG-BARAIL TRANSITIONAL SEQUENCES (DBTS)

The Disang-Barail Transitional Sequences (DBTS) comprises of heterogeneous succession of alternating sand-mud lithology. They display gradational base and erosional top where the sand-silt unit in the succession exhibits numerous alternations of thin, flaggy, fine grained sandstone and silty/sandy shale. The contact between sand and shale is usually found to be erosional. The sedimentary structures present in the fine sand-silt units are micro-hummocky cross stratification, cross and parallel laminations, wave ripples and gently dipping fine laminations (Pandey and Srivastava, 1998; Srivastava *et al*., 2004; Srivastava and Pandey, 2005).

2.3.7 BARAIL GROUP

It was Mallet in 1876, who first studied the rock succession of this group. But later, it was Evans (1932) who coined the term Barail and accorded the status of ‘series’ to the similar rock associates exposed in the Barail range. Barail Group is represented by the oldest Laisong Formation, the middle Jenam Formation and the youngest Renji Formation in the Belt of Schuppen. However, in the Inner Fold Belt they are undifferentiated. In the north-

eastern segment, they are known by the nomenclature viz. Naogaon Formation, Baragoloi Formation and Tikak Parbat Formation respectively. A seismic survey (GSI, 1975) conducted in Dhansiri valley suggests that the Barail Group of rocks (Upper Eocene to Oligocene) continues with a reduced thickness in the sub thrust block of the Naga Hills. In the north-eastern part of Nagaland, mineable reserves of coal are present in these rocks. A coal bearing environment is believed to have formed in the north-eastern part during the deposition of these sediments, while there was restraining towards the south west due to deepening of basin which resulted in paucity of coal in the region (GSI, 2011). The sedimentary structures present in the Barail lithology include ripples marks, plane laminations, flute casts, load casts, and channel and small to medium scale planer cross beddings.

The three formations of the Barail Group are briefly discussed below:

1) Laisong Formation: In the Schuppen Belt, the Laisong Formation is the oldest litho unit recorded. It consists of hard compact and well bedded sandstones. The sandstone show different shades of colour from white to grey and becomes reddish brown and pink on weathering. The thickness of the formation measured along Dimapur-Kohima road section is about 1730 m (Rangarao, 1983). Along Mokokchung Mariani road section, a 200 m sequence of current bedded sandstones on the upthrust block of the Chongliyimsen Thrust has been recorded. This is referred to as Laisong Formation on the basis of lithological characters. The Laisong Formation have yielded *Nummulites* and *Dictyoconoids* of Middle and Upper Eocene affinity in the northeast of Ngalwa (Acharyya, 1982) and *Operculina sp.*, *Nummulites chavanessa* of Upper Eocene affinity from Heningkunglwa area (Rangarao, 1983). Laisong Formation, in the Inner Fold Belt, gradationally overlies the Disang sediments in different synclinal troughs of Konya, Mokokchung, Zunheboto and Kohima Syncline (GSI, 2011). It consists of medium to fine grained, well bedded, hard, light grey laminated sandstone alternating with minor grey and sandy shale with siltstone.

2) Jenam Formation: In the southern part of the Schuppen Belt, it is represented by a predominantly argillaceous sequence of dark siltstone, shale, thin sandstone bands, carbonaceous bands and a number of coal streaks. The thickness of this formation along Dimapur-Kohima road section is about 800 m (Rangarao, 1983). Jenam Formation of Schuppen Belt is equated with Baragoloi Formation of Upper Assam and lower part of Tikak Parbat Formation is correlated with upper units of Jenam Formation and the lower units of Renji Formation. Evans (1932) synthesized that Jenam Beds within Schuppen Belt are argillaceous in the upper part, thus forming a transition into the overlying Renji Formation.

3) Renji Formation: This Formation is dominated by thick ferruginous sandstone beds alternating with grey siltstones and fine sandstone beds. Thin shale beds are commonly encountered with parallel laminations. They are exposed as the footwall of Piphema thrust for a length of about 2.8 km road traverse towards Dimapur. The thickness of Renji Formation in

the different tectonic slices of Schuppen Belt varies widely due to changes in depositional environment and unconformable overlap of Surma rocks. It is the youngest formation of the Barail Group in the Belt of Schuppen. Evans (1932) described this unit as "a great thickness of hard, ferruginous, usually massive sandstone occurring above the soft Jenam Beds". It is made up of very thick multi-storeyed sandstone units with a number of grit beds (2000 m) (GSI, 2011). Based on available palaeontological records (Acharyya, 1982; Rangarao, 1983), it is interpreted that Barail sedimentation commenced in Upper Eocene period, but in absence of diagnostic fossil beds, the period of Oligocene sedimentation is yet to be precisely confirmed.

2.3.8 SURMA GROUP

The Surma Group of rocks unconformably overlies the Barial rocks, often characterised by basal conglomerate (GSI, 2011). They are exposed in the Belt of Schuppen in the form of a number of long, narrow strips running along almost the entire length of Nagaland on the western margin. They gradually thin out towards the north. The rocks of this group are also reported to be in the core of the Kohima Synclinorium (DGM, 1978; GSI, 2011). They show a pattern of progressive transgression within the Belt of Schuppen (GSI, 2011). Alternating succession of well bedded sandstones, shaly sandstone, mudstone and sandy shale and a basal conglomerate characterize these rocks. The Surma rocks in Nagaland are of lower Miocene age (Yadekar and Ray, 1984). The overall thickness of this group varies from 300-1250 m. The Surma Group is subdivided into the Bhuban and Bokabil Formations.

2.3.9 TIPAM GROUP

A group of massive sandstones, that are highly friable and contain subordinate clay and shale, known as the Tipam, unconformably overlie the Surma rocks. However, in Nagaland, the unconformity is not clear and the contact between the Tipam and Surma is usually thrusted. The Tipam Group is divided into two Formations, *i.e.* the older Tipam Sandstone Formation and the younger Girujan Clay Formation. The Tipam sandstones are of Mio-Pliocene age and are massive and very friable in nature. These rocks are generally coarse grained, occasionally gritty and ferruginous and characterized by multi storied, channelled false-bedded sandstones with little lithological variation (GSI, 1983). The Girujan Clay Formation is dominated by thick sequence of mottled and varied clays with a few silt and sandstone beds.

2.3.10 NAMSANG BEDS

The Namsang Beds, which belong to the Dupitila Group, lie unconformably over Girujan Clay Formation and are confined towards the northern part of the Schuppen Belt.

These beds of Mio-Pliocene age consist of sandstone, lignite pebbles, conglomerate, grit, mottled clay and lenticular streaks of lignite. Thickness varies between 400-1080 m.

2.3.11 DIHING GROUP

The Dihing Group comprises mainly of thick pebble beds with clays and soft sands that unconformably overlie the Namsang Bed Formation and Girujan Clays (Chakradhar and Gaur, 1985). They occur in few patches in the western margin of the Belt of Schuppen.

2.3.12 ALLUVIUM AND HIGH LEVEL TERRACES

Pleistocene sediments deposited in fluvial regimes are seen as boulder beds, pebbles and gravel with coarse sand and clay. They occur as high level terraces of old. The younger Holocene alluvium are seen as thin layers of sand, silt and clay over the underlying Dihing rocks. They are extensively scattered in the plains of Nagaland and Assam. Neotectonic movements in these sediments have been reported (Longkumer *et al*., 2019).

Table 2.1: Stratigraphic succession of Nagaland (after Mathur and Evans, 1964; Agarwal and Ghose, 1986 and Imchen *et al*., 2014)

Age	**Group**	**Litho-formations**	
		Outer and Intermediate Hills	Eastern High Hills
Recent - Pleistocene		Alluvium And High Level Terraces	
	Dihing	Boulder Beds	
--------Unconformity---------			
Mio-Pliocene	Dupitila	Namsang Beds	
--------Unconformity---------			
Miocene	Tipam	Nazira Sandstone Girujan Clay Tipam Sandstone	
	Surma	Upper Bhuban	

		Lower Bhuban		

--------Unconformity---------

Oligocene	Barail	Renji	Tikak Parbat	Jopi / Phokphur Formation Tuffaceous shale, sandstone, greywacke, grit and conglomerate. Minor limestone and carbonaceous matter
		Jenam	Baragoloi	
		Laisong	Naogaon	
Upper Cretaceous - Eocene	Disang	Upper		Shale/slate/phyllite with calcareous lenses in basal sections and invertebrate and plant fossils in upper sections with brine springs
		Lower		

-------Base not seen------- -------Fault/Thrust-------

Chert Kimmeridgian to mid-Tithonian Middle Jurassic - Cretaceous	**Naga Ophiolite Complex**	Zepuhu Formation Marine sediments (shale, phyllite, greywacke, iron-rich sediments, chert and limestone with radiolaria and coccoliths), volcanics (basalt, spilite, volcaniclastics), metabasics, greenschist, glaucophane schist/ glaucophane-bearing metachert, eclogite), layered cumulate sequence (peridotite, pyroxenite, gabbroids, plagiogranite, anorthosite), and peridotite tectonite and serpentinite associated with deposits of podiform chromite and nickeliferous magnetite, minor Cu-Mo sulphides associated with

		late felsic intrusions and some dolerite dykes

------Fault/Thrust-------

Pre-Mesozoic (?)	**Naga Metamorphic Complex**	Nimi Formation Weakly metamorphosed limestone, phyllite, quartzite and quartz-sericite schist Naga Metamorphics Mica schist, granitoid gneiss and feldspathic metagreywacke with tectonic slices of ophiolite in variable dimensions

2.4 GEOLOGY OF THE STUDY AREA

The study area comes within the Belt of Schuppen. The Barail Group of rocks classified as the Laisong (oldest), Jenam (middle) and the Renji (youngest) Formations, range in age from Upper Eocene to Oligocene age.

Disang Thrust which forms the eastern limit of the Belt of Schuppen, along with the Piphema Thrust and Sanis-Chongliyimsen Thrust bound the Barail Group of rocks. The geological map of the study area (Figure 2.3) shows the distribution of various litho-units belonging to the Barail Group. Locations of rock samples and vertical profile sections have been shown in Figure 2.4.

Due to the extensive thrust pattern in the area, the appearance of the litho units in the field according to stratigraphy is not realized. The general trend of the BoS is NE-SW trending reverse faults and overturned folds, NNW-SSE and WNW-ESE strike-slip faults and NW-SE normal faults (Mathur and Evans, 1964). The Geological Map of Nagaland is shown in Figure 2.2, displaying the various geological arrays for reference.

The Barail sediments are exposed between the foot of the Disang Thrust and the eastern margin of the Medziphema town (Sanis-Chongliyimsen Thrust), where Quaternary Dihing Boulder Bed is exposed. The Jenam Formation occurs in two tectonic slices, one between Disang and Piphema Thrusts and the other overlying the Laisong Formation east of Pherima Village. The Jenam Formation has a NE-SW linear strike with a width of 5.1 km.

The Jenam Formation is represented by well bedded, dark grey shale, siltstone and sandstone beds and they exhibit high degree of structural deformations. Jenam Formation is defined by dominance of argillaceous sequences. Coal streaks/streaks are common in these sediments. The Piphema Thrust is located 5.1 km away from the Disang Thrust towards Medziphema.

The youngest, Renji Formation occurs as massive sandstone beds, ferruginous in nature with alternating sequences of siltstone and shale. Ripple marks (asymmetrical) are very common in these sequences. In the study area, they dramatically occur as vertical cliffs with almost perpendicular dip. They are exposed as the footwall of the Piphema Thrust for a length of 2.8 km along the road towards Dimapur.

The Laisong Formation occurs as a NE-SW linear tectonic slice on the hanging wall of the Sanis-Chongliyimsen Thrust. They are exposed for about 5.3 km on road from Medziphema towards Kohima. Two distinct units of Laisong sediments are observed in the field, the upper unit being thick bedded, and medium to coarse grained sandstones while the lower unit has more argillaceous beds within the coarse sands. Intercalation of mud and shale is common in these sediments. Coal streaks are common and found associated with shale beds.

The Sanis-Chongliyimsen Thrust separates the Palaeogene and Neogene rocks as no Palaeogene sediments are recorded west of this tectonic break.

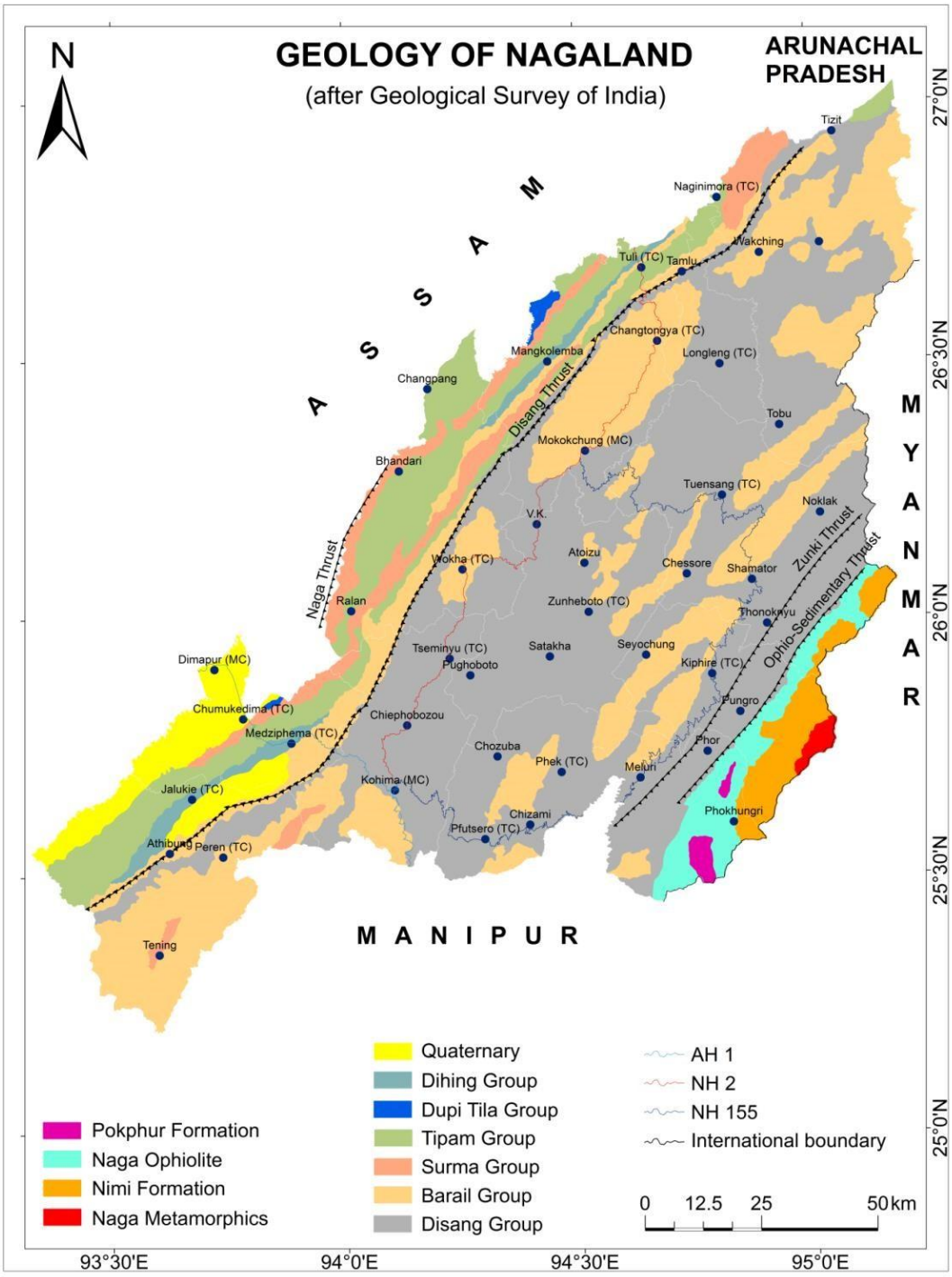

Figure 2.2: Geological Map of Nagaland (after GSI, 2011)

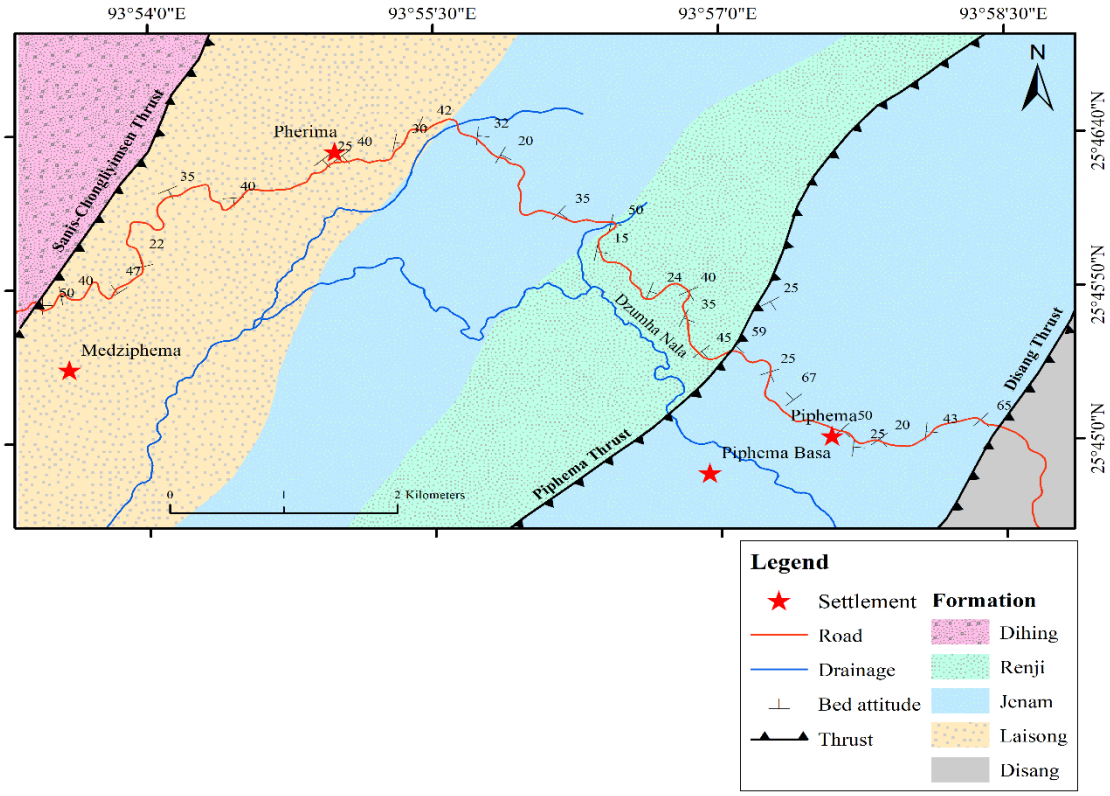

Figure 2.3: Geological Map of the Study Area

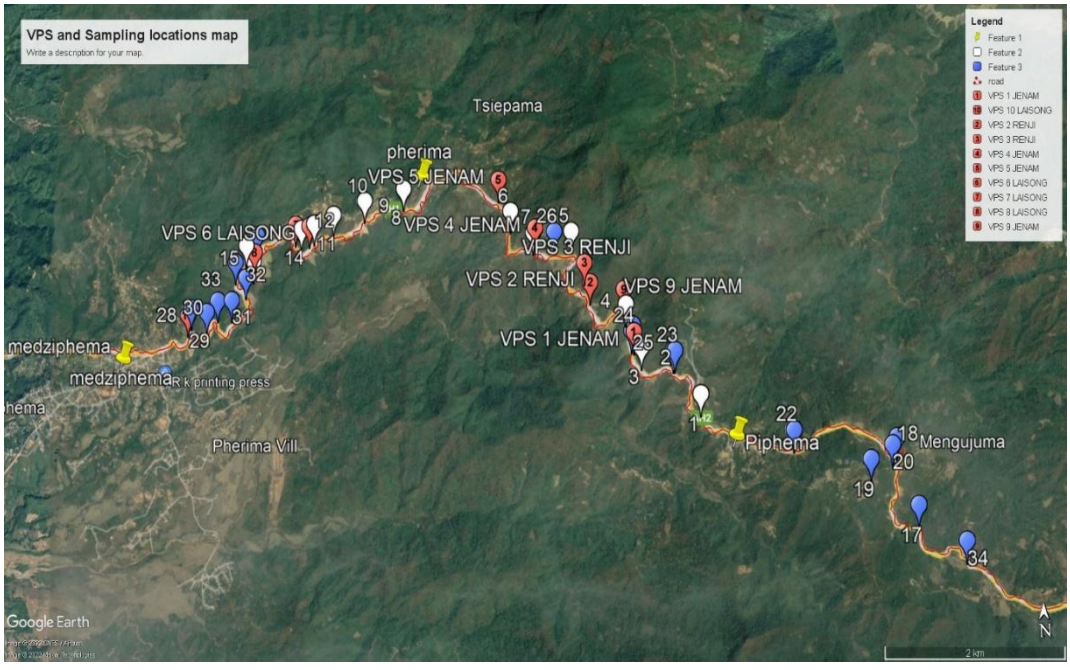

Figure 2.4: Map showing Sample and VPS locations

CHAPTER 3

METHODOLOGY

The research methodology involved detailed fieldwork and laboratory investigations. The investigation dealt and advanced along the following lines:

3.1 FIELD INVESTIGATIONS

a) Demarcation of different lithologic units and recording of bed attributes

b) Identification of structural indices such as thrusts, faults and folds

c) Collection of random and oriented samples from suitable rock exposures

d) Identification and recording of sedimentary structures including biogenic structures

e) Measurement of vertical profile sections

f) Recording and identification of lithofacies

The instruments utilized during fieldwork are hand held Garmin GPS (Global Positioning System Oregon 650), base map, brunton compass, geological hammer, chisel, hand lens, measuring tape, sample bags, field notebook, marker, haversack, and camera. Reconnaissance survey has been done along the section to locate suitable exposures for detail study which was followed by extensive fieldwork in the area. All lithological variations have been marked on the GPS with coordinates for referencing with the map. Major thrusts, faults and folds have been identified and photographed. The structural aspects have also been noted. Bed wise sampling has been done along a litho column to correlate with variation in lithofacies. Random sampling has also been carried out in the field for petrographic studies in the laboratory. Care has been taken to remove any weathered cover and vegetation to collect fresh samples. The location of each sample has been geotagged with bed attributes. Field photographs of significant features including inorganic and biogenic sedimentary structures were recorded and photographed. Litho-sections were measured at suitable locations and profiles were constructed for litologic variations in time and space.

3.2 LABORATORY ANALYSES

The various laboratory analyses undertaken in the present study is shown in the following Table 3.1:

Table 3.1: Table showing details of laboratory analyses

Objective	Methodology/Instrumentation	Laboratory
To study the lithofacies variations, textural properties, and depositional environment	Preparation of geological map, cross section, construction of VPS, preparing lithofacies scheme	Department of Geology Nagaland University Kohima Campus, Meriema
	Modal analysis	
	Grain size analysis	
To determine the provenance and tectonic setting	Rock thin section	Department of Geology Nagaland University Kohima Campus, Meriema
	Heavy mineral analysis	
	X-ray Fluorescence Spectrometry (XRFS) analysis	Sophisticated Analytical Instrument Facility (SAIF), Dept of Instrumentation and USIC Gauhati University Guwahati, Assam
To identify clay minerals and understand the diagenetic history	X-ray Diffraction (XRD) analysis	Sophisticated Analytical Instrument Facility (SAIF), Dept of Instrumentation and USIC Gauhati University Guwahati, Assam
	Scanning Electron Microscope (SEM) analysis	Central Research Facility (CRF) Indian Institute of Technology (IIT), Kolkata

3.3 PROCEDURES FOR LABORATORY ANALYSES

3.3.1 PREPARATION OF GEOLOGICAL MAP

Global Positioning System (GPS) has been used during the fieldwork to navigate and record the coordinates of outcrops and sampling points as well. Google Map has been used for better navigation during the fieldwork. The bed attitudes and structural attributes were measured using Brunton Compass. All important and necessary field photographs and megascopic structures were captured using a camera. Sedimentary structures were also photographed.

For the preparation of geological traverse map, the mosaic of the toposheet no. 83G/13 and 83G/14 (1:50000 scale) were prepared by geo-referencing the field data in ArcGIS software. The prepared geological traverse map and geological cross-sections and were refined in Corel DRAW software. The sampling locations, VPS locations, attitude of the different beds (dip and strike), structural data recorded in the GPS (Global Positioning System) as coordinates was transferred to a windows operating system and generated as digital media. Field photographs captured were tagged and described accordingly.

3.3.2 VERTICAL PROFILE SECTION (VPS) AND LITHOFACIES ANALYSIS

For lithofacies analysis, ten (10) detailed vertical profile sections (VPS) have been measured and recorded in the field and the data has been converted into digital media using SedLog and CorelDRAW softwares respectively. Different litho-units and their contacts exposed in the study area were measured. The distinctive megascopic characteristics, lithological characteristics, thickness of the beds, grain size, and sedimentary structures were observed and noted.

Lithofacies analysis was conducted in the present study to reconstruct the depositional environment of the Barail Group in the study area. From the VPS, ten (10) different Facies Codes have been generated according to the parameters given by Selley (1970; 1976); bed geometry, lithology including grain-size, primary sedimentary structures, palaeo-current patterns, and fossils.

3.3.3 ROCK THIN-SECTION STUDY

Fresh sandstone samples from all three formations of the Barail Group were selected for rock thin section analysis. A total number of sixty (60) thin sections were prepared for petrographic studies. The thin sections have been prepared at the Department of Geology, Nagaland University, Kohima Campus, Meriema.

The rock samples are mechanically cut into thin slices approximately 1/8 inches thick with the help of a cutting machine. Since the rock samples were indurated, no other treatment has been applied. After acquiring a thin section of the sample, it is placed face down on a glass

and grinded with silicon carbide powder with mesh sizes of 300, 600, 800, 1000, and 1200. This process results in a finely polished surface which is then put on a hot plate. Araldite is used to mount the smooth surface on the glass slide and left for 24 hours to bind and harden. The uneven surface is grinded again with silicon powder until the grains give the desired interference color. Once the required thickness 0.03mm (approximate) is attained, the polished side of the sample is covered with a coverslip, and the slide is ready for study under petrological microscope.

3.3.4 MODAL ANALYSIS

For modal analysis, the Gazzi-Dickinson (1966) method was used by counting at least 250 or more points per thin section. Forty-five (45) sandstone thin sections from the Barail Group of rocks have been counted for modal composition. Framework grains of fifteen (15) samples each from the Laisong, Jenam and Renji Formation were meticulously counted. Composition of framework grains and matrix were identified under a petrological microscope using their optical properties, details of which are discussed in the following chapters. The counted data has been plotted in representative ternary and diamond diagrams. Important diagenetic features have been observed and studied as well from the thin sections. Photomicrographs have been acquired for petrographic studies as well. Thin section study and all petrographic data were generated at the Department of Geology, Nagaland University, Kohima Campus, Meriema using the LEICA (TL/RL) DM 2700P Trinocular Polarizing Microscope fitted with CCD camera and Leica Application Suite (LAS).

3.3.5 GRAIN SIZE ANALYSIS

The rock samples in the study area are hard and compact indurated sandstones and therefore the grain size analysis has been performed using thin sections. Friedman (1962), Stauffer (1966), Conner and Frem (1966), Smith (1966) and Textoris (1971) have justified the use of thin sections for grain size measurements.

Twenty one (21) thin sections, seven (7) samples each from the three rock formations have been used for grain size measurements. Minimum of 200 grains or more have been measured in each thin section. Grain size values obtained were grouped into half phi (Ø) scale intervals and were used in plotting cumulative curves on arithmetic paper.

3.3.6 HEAVY MINERAL ANALYSIS

Folk's (1980) method and Middleton's (2003) Funnel Separation method for Heavy Mineral separation has been adopted in the present study. Bromoform (Tribromo methane, $CHBr_3$) is a chemically inert and non-viscous heavy liquid with a specific gravity of 2.89.

The samples are gently crushed with the help of hammer, mortar and pestle. Crushed samples are then sieved in 100, 120 and 140 ASTM (American Standard for Testing Machine) sizes respectively. Approximately 50 grams of crushed samples were obtained after sieving of each sample for heavy mineral separation. The samples are transferred in a 250ml beaker and soaked in Hydrogen Peroxide (H_2O_2) for 24 hours to remove clay and carbonate coatings on the grains. The treated sample is thoroughly washed and rinsed with water repeatedly until no impurities and residue are left behind. The samples are then boiled with dilute hydrochloric acid (N/10 i.e., 1:10 ratio where 100ml of concentrated HCl is diluted in 1000ml of water) and a pinch of stannous chloride ($SnCl_2$) is added. This is done to remove any authigenic clay and carbonate or ferruginous coatings over the grains. Zinc powder is also added in case the sample appears murky. On cooling, the boiled sample is thoroughly washed again with distilled water repeatedly so as to eliminate the acid. The sample is then oven dried and is ready for separation.

In a separating funnel, Bromoform liquid is placed then the treated dried sample is added and kept for about 5 minutes to allow the heavies to sink. Heavy minerals settle down at the bottom of the funnel and are collected on filter paper which is then oven dried. Heavy mineral grains separated out are mounted on glass slides using adhesive Canada balsam and covered with cover slip. The mounted slide is kept to dry and set for a day. The above process is repeated until the desirable amounts of heavy minerals is recovered. Each grain mounted is studied under the petrological microscope for identification and further detailed study. Identified heavy minerals are counted and data generated is represented in histograms. All sample preparation, steps involved, laboratory studies and petrographic studies for heavy minerals have been undertaken at the Department of Geology, Nagaland University, Kohima Campus, Meriema.

3.3.7 X-RAY FLUORESCENCE SPECTROMETRY (XRFS) ANALYSIS

X-ray Fluorescence Spectrometry (XRFS) analysis was done at Sophisticated Analytical Instrument Facility (SAIF), Department of Instrumentation and USIC, Gauhati University, Guwahati, Assam to determine the major oxides. A total of thirty (30) samples were chosen for XRF analysis. Ten (10) representative sandstone samples each from the Laisong, Jenam and Renji Formations were powdered using hammer, mortar and pestle. The powdered sample is then grinded with agate mortar and pestle to make it into finer powder at the Department of Geology, Nagaland University, Kohima Campus, Meriema. After grinding and sieving at mesh size 200 mesh size (ASTM), 20 grams of each sample was packed in plastic sample containers and tagged to avoid contamination. X-ray Fluorescence Spectroscopy (XRFS) analysis is based on the excitement of a sample by bombardment with x-rays which causes the sample to fluorescence which is recorded in terms of energy spectrum.

The different intensities of the energy spectrum are calibrated for instrumental errors and corrected accordingly. Quantitative analysis of silicate rocks for 10 major oxides: SiO_2, Al_2O_3, Fe_2O3 (T), MnO, MgO, Na_2O, CaO, K_2O, TiO_2, P_2O_5 have been acquired and is represented in table and respective bivariate plots in the following chapters.

3.3.8 X-RAY DIFFRACTION (XRD) ANALYSIS

Eighteen (18) samples have been analysed for XRD analysis taking six (6) from each formation of the study area. Preparation of sample for XRD was carried out at the Department of Geology, Nagaland University, Kohima Campus, Meriema. The investigation has been carried out at the Sophisticated Analytical Instrument Facility (SAIF), Gauhati University, Guwahati, Assam. X-ray Diffraction (XRD) Analysis was done in order to study the clay fractions present in the samples. The rock samples were grinded with agate mortar and pestle uniformly and sieved using 200 (ASTM) mesh. 20 gm of finer rock powder was collected and sealed a plastic airtight cylindrical container and labelled. The sample is transferred to a measuring cylinder and stirred with 1000 ml distilled water. It is then kept undisturbed for three hours. A pipette is then used to draw out 50 ml of the upper solution water where the finer clay mixtures float. A filter paper is used to retain this clay mixture. This process is repeated until a considerable amount of clay particles are acquired. The filter paper containing the particles is over dried so as to remove all excess water. The dried clay fractions undergo XRD analysis in the Automated Computerized Powder X-ray Diffractometer. The output consists of X-ray Diffractogram, Peak Position, d values and relative intensity data which are then studied and interpreted.

3.3.9 SCANNING ELECTRON MICROSCOPE (SEM) ENERGY DISPERSIVE X-RAY (EDX/EDS) ANALYSIS

Three (3) thin section samples were chosen for Scanning Electron Microscope (SEM) EDX Analysis which was carried out at Central Research Facility (CRF), Indian Institute of Technology (IIT), Kolkata. The output is high-resolution three-dimensional images of the specimen surface showing topographical, morphological, and compositional characteristics. The thin sections were coated and observed under the SEM.

Scanning Electron Microscopy-Energy Dispersive Spectroscopy (SEM-EDX) is useful in studying several aspects of sandstones such as detrital mineralogy, diagenesis, grain size, grain shape, sorting, angularity, cement and matrix content. SEM-EDX exhibits lower errors than optical microscopy in determining grain mineralogy, type, boundary, cement and matrix composition as it is apparently easier to differentiate the discrete entities (Worden and Utley, 2022). This technique is an intermediary between sediment mineralogy and petrology and core-based sedimentology (Armitage *et al*., 2010).

CHAPTER 4
LITHOFACIES ANALYSIS AND VERTICAL PROFILE SECTION

4.1 GENERAL

It was Nicolas Steno who introduced the term 'facies' in 1669 (Teichert, 1958). Moore (1979) described facies as 'any aerially restricted part of a designated stratigraphical unit which exhibits characters significantly different from those of other parts of the unit'. Middleton (1973) describes sedimentary facies as the sum total of the characteristics of a sedimentary unit. According to Reading and Levell (1996), a rock facies is a body of rock with specified characteristics that reflect the conditions under which it was formed. Reading (1978) has expanded the definition and describes facies as a rock unit bounded by typical lithologic features, guided sedimentation, reflecting a particular process, set of conditions or environments. Lithofacies analysis involves facies differentiation and interpretation on the basis of lithology and associated features. To determine the lithofacies type of sediments, it is important to document all the characteristics including lithology, texture, sedimentary structures, palaeocurrents and fossil content. This aids in unravelling the processes of deposition of the sediments. The relation between lithofacies and the environment of deposition was first proposed by Walther in 1894 when he suggested that the two environments lying side by side would appear overlapping each other in crustal profile. Facies association which is a group of facies in a sedimentary succession and environment of deposition provide information on the depositional environment as they result from association of various processes (Nichols, 2009). Facies analysis has undoubtedly become a very significant tool in interpreting past environments and reconstruction of the same (Anderton, 1985).

4.2 LITHOFACIES ANALYSIS

For clastic sedimentary rocks, diagnostic characters as bed geometry or dimension, lithology including grain-size, primary sedimentary structures, palaeo-current patterns, and fossils constitute the five parameters of sedimentary facies (Selley, 1970; 1976).

4.2.1 GEOMETRY

In the study area well bedded, both thick and thin bedded litho-units are exposed. Bed contacts are mostly observed to be straight and gradational. The vertical sections provide substantial amount of data for lithofacies description.

4.2.2 LITHOLOGY AND GRAIN-SIZE

Mineralogical and textural variations in a clastic sedimentary rock point towards the nature of source terrain, mechanism of transportation and depositional environment. Though grain size analysis has found use, the reliability and effectiveness of grain size parameters as environmental indicators has been questioned (Pettijohn, 1975; Selley, 1976; Friedman and Sanders, 1978; Walton *et al*., 1980; Reineck and Singh, 1980). The grain-size variations within the Oligocene Barail sediments in the study area range from clay to coarse sand fractions. The Laisong sediments are represented by medium/coarse to occasional very coarse grained sandstones with minor amount of shale and siltstones. The Jenam Formations comprise of shale and sandstones where sand size vary between very fine to fine and medium to coarse sand fractions. Renji Formation is represented by both shale and sandstones where sand size ranges from very fine to fine and medium to coarse sand sizes. Coal streaks are not uncommon in all three formations.

4.2.3 SEDIMENTARY STRUCTURES

Sedimentary structures reflect environmental conditions that prevailed at or very shortly after the time of deposition, therefore serve as a very significant feature in deducing ancient depositional environment. They not only provide insight to the flow regime but also reflect the processes which has produced them (Allen, 1982; Collinson and Thompson, 1994). Sedimentary structures can be used to determine top and bottom of beds and also to evaluate sediment transport mechanism, palaeocurrent flow directions, relative water depth, and relative current velocities.

In the study area a wide variety of primary and post depositional features have been observed. Primary sedimentary structures, observed in the study area include parallel laminations, cross laminations, sole marks, load casts, ripple marks and channels.

4.2.4 PALAEOCURRENTS

Palaeoflow or the direction of flow at the time of sedimentation is an important attribute of palaeoenvironmental interpretation. The use of palaeocurrent in reconstructing palaeoevironment have been described by Allen (1966, 1967) and Selley (1968). Primary sedimentary structures and scalar features of rocks have been used to deduce the palaeocurrent direction. Palaeocurrent analysis is accomplished by measuring the orientation of directional sedimentary structures such as flute casts, ripple marks, cross-beds or the long axis orientation of pebbles.

4.2.5 BIOGENIC STRUCTURES/ FOSSILS

Body/trace fossils provide substantial information for palaeoenvironmental studies. Fossils are often utilised as palaeoenvironmental indicators thereby ascertaining their importance (Howard, 1972; Ekdale *et al*., 1984). Tracks, trails, burrows, borings and other structures made by organisms on bedding surfaces or within beds are known as trace fossils also referred to as ichnofossil. Where body fossils are absent trace fossils provide significant information on the depositional environment. These are characterized by the disturbance of sediment due to the activities of organisms and bioturbation. Study of trace fossil assemblages is significantly important than study of individual ichnogenera or ichnospecies. Body fossils are absent in the study area however, leaf imprints (Plate 4.1a) and carbonized plant materials (Plate 4.1b), have been recorded from the field. Trace fossils can also provide valuable information on sedimentation rate, water depth, salinity, energy level and oxygenation at the time of deposition of sediments. Trace fossil distributions are indirectly controlled by bathymetry (Seilacher, 1967; Bromley, 1996). Body fossils are rarely wholly preserved, therefore trace fossils play a significant role in environmental interpretation where body fossils are absent or sparse (Frey, 1975).

4.3 DESCRIPTION OF SEDIMENTARY STRUCTURES

Various primary sedimentary structures, varying in scale and geometry, observed and recorded and have been placed into four categories of sedimentary structures; namely depositional, post-depositional, erosional and biogenic (Tucker, 1993).

4.3.1 DEPOSITIONAL SEDIMENTARY STRUCTURES

Depositional sedimentary structures are formed during the time of deposition and are found on the upper surface of beds and also within them. Depositional sedimentary structures observed in the study area includes bedding, laminations, ripple marks, cross-stratification.

4.3.1 (A) Bedding

Beds are tabular or lenticular layers of sedimentary rock with each bed having distinguishable properties in composition, size, shape, orientation and packing of sediments. Bedding represents changes in the sedimentation pattern. Thickness of a bed in a succession is an important and useful parameter to measure. Campbell (1967) suggested that beds have no limiting thickness.

The Barail sediments in the study area exhibit variations in bedding style, thickness, ranging from very thinly bedded (Plate 4.1c) to very thickly bedded (Plate 4.1d). Planar bedding is a common feature in all the three formations. Thickening as well as thinning upwards of beds has been observed along the exposure.

4.3.1 (B) Lamination

Laminations are horizontal layering which are essentially parallel to bedding surfaces. Individual laminae displaying thickness of less than 1 cm are considered as planar laminations. Colour changes accentuate the presence of some laminae. Planar lamination occurs in fine grained to coarse grained sediments in the study area (Plate 4.1e, f). Wave ripple cross lamination has also been observed.

4.3.1 (C) Cross-Stratification

Cross stratification is layering in sediment that is oriented at an angle to the depositional surface (Collinson *et al*., 2006). Presence of cross stratification suggests variations in current or wave activity or sediment supply due to changing current strength or wave power. In the study area, cross stratification is not a common feature. It has been recorded in a few exposures only (Plate 4.2a, b and c).

4.3.1 (D) Ripple Marks

The most common sedimentary structure found in sediments and sedimentary rocks are ripple marks. Ripples are oscillatory/unidirectional motion of the top surface of water body produced by waves or current. They are considered to be the smallest bedforms. Type of ripple, their orientation, geometry throws light on the depositional environment. The Barail sediments in the study area record abundance of ripples, in both sandstones and the fine grained sediments (Plate 4.2d, e, f, and g).

4.3.2 POST-DEPOSITIONAL SEDIMENTARY STRUCTURES

These structures are the result of deformation. These are termed post-depositional as they only form after sediment has been laid down. In the study area, such structures include load casts (Plate 4.3a) and intraclasts (Plate 4.3b). Potter and Pettijohn (1977) described load casts as swellings ranging from slight bulges, deep or shallow rounded sacks, knobby excrescences, or highly irregular protuberance. They occur on the soles of sandstone beds that overlie softer material. Load casts do not display preference to current direction and occur in many types of environment.

4.3.3 EROSIONAL SEDIMENTARY STRUCTURES

Partial and localised removal of sediments which have been recently deposited may occur when a turbulent overrides the sediment surface. Channels are a common structure of this group observed in the study area.

4.3.3 (A) Channels

Channels are recognized by their cross-cutting relationship with underlying sediments. (Plate 4.3c, d, e, and f). Channelled sediments are texturally different than the sediments below or adjacent. They may range in size from a few cm to a meters.

4.3.4 BIOGENIC SEDIMENTARY STRUCTURES/TRACE FOSSILS

Trace fossils are fossilized records of the activities of the past life. These sedimentary structures are characterized by the disturbances in the sediment due to the activities of organisms and provide important information of the past. They play a very important role in environmental interpretation especially where body fossils are absent. In the studied Barail sediments trace fossils are sparse and less abundant. Trace fossils recorded from the Barail sediments are mostly horizontally disposed except *Skolithos*, *Monocraterion* and *Laevicyclus* which are vertical to the bedding plain. Trace fossils observed in the study area belong to either *Skolithos* or *Cruziana* ichno-assemblages. However, *Nerites* ichnofacies have been recorded form Jenam Formation only.

Following are the descriptions of the identified trace fossils in the study area:

Skolithos verticalis (Hall, 1843): This is one of the most common trace fossil recorded from the fine grained sandstone of the Laisong Formation. They are straight, un-branched structures having a diameter between 1-7 mm showing full relief (Plate 4.4a and b).

Ophiomorpha nodosa (Lundgren, 1891): Horizontal burrows where burrow fill is different than the sediments it is found associated with. Exterior surface is line with ridges covering the tube (Plate 4.4c).

Chondrites isp, is a three dimensional cylindrical tunnels systems with individual tunnel segments are generally straight and do not intersect each other. Diameter of individual branch varies between 0.5 and 1.0 mm. These are recorded from Laisong sandstones only (Plate 4.4d).

The vertical or vertical to slightly inclined biogenic structures are commonly recognized from semi-consolidated substrate (Frey and Pemberton, 1985) and they are characteristic features of the nearshore/foreshore marine environment, with moderate to high energy conditions (Seilacher, 1967). The horizontal structures are the members of the *Cruziana* ichnofacies and generally occur in shallow water marine environment with reducing energy (Seilacher, 1967).

Thalassinoides horizontalis (Myrow, 1995): They are three dimensional structures with horizontal network and are generally swollen at Y-shaped junction. These are found to be associated with very fine sandstones of Jenam Formation (Plate 4.4e and f).

Planolites beverleyensis (Billing, 1862): These are horizontally disposed trace fossil recorded from Jenam Formation and are straight to gently curved. They are cylindrical or sub-cylindrical and unbranched burrows showing a circular or elliptical shape in cross section (Plate 4.5a).

Laevicyclus isp (Quenstedt, 1879): These vertical cylindrical burrows consist of a central shaft which is surrounded by circles and are right angle to the bedding plane. Sediments making the outer rings are coarser than the inner shaft. These are reported from Jenam Formation only (Plate 4.5b).

Nerites isp (Weller, 1899): These are unbranched meandering trail having a width of 5 mm with 15 mm length made up of a central zone having a smooth upper part and showing laminations in the lobes though poorly visible. This has been reported from Jenam Formation only and has been recorded from both mudstones as well fine sandstones (Plate 4.5c).

Monocraterion isp (Torell, 1870: Simple vertical funnel shaped burrow structure perpendicular to the bedding plane having a central raised knob. Diameter ranges between 1 to 4 mm (Plate). This is reported from Jenam Formation only (Plate 4.5d).

Scolicia prisca (Quatrefages, 1849): Meandering burrows is parallel to the bedding planewhere central furrow is flanked by redges. This is recorded from the mudstones and very fine grained sandstones of the Jenam Formation (Plate 4.5e).

Palaeophycus striatus (Hall, 1852): These are straight, horizontal unbranched tunnel with wall lining. Wall surface is covered with straight faint linings. This is the only trace reported from fine sandstones of Renji Formation (Plate 4.5f).

4.4 FACIES SCHEME

On the basis of the various facies parameters and field observations total ten (10) lithofacies have been identified and allotted distinct facies codes. The scheme includes description of the lithofacies types in each of the formation of the Barail Group of rocks. Table 4.1 shows the composite table for facies code and lithofacies type.

4.4.1 DESCRIPTION OF LITHOFACIES

4.4.1 A) Laisong Formation: Altogether four (4) lithofacies have been identified in the field, descriptions are given below. Trace fossils recorded from the various facies of the Laisong Formation includes *Ophiomorpha, Laevicyclus, Skolithos, Monocraterion* and *Chondrites*.

a. **Fine to medium massive sandstone facies (*Sm*):** This facies is characterized by fine to medium grained sandstone occasionally having coarse grained sandstones. Thickly bedded massive sandstones are found associated with vertical burrows. The thickness of sandstone beds varies between 1 to 4 metres. However coarse grained beds show a maximum thickness of 10 meters. Coal streaks have also been observed in this facies (Plate 4.6a).

b. **Lenticular/wavy sandstone facies (*Sw*):** This facies is represented by fine to medium sandstone showing wavy or lenticular bedding pattern (Plate 4.6b, c).

c. **Rippled sandstone facies (*Sr*):** This facies is represented by fine to medium sandstone lithologies. Asymmetrical ripples with low crests are found in this facies. Its thickness ranges from a few cms to 3 meters (Plate 4.6d).

d. **Fine cross laminated sandstone facies (*Sx*):** Fine to medium sandstones possessing fine cross lamination with occasional wave ripple cross laminations are the main characteristics of this facies. Its thickness ranges between 10 cm to less than a meter (Plate 4.6e).

4.4.2 B) Jenam Formation: Altogether three (3) lithofacies have been identified in the field, descriptions are given below. Jenam Formation records the presence of horizontally disposed trace fossils including *Planolites beverleyensis, Thalassinoides horizontalis*, *Scolicia prisca* and *Nerites*.

a. Sandstone-shale facies (*Ss*): Fine to medium grained sandstones alternating with shale in a rhythmic pattern are a common feature of this facies. Sandstone beds are thicker than shale beds. Laminations, ripples, wavy contacts, coal streaks mark this facies. The thickness varies from approximately 30 cm upto a stretch of alternating sand-shale facies over 4 meters long (Plate 4.7a, b).

b. Fine siltstone-shale facies (*Fl*): This facies is characterized by alternating sequences of siltstone and shale. Thin compact siltstone beds with repetitive thin shale beds in between extend upto 3 meters at places. Shales are grey to dark grey in colour. Siltstone and shale is plane laminated. Coal streaks are a common feature of this

facies. This is the most dominated lithofacies among the Jenam Formation (Plate 4.7c).

c. Channelled sandstone facies (*Sch*): This facies is represented by very fine to fine grained sandstones showing channel geometry. At places within this facies bidirectional cross/ form ripples and ripple cross laminations (Plate 4.7d, e).

Trace fossils recorded from the Jenam Formations are all horizontally disposed and are general found associated with the very fine grained sediments.

4.4.3 C) Renji Formation: Altogether three (3) lithofacies have been identified in the field, descriptions are given below. Only one trace fossil *Palaeophycus striatus* has been reported from the Renji Formation.

a. **Lenticular sand-mud facies (*Sw*):** Fine to medium sandstone facies showing wavy or lenticular bedding patterns. Sand lenses found within the shale units are cross laminated. Shales are carbonaceous in nature (Plate 4.8a).

b. Plane laminated fine to medium sandstone facies (*Sl*): This facies is characterized by fine to medium grained sandstones showing plane laminations, ripples, horizontal bedding showing colour variations and moderate bioturbation are common in this facies. Its thickness ranges between a few centimetres to a meter (Plate 4.8b, c).

c. Fine to medium sandstone facies *(Sch)*: This facies is represented by ferruginous fine to medium sandstones with minor intercalations of shales. This facies also shows the presence of channel showing lateral accretions (Plate 4.8d, e).

Table 4.1: Summary table showing the Lithofacies and description for Barail Group of rocks

Formation	Facies Code	Lithofacies	Lithology	Sedimentary structures	Interpretation
	Sm	**Fine to medium massive sandstone facies**	Fine to medium grained sandstone	Massive sandstone, thickly bedded, Vertical burrows	Upper shoreface, high energy

Laisong Formation	***Sw***	**Lenticular/ wavy sandstone facies**	Fine to medium grained sandstone	Fine to medium sandstone, wavy or lenticular bedding pattern	Inter tidal, upper shoreface
	Sr	**Rippled sandstone facies**	Fine to medium grained sandstone	Asymmetrical ripples with low crests, symmetrical ripples	Inter distributary bay; Crevasse channel fill
	Sx	**Fine cross laminated sandstone facies**	Fine to medium grained sandstone	Cross lamination, wave ripple cross laminations	Beach face

	Facies Code	**Lithofacies**	**Lithology**	**Sedimentary structures**	**Interpretation**
Jenam Formation	***Ss***	**Sandstone-shale facies**	Fine to medium grained sandstones alternating with shale	Laminations, ripples, wavy contacts, coal streaks	Low energy tidal current
	Fl	**Fine siltstone-shale facies**	Siltstone and shale	Plane lamination, Carbonaceous shale, coal streak	Channel bank

	Sch	**Channeled sandstone facies**	Very fine to fine grained sandstones	Bidirectional cross/ form ripples and ripple cross laminations	Low energy tide deposits

	Facies Code	**Lithofacies**	**Lithology**	**Sedimentary structures**	**Interpretation**
Renji Formation	***Sw***	**Lenticular sand-mud facies**	Fine to medium sandstone facies carbonaceous shales	Wavy or lenticular bedding, Cross laminated Sand lenses	Inter-tidal deposits
	Sl	**Plane laminated fine to medium sandstone facies**	Fine to medium grained sandstones, colour variations in adjacent beds	Plane laminations, ripples	Levees & Marsh
	Sch	**Fine to medium sandstone facies**	Fine to medium sandstones with minor intercalations of shales	Channel showing lateral accretions	Distributary mouth bar

4.5 VERTICAL PROFILE SECTIONS (VPS)

4.5.1 VPS 1 Pherima Village (N25° 46' 18.58'' E 93° 54' 26.53'')

This VPS (13 metres) was measured at Pherima village along the national highway and exposes the Laisong sediments. Sandstone in this exposure are less compacted, light brown to buff coloured and coarse grained to very coarse grained in some instances. Thickly

bedded massive sandstone beds with clayey material in between have been observed. Sandstone siltstone alternating beds have been recorded in between thick sandstone beds. Coal is common in this section. Small scale cross bedding, wavy laminations are some structures in this outcrop. The bed contacts are rippled. *Sm* and *Sx* are the lithofacies in this lithocolumn (Figure 4.2a).

4.5.2 VPS 2 Pherima Village (N25° 46' 19.4'' E 93° 54' 20.1'')

This vertical profile section (22 metres) was measured at Pherima village and the rocks belong to the Laisong Formation of the Barail Group. Thickly bedded, brown to greyish coloured massive sandstones are seen here with thin intercalations of shale beds. The sandstones are friable though they appear compact in the outcrop. Planar laminations and wave ripple cross laminations are seen in sandstone beds. Shales are plane laminated. Bed contacts are wavy. Few hard and compact reddish medium grained sandstone bed are also seen between friable sandstone beds. Coal streaks occur in between shale beds. The lithofacies present in this profile are *Sm*, *Sw*, *Sr* and *Sx* (Figure 4.2b).

4.5.3 VPS 3 Pherima Village (N25° 46' 09.9'' E 93° 54' 00.9'')

The lithocolumn (24 metres) presents rocks of the Laisong Formation measured at Pherima village. The sandstones are light brown to greyish coloured with a buff appearance. The rocks in the profile are thickly bedded coarse grained massive sandstones with shale in between (soft clay). Ripple marks and intra clasts occur in sandstone beds. Coal occurs as thin laminations in between shale beds. *Sm* and *Sr* are the lithofacies represented in this vertical profile section (Figure 4.2c).

4.5.4 VPS 4 Medziphema Town (N25° 45' 49.16'' E 93 53' 31.53'')

This lithocolumn (22 metres) was measured right before reaching Medziphema Town junction from Pherima. The area exposes the Laisong Formation of the Barail Group of rocks. The Laisong sandstones in this area are argillaceous compared to the more arenaceous sandstones around Pherima area. The sandstones are medium grained to coarse grained, grey and brown coloured and friable in nature. Massive sand beds alternate with shale beds and coal streaks appear frequently. Contact between beds is gradational. The lithofacies present in this section are *Sm* and *Sr* respectively (Figure 4.2d).

4.5.5 VPS 5 Piphema Village (N25° 45' 34.4'' E 93° 56' 50.3'')

This vertical profile section (9 metres) was measured at Piphema village, along the national highway. The rocks belong to the Jenam Formation of the Barail Group of rocks. Sandstones here are mostly grey in colour while shales appear dark grey to blackish color. The lithology of this section displays very fine to fine grained and medium grained sandstones alternating with siltstone and shale beds. Sandstone and shale beds are generally thinly bedded. Planar and cross laminations in sand and shale are common here. Massive sandstone

beds also occur. Bedding planes are rippled. A series of fining upward sequences have been observed. The lithofacies schemes present in this section are *Ss* and *Fl* (Figure 4.3a).

4.5.6 VPS 6 Piphema Village (N25° 46' 14.0'' E 93° 56' 08.4'')

This lithocolumn (42 metres) has been measured above Anghya Hotel at Piphema towards the right of road enroute Dimapur. The rocks exposed belong to the Jenam Formation. Sandstone beds vary in colour from grey to brown in this area. Fine grained sediments are dark grey to black in colour. Fine to medium grained sandstones with laminated shales occur in alternating bands. The sandstones are thinly bedded. Massive sand beds as well as laminated sandstone beds occur here. Ripple marks have been observed. The lithofacies presented in this lithocolumn are *Ss* and *Fl* (Figure 4.3b).

4.5.7 VPS 7 Pherima Village (N25° 46' 32.65'' E 93° 55' 52.58'')

The rocks in this lithocolumn (9 metres) belong to the Jenam Formation and has been recorded at Pherima village. Sandstones are dark grey to grey colour while the siltstone and shale appear to be darker than sandstone. The sandstones in this area are medium to coarse grained; compact, massive and laminated sandstone variety also occurs. Siltstone and shale are plane laminated. Thin sandstone beds occur within siltstone and shale beds. The outcrop is highly weathered and show convolute weathering pattern. This vertical profile section is represented by the lithofacies *Fl* and *Sch* (Figure 4.3c).

4.5.8 VPS 8 Piphema Village (N25° 45' 52.98'' E 93° 56' 31.96'')

This VPS (14 metres) was measured at Piphema village where it exposes vertical beds of Renji sandstones. Sandstone appear dark grey to dark brown with a reddish hue. Ferruginous sandstones are the trademark of this exposure. The rocks are hard and compact, medium grained to coarse grained sandstones. Alternations of sandstone and shale beds is common here. Shale are laminated and occurs as intercalations within coarse sand beds. Coal streaks also occur frequently within shale beds and taper out. Bedding contact is curved. Ripple marks are abundant in both coarse and fine material. This VPS represents the lithofacies *Sw* and *Sl* (Figure 4.4a).

4.5.9 VPS 9 Piphema Village (N25° 45' 57.80'' E 93° 56' 29.60'')

This VPS (26 metres) presents the same lithological characters as the preceding one since both have been measured at very close intervals. The lithofacies present are *Sw* and *Sl* (Figure 4.4b).

4.5.10 VPS 10 Tsiepama Village (N25° 45' '50.0' E 93° 56' 46.7'')

The vertical profile section (32 metres) was constructed at Tsiepama village exposing the Renji Formation. The sandstones are medium grained to coarse grained, greyish in colour and bioturbated. Massive sandstones as well as laminated sandstone beds are encountered in this profile section. Trace fossils and low crested ripple marks have been observed as well.

Coal is also found to occur within sand beds. A series of coarsening upward sequences have been observed. *Sw* and *Sl* are the facies present (Figure 4.4c).

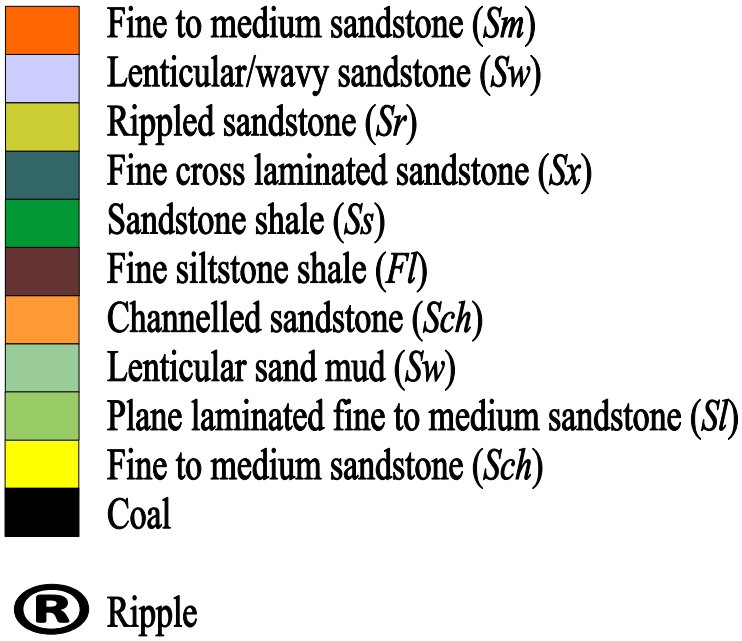

Figure 4.1: Colour index for various Lithofacies used in VPS

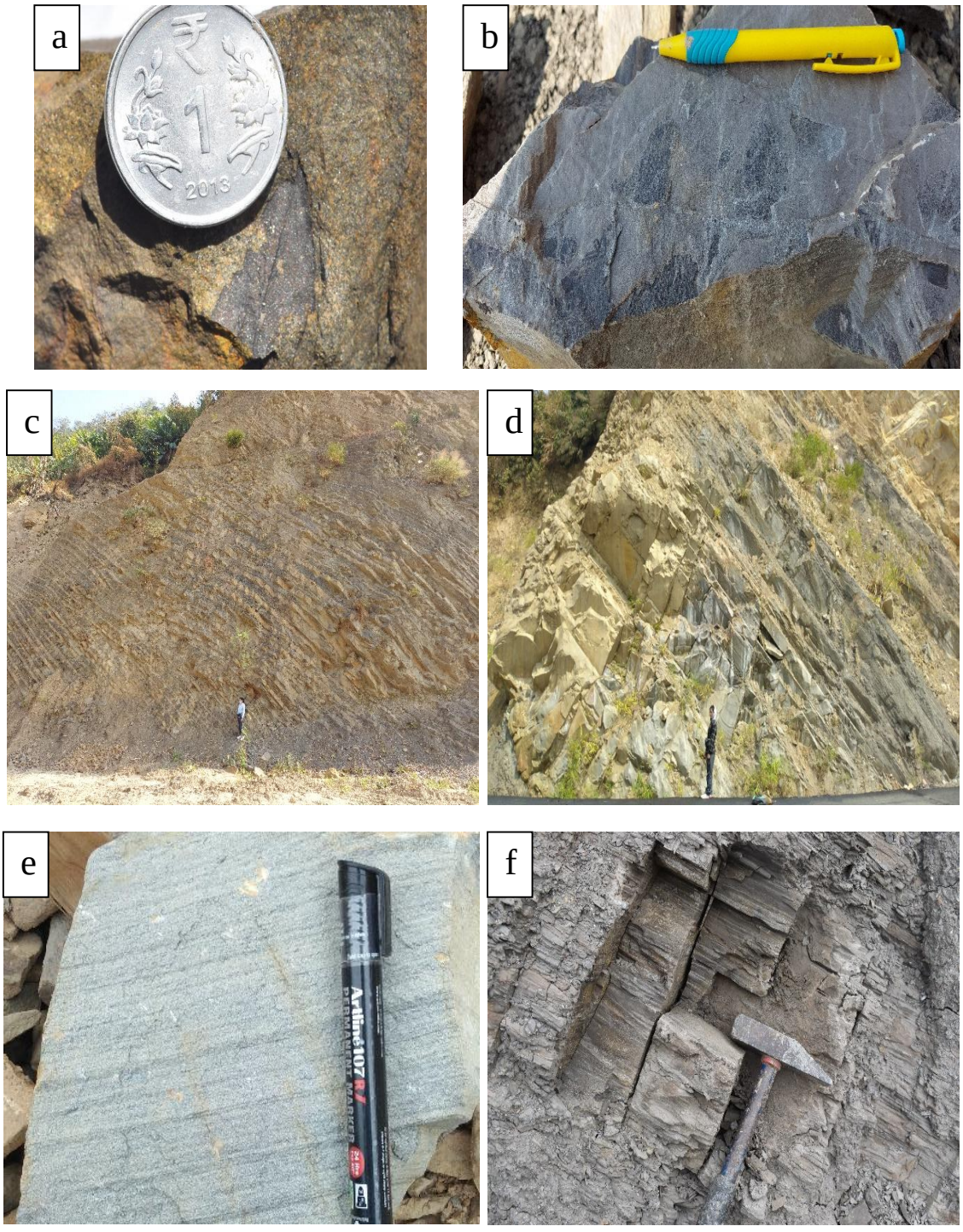

Plate 4.1: Field photographs showing a) leaf imprint (J); b) carbonized plant material (J); c) thinly bedded sandstone (J); d) thickly bedded sandstone (L); e) and f) planar laminations

*L for Laisong Formation; J for Jenam Formation; R for Renji Formation

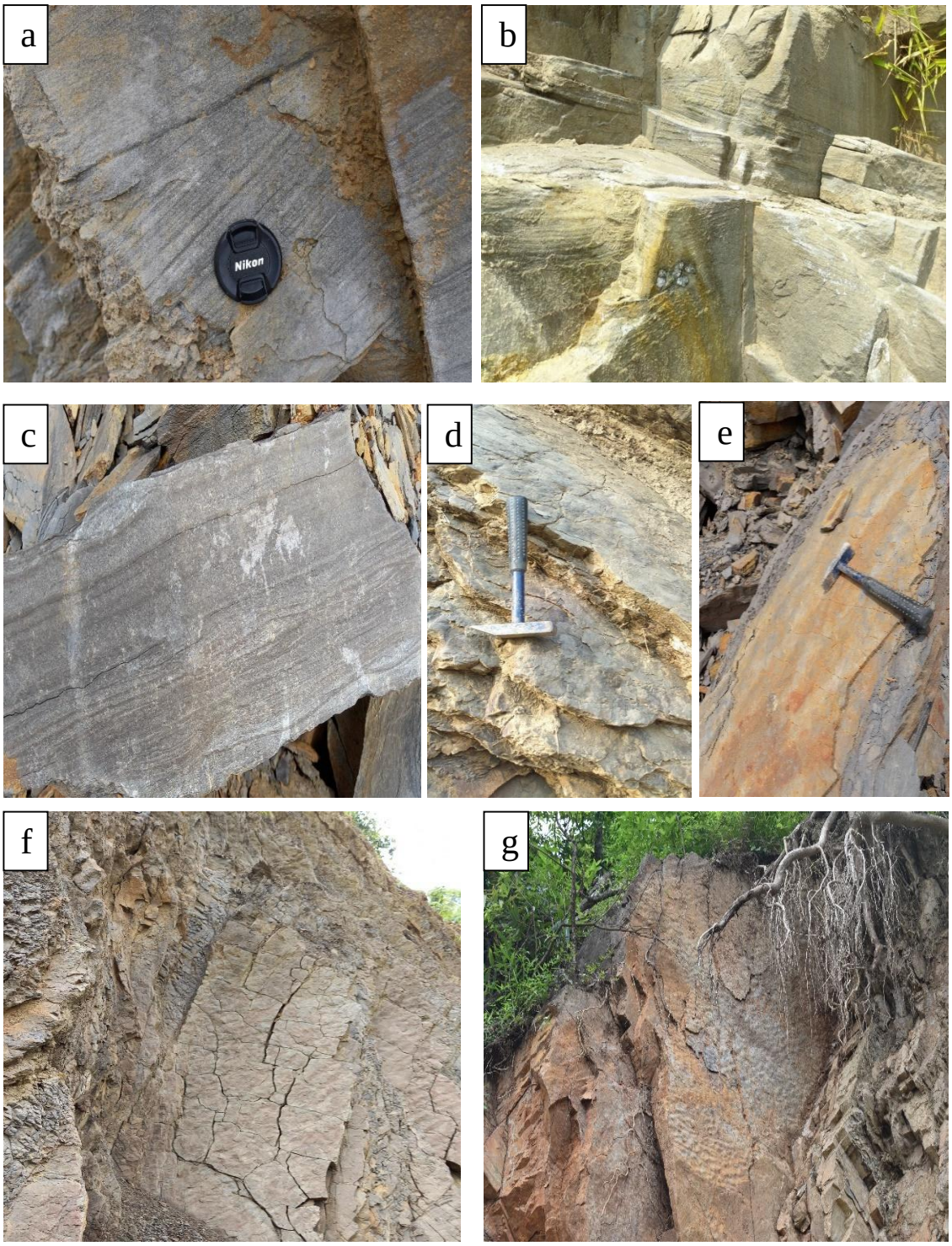

Plate 4.2: Field photographs showing a), b) and c) cross stratification; d) and e) asymmetrical ripples (L); f) asymmetrical ripples (J); g) asymmetrical ripples (R)

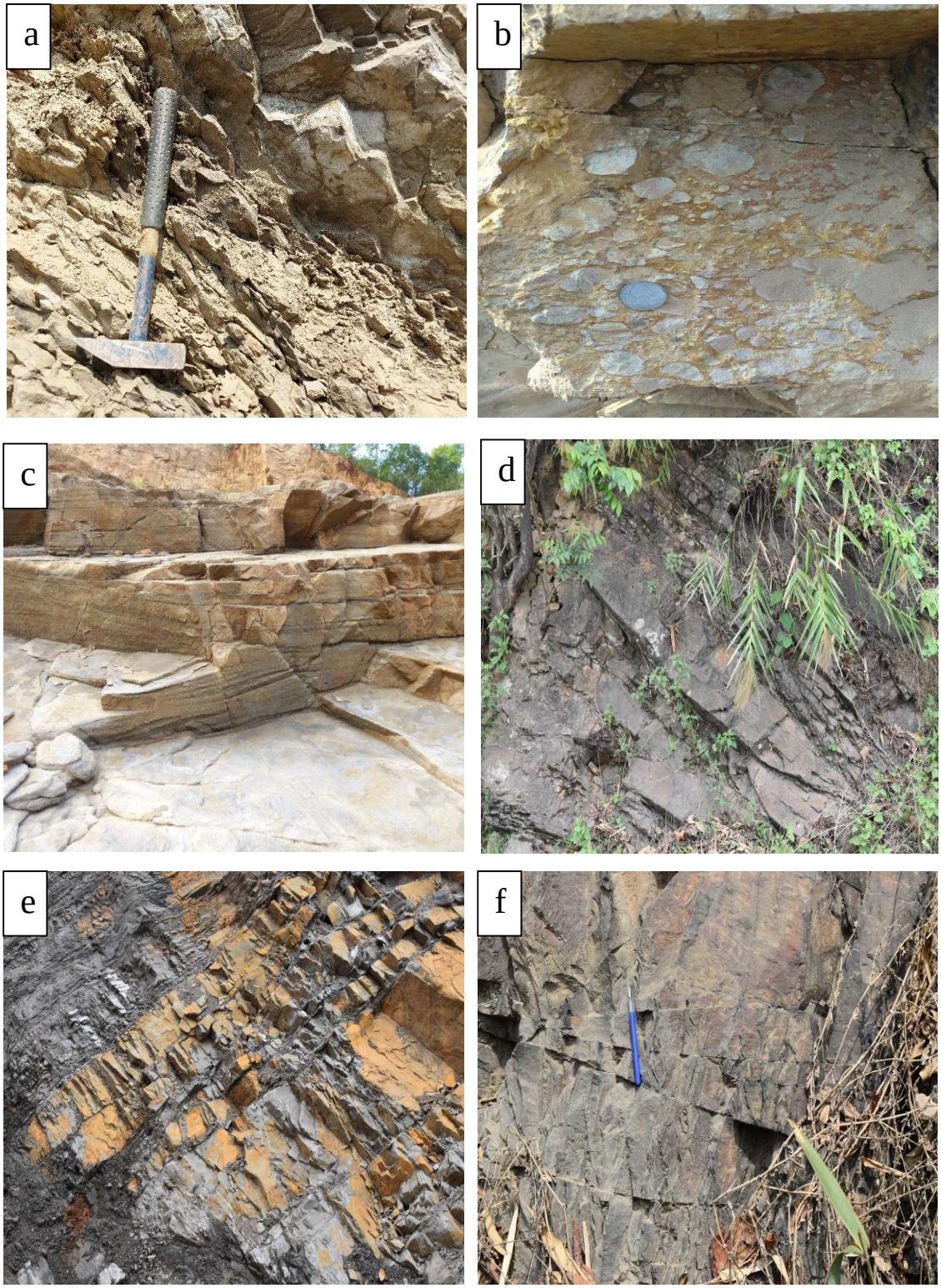

Plate 4.3: Field photographs showing a) load casts (L); b) intraclasts (L); c) channels (L), d) (R), e) (J) and f) (R)

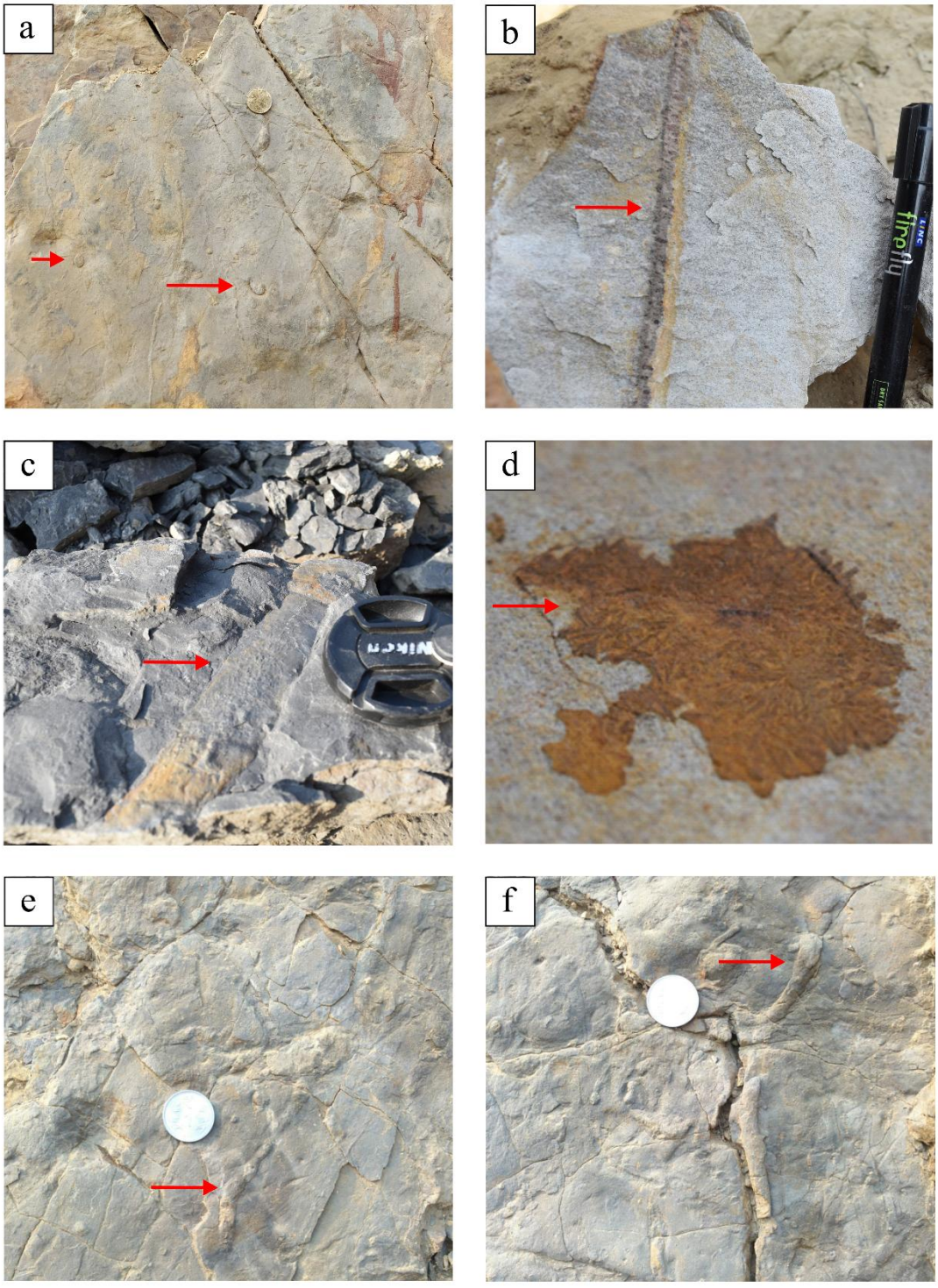

Plate 4.4: Field photographs showing trace fossils a) and b) *Skolithos verticalis* (L); c) *Ophiormorpha nodosa* (L); d) *Chondrites* isp (L); e) and f) *Thalassinoides horizontalis* (J)

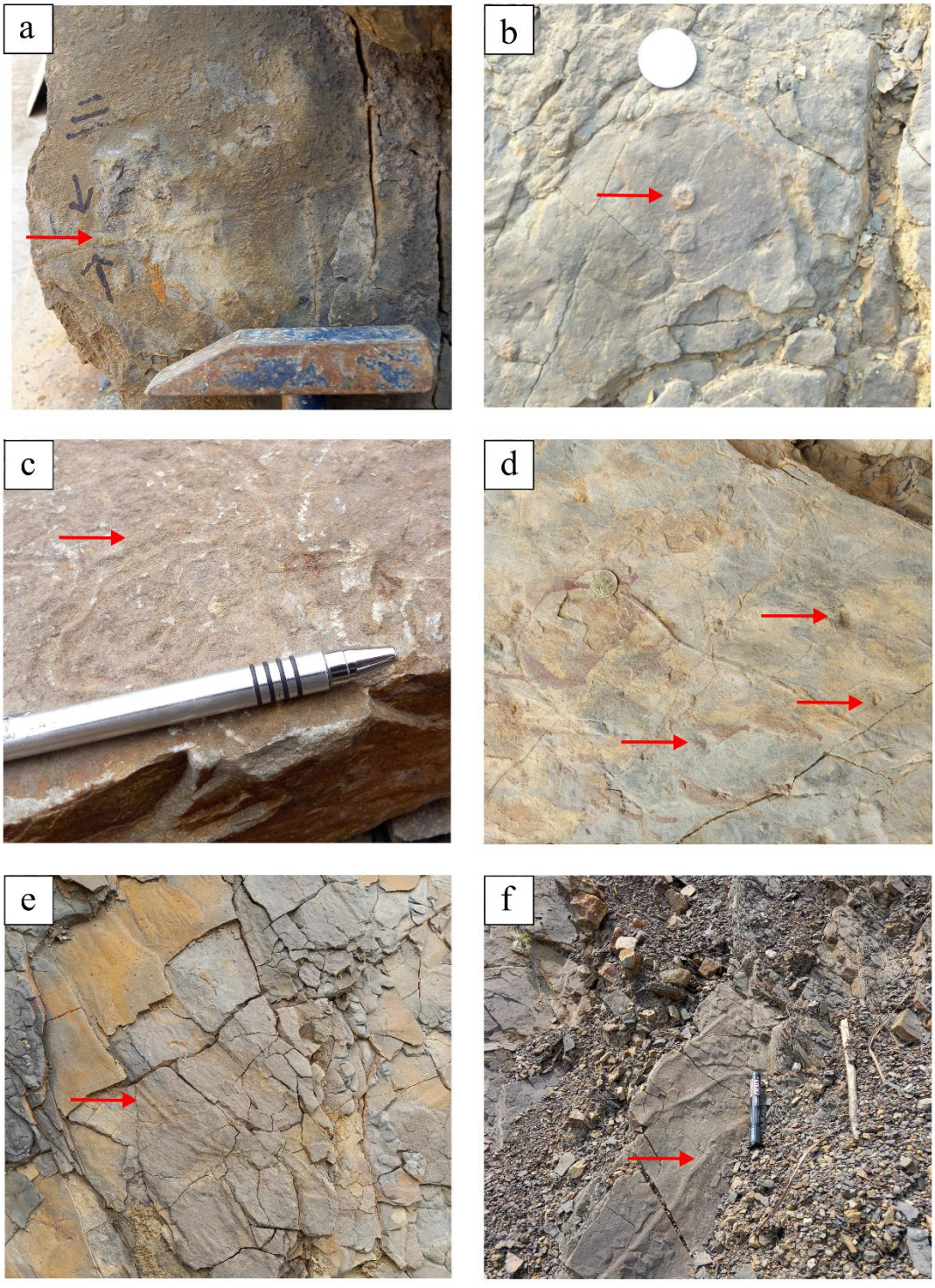

Plate 4.5: Field photographs showing trace fossil a) *Planolites beverleyensis* (J)*;* b) *Laevicyclus* isp (J); c) *Nerites* isp (J); d) *Monocraterion* isp (J); e) *Scolicia Prisca* (J); f) *Palaeophycus striatus* (R)

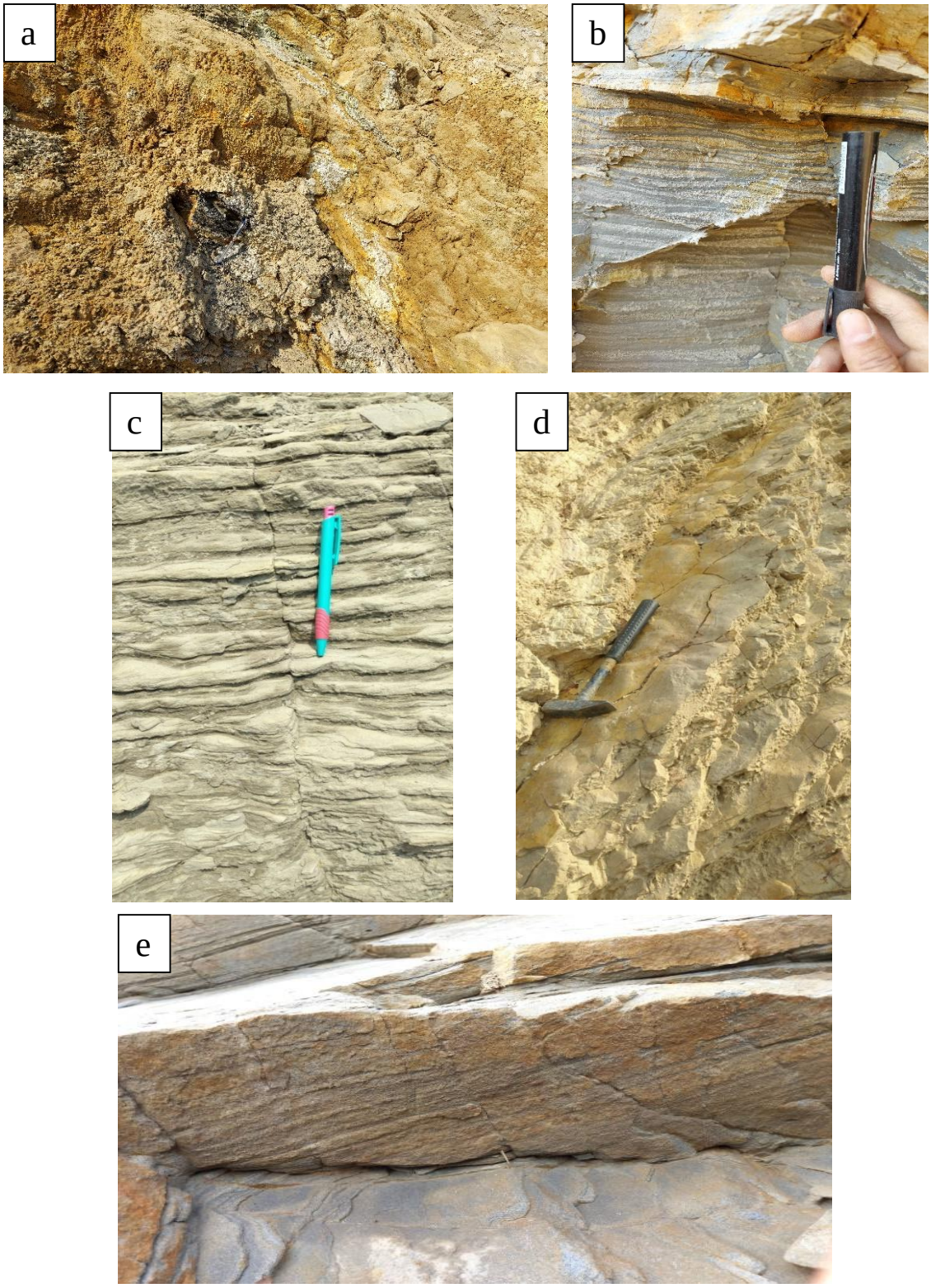

Plate 4.6: Field photographs showing different facies in Laisong Formation a) Fine to medium massive sandstone facies (*Sm*); b) and c) Lenticular/wavy sandstone facies (*Sw*); d) Rippled sandstone facies (*Sr*); e) Fine cross laminated sandstone facies (*Sx*)

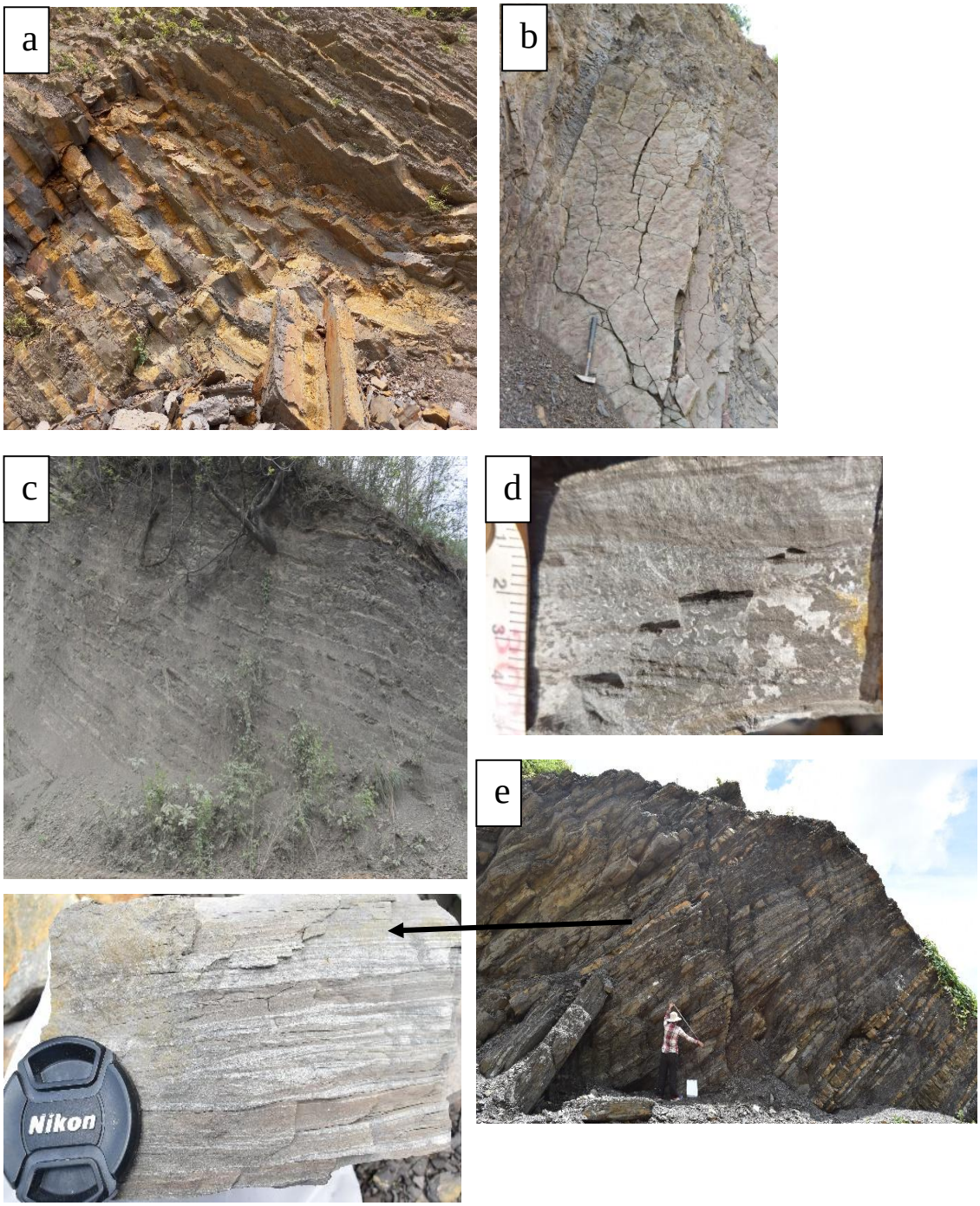

Plate 4.7: Field photographs showing different facies in Jenam Formation a) and b) Sandstone-shale facies (*Ss*); c) Fine siltstone-shale facies (*Fl*); d) and e) Channelled sandstone facies (*Sch*)

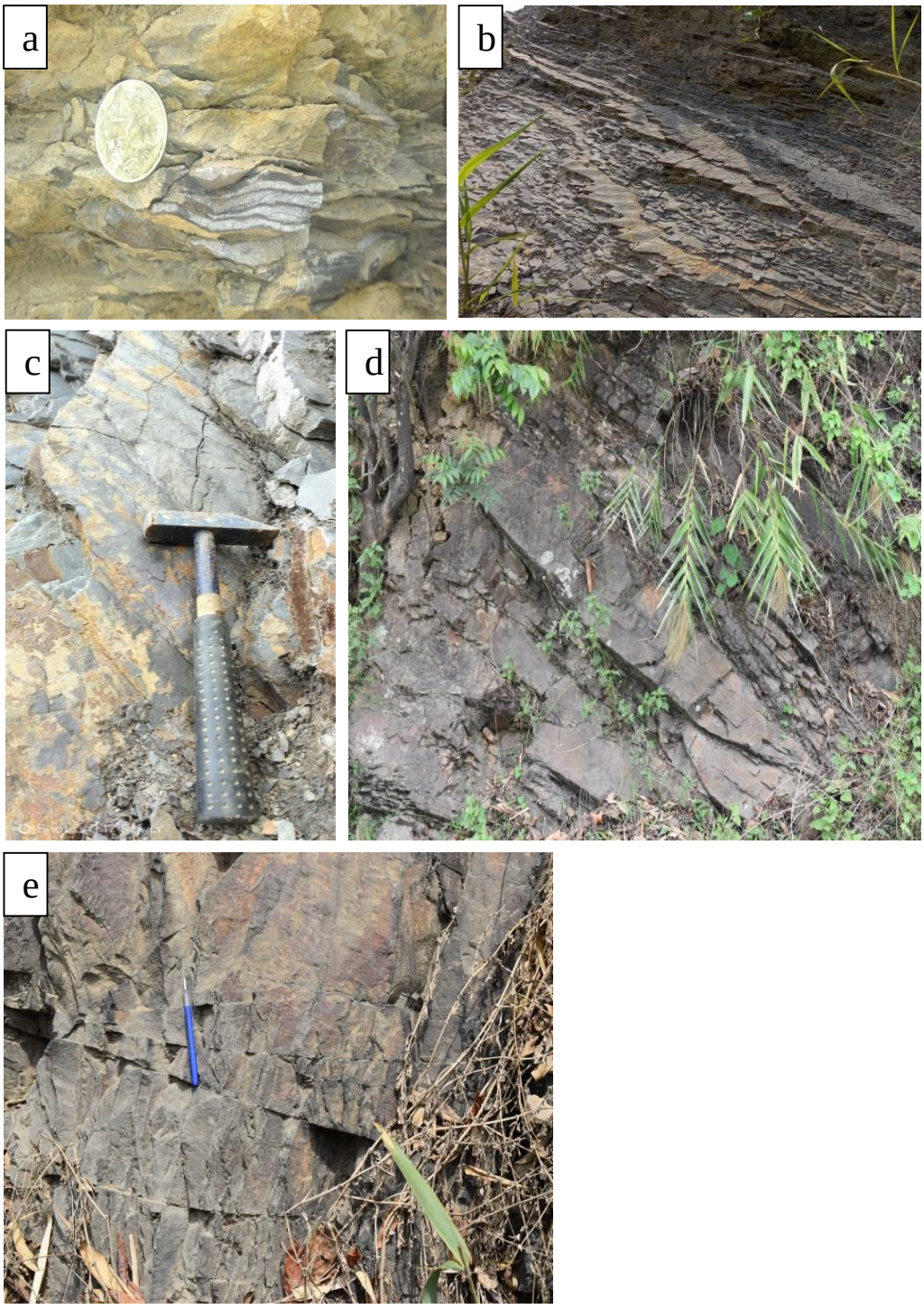

Plate 4.8: Field photographs showing different facies in Renji Formation a) Lenticular sand-mud facies (*Sw*); b) and c) Plane laminated fine to medium sandstone facies (*Sl*); d) and e) Fine to medium sandstone facies *(Sch)*

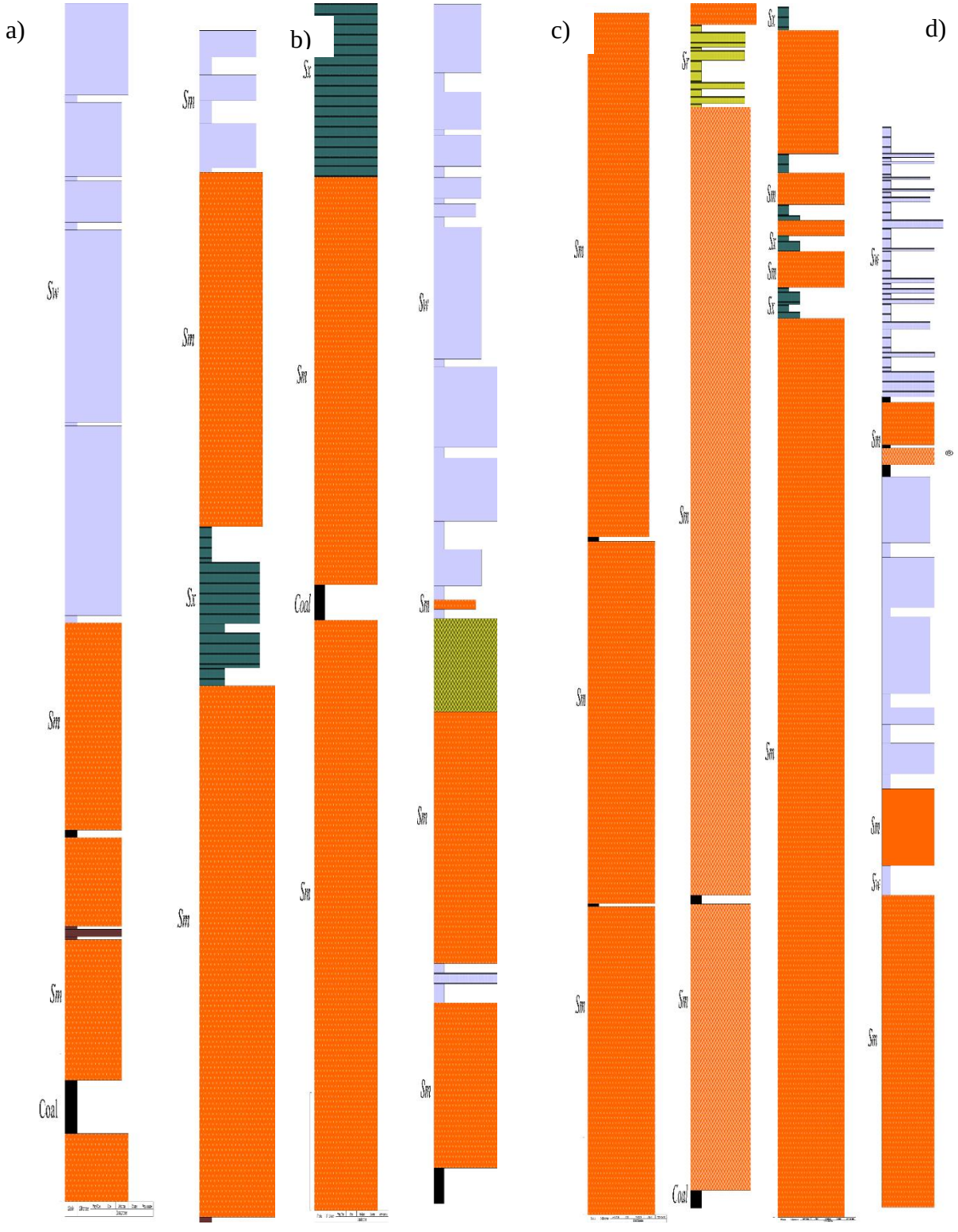

Figure 4.2: Vertical Profile Sections of Laisong Formation a) VPS 1; b) VPS 2; c) VPS 3; d) VPS 4

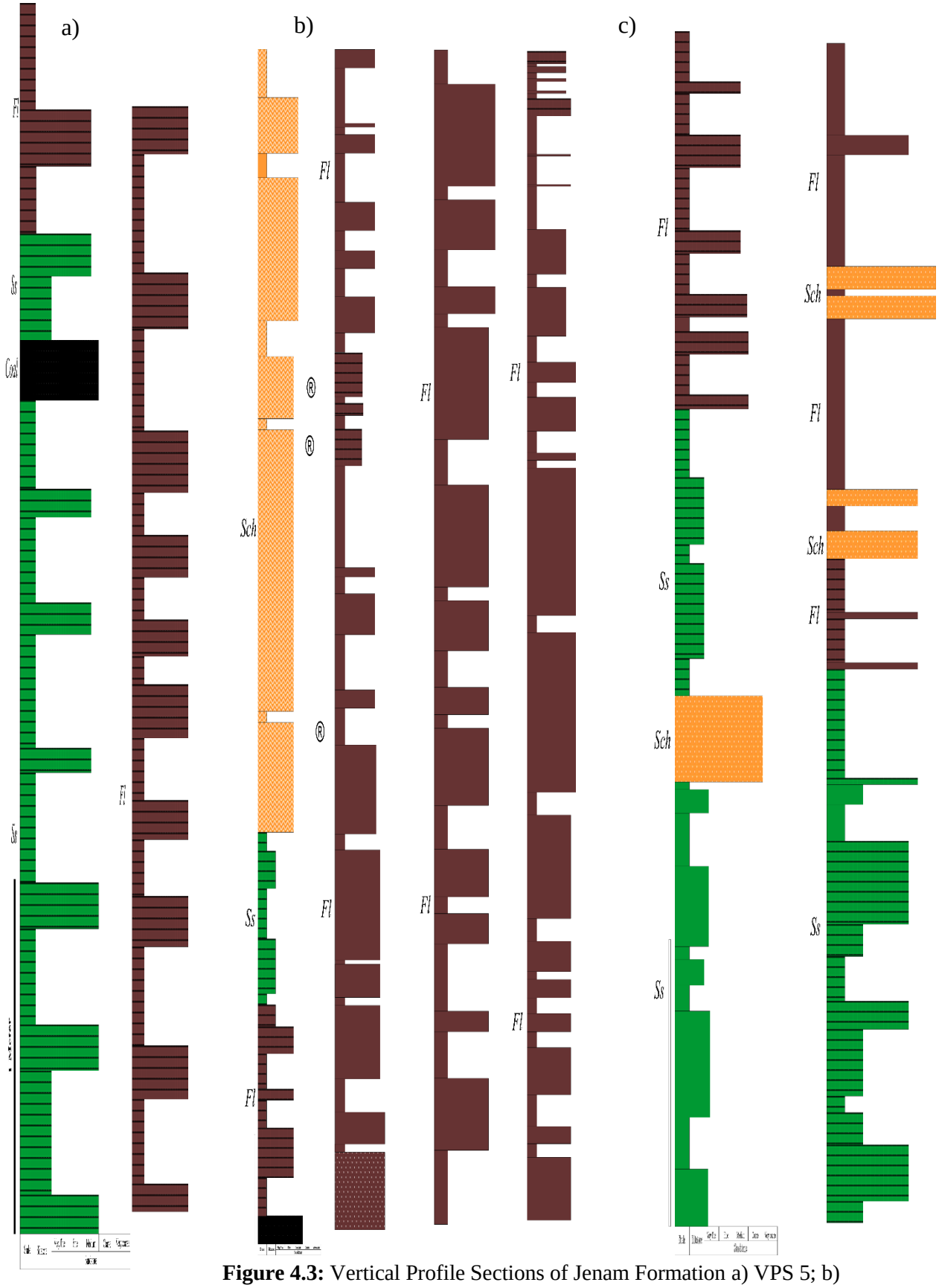

Figure 4.3: Vertical Profile Sections of Jenam Formation a) VPS 5; b) VPS 6; c) VPS 7

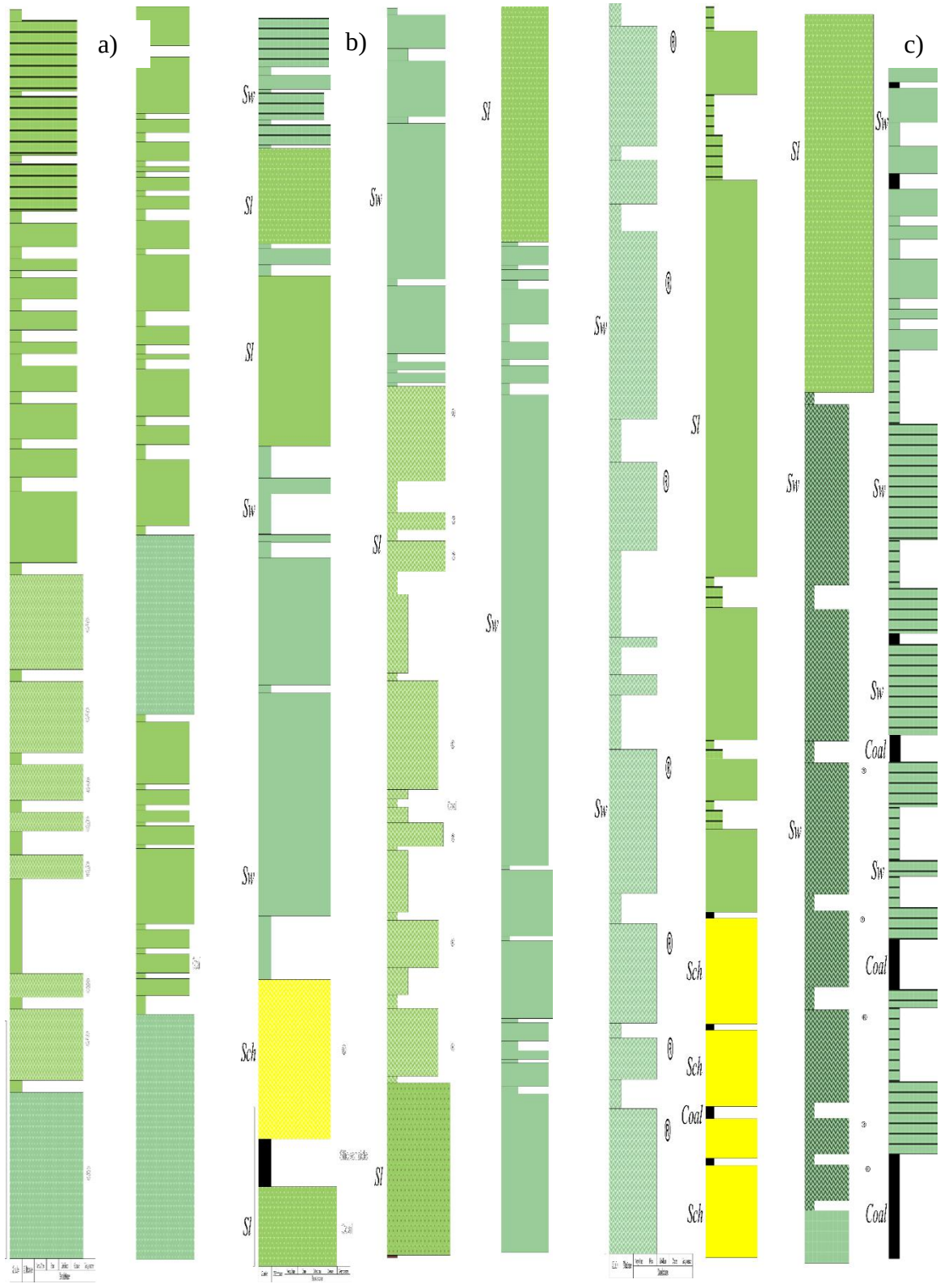

Figure 4.4: Vertical Profile Sections of Renji Formation a) VPS 8; b) VPS 9; c) VPS 10

CHAPTER 5
GRAIN SIZE ANALYSIS

5.1 GRAIN SIZE

Grain size is a fundamental attribute of siliciclastics rocks and thus one of the important descriptive properties of such rocks. The grain size of the clastic sediments is a measure of the energy condition of the depositional environment as well as the depositing medium. Folk and Ward (1957) and Sahu (1964) were some of the early workers who contributed towards determination of the depositional environments using various grain size parameters and discriminant functions. Sedimentologists are particularly concerned with three aspects of particle size (1) techniques for measuring grain size (grade scale), (2) methods for summarising large amounts of grain size data and presenting them in graphical or statistical form for easy evaluation, and (3) the genetic (e.g. environmental) significance of these data (Boggs Jr., 2012).

Grain size attributes in environmental analysis has been attempted by many workers like Wentworth (1922), Krumbein and Pettijohn (1938), Folk (1966), Friedman (1967), Visher (1969), Sengupta (1982), and McLennan *et al*., (1993). Debate still exists among the sedimentologists regarding the effectiveness of various techniques available for classifying and discriminating the sedimentary environment through grain size attributes.

In the present study, thin section technique of grain size analysis has been employed to reconstruct the depositional environment of the Barail sediments. The grain size measurement of twenty one (21) representative sandstone samples of the Barail Group of rocks was carried out with the help of Leica microscope at the Department of Geology, Nagaland University, Kohima Campus, Meriema. More than 200 grains in each of the thin section were measured. Grain size values thus obtained were grouped into half phi (Ø) intervals and were used in plotting cumulative curves on arithmetic probability paper.

5.2 GRAIN SIZE STATISTICS

The cumulative curve is one of the simplest but most useful of the grain size plots. The shape of the log probability curve reflects conditions of the sediment transport process and thus can be used as a tool in environment interpretation. Comparative studies of different cumulative curves were carried out in order to understand the transport mechanism and probable depositional environments following Visher's (1969) method. Phi-values (Ø) for different percentiles were read from the cumulative curves and presented in Table 5.1.

5.2.1 UNIVARIATE GRAIN SIZE PARAMETERS

Folk and Ward's (1957) formulae later modified by Friedman and Sanders (1978), was used to calculate the statistical measures of grain size distribution. The grain size

statistical parameters median, mean, standard deviation, skewness and kurtosis were used to represent grain size characteristics of the Barail sandstones. The grain size distribution and descriptive statistical measures of the samples have been shown in Table 5.2.

i. **Median (Md):** Median or Ø50 represents the middle of the population (s) (i.e. half the percentiles are finer and half coarser than Ø50).

ii. **Mode:** The mode corresponds to maximum frequency and can be read directly from size frequency distribution, it corresponds to the diameter of grains represented by the steepest point on a cumulative curve or the highest point on a frequency curve.

Other statistical parameters were determined using the following formulae:

i. **Graphic mean (M_z)**

$$M_z = \frac{Ø16 + Ø50 + Ø84}{3}$$

ii. **Inclusive Graphic Standard Deviation (σ_I)**

$$\sigma_I = \frac{Ø84 - Ø16}{4} + \frac{Ø95 - Ø5}{6.6}$$

Verbal Classification:

σ_I under Ø0.35	very well sorted
0.35 to Ø0.50	well sorted
0.50 to Ø0.71	moderately well sorted
0.71 to Ø1.00	moderately sorted
2.00 to Ø5.00	very poorly sorted
Over Ø5.00	extremely poorly sorted

iii. **Simple Sorting Measures (SO_S)**

$$SO_S = Ø95 - Ø5$$

iv. **Simple Skewness Measures (σ_S)**

$$1\sigma s = (Ø95 + Ø5) - 2\,Ø50$$

v. **Inclusive Graphic Skewness (SK_I)**

$$SK_I = \frac{(Ø84 + Ø16) - 2\,Ø50}{2(Ø84 - Ø16)} + \frac{(Ø95 + Ø5) - 2\,Ø50}{2(Ø95 - Ø5)}$$

Verbal Classification

SK_I from +1.00 to + 0.30	strongly define- skewed
+0.30 to +0.10	define- skewed
+0.10 to -0.10	near symmetrical
$SK_I = 0.00$	symmetrical
SK_I -0.10 to -0.30	coarse- skewed
-0.30 to -1.00	strongly coarse skewed

viii. Graphic Kurtosis (K_G)

Verbal Classification

$$K_G = \frac{Ø95 - Ø5}{2.44\ (Ø75 - Ø25)}$$

K_G under 0.67	very platykurtic
0.67 to 0.90	platykurtic
0.90 to 1.11	mesokurtic
1.12 to 1.50	leptokurtic
1.51 to 3.00	very leptokurtic
Over 3.00	extremely leptokurtic

The normal Phi-curve has a Kurtosis of 1.00.

5.2.2 (a) Mean Grain Size (M_z)

Graphic mean or mean grain size reflects the average grain size of sediments and thus relates to hydraulic conditions of the depositional environment. It is represented by Ø mean size and denotes the index of energy conditions (Passega, 1964). Average M_z value of the studied sediments lies at 2.89 Ø.

(b) Standard Deviation (σ_I)

Standard deviation is the mathematical expression for sorting in sediments. The inclusive graphic standard deviation measures the sorting of the grain size distribution. It also reflects the hydrodynamic energy conditions of the depositional environment (Sahu, 1964). The average sorting value for the Barail sediments is 0.60 showing moderately well sorted sediments.

(c) Skewness (SK_I)

The graphic skewness reflects the deviation of mean from the median or the degree of asymmetry of the grain size distribution. Majority of the samples of Barail Group are near symmetrical.

(d) Kurtosis (K_G)

It measures the degree of peakedness of the grain size distribution with respect to normal probability curve. The samples are mostly mesokurtic, with a few leptokurtic peakedness. The range varies from 0.00 near symmetrical to -0.13 coarse skewed.

5.2.3 BIVARIATE GRAIN SIZE PARAMETERS

In the present investigation, bivariate plots used include Graphic Mean versus Inclusive Graphic Skewness, Simple Skewness measures versus Simple Sorting measures, Inclusive graphic standard deviation versus Inclusive graphic kurtosis. The values used in this exercise correspond to the sieve equivalents.

(a) Graphic Mean (M_z) Vs Graphic Skewness (SK_I)

This plot is used in discriminating river, wave and slack water processes (Stewert, 1958), besides differentiating inland and coastal dune sands (Moiola and Weiser, 1968) and beach and dune sands (Friedman, 1967; Moiola and Weiser, 1968). The scatter plot indicates that the deposition of Barail sediments was influenced mainly by wave processes. The Friedman (1967) and Moiola and Weiser's (1968) plots reflect that the samples also have the imprint of a beach complex (Figure 5.1).

(b) Graphic Standard Deviation (σ_I) Vs Graphic Kurtosis (K_G)

The plot of Inclusive Graphic Standard Deviation (σ_I) versus Inclusive Graphic Kurtosis (K_G) is used to understand the degree of sorting in the sediments. Almost all the plot points fall within moderately well sorted sediments with a few well sorted and moderately well sorted sediments (Figure 5.2).

(c) C-M Diagram

Many attempts of utilizing grain size statistical parameters to interpret different depositional environments have been made (Folk and Ward, 1957; Mason and Folk, 1958; Harris, 1958; Friedman, 1961, 1962, 1967; Sahu, 1964; Chappel, 1967). However, the reliability of such techniques remains questionable. Passega (1957, 1964) obtained the C-M diagram to reflect the processes of sediment deposition where C represents coarsest grain diameter and M is the median grain diameter. By plotting M (the median or 50th percentile particle diameter in microns) against C (1 percentile, approximate value of maximum grain size in microns) on a log-log paper, the samples from a given environment will fall within a specific environment field in these diagrams. The position of the scatter points depends on the mode of deposition of the sediments.

In the present case, the C-M diagram or pattern for the Barail sediments corresponds to generally Class V and VI suggesting that the sediments have been deposited by both graded and uniform suspension with some sediment transported as bed load. The C-M diagram or pattern for the Barail sediments is shown in Figure 5.3. A depth of approximately very shallow 60/70 meters has been interpreted from the C-M plot.

(d) Cumulative Curve Analysis

Many workers have related log normal distributions to specific sediment transport mechanism during the depositional history of the sediments i.e. the coarsest sub-population represents the bed load or surface creep mechanism of transportation and the finest represents the suspension, the intermediate size being the saltation sub-population (Visher, 1970; Moss, 1972; Middleton, 1976; Sagoe and Visher, 1977). However, interpretation of cumulative curves must be made with caution with respect to minimum number of grain measure, loss of finer grain size due to diagenetic changes and sampling error (Tanner, 1964; Middleton, 1976; James and Oaks, 1977; Walton *et al*., 1980).

In the present investigation, cumulative curves for twenty one (21) samples have been plotted for understanding the depositional history of Barail sediments (Figures 5.4, 5.5 and 5.6). Sediments in the study area appear to have been transported under graded suspension mechanism with little influence of uniform suspension and rolling.

(e) Linear Discriminant Functions

Sahu (1964) established four discriminant functions based on graphical parameters to distinguish between various depositional environments. Following are the four empirically established discriminant functions of Sahu (1964) employed in the present investigation to differentiate sediments from eolian, beach, shallow agitated marine, fluvial (deltaic) and turbidite environments.

i. Y_1: Differentiates eolian from beach environment. It is expressed as,

$Y_1 = -3.5688\ M_z + 3.7016\ \sigma_I^2 - 2.0766\ SK_I + 3.1135\ K_G$

If, Y_1 =< -2.7411, it indicates eolian deposition

Y_1 => -2.7411, it indicates beach deposition

ii. Y_2: Differentiates beach from shallow agitated marine environment. It is expressed as,

$Y_2 = 15.6534\ M_z + 67.7091\ \sigma_I^2 - 18.1071\ SK_I + 18.5043\ K_G$

If, $Y_2 < 65.3650$, it indicates beach deposition

$Y_2 > 65.3650$, it indicates shallow agitated marine processes

iii. Y_3: Differentiates shallow agitated marine processes from fluvial (deltaic) deposition. It is expressed as,

$Y_3 = 0.2852\ M_z + 8.7604\ \sigma_I^2 - 5.8932\ SK_I + 0.04821\ K_G$

If, $Y_3 < -7.4190$, it indicates fluvial (deltaic) deposition

$Y_3 > -7.4190$, it indicates shallow agitated marine deposition

iv. Y_4: Differentiates fluvial (deltaic) environment from turbidity current deposition. It is expressed as,

$Y_4 = 0.7215\ M_z + 0.4030\ \sigma_I^2 - 6.7322\ SK_I + 5.2927\ K_G$

If, $Y_4 < 9.8433$, it indicates turbidity current deposition

$Y_4 > 9.8433$, it indicates fluvial (deltaic) deposition

Where M_z = Graphic Mean σ_I^2 = Standard Deviation

SK_I = Inclusive Graphic Skewness K_G = Graphic Kurtosis

Results obtained through these four discriminant functions have been presented in Table 5.3. Y2 and Y3 values suggest that the Barail sediments have been deposited in a shallow marine agitated condition. While Y1 suggests eolian deposition and Y4 shows turbidity current deposition.

Based on the status of the discriminant functions, the Barail sediments have been found to be associated dominantly with shallow agitated marine deposition with minor elements of eolian and to some influence of turbidity currents.

(f) Log-Log Plot

The log-log plot of mean phi deviation (σ_I^2) of all samples versus the ratio of standard deviation of kurtosis (SK_G) to standard deviation of mean size (SM_z) times the standard deviation of variance $S(\sigma_I^2)$ of samples belonging to Barail sediments have also been used after Sahu (1964) for further discrimination among environments (Figure 5.7). The log-log plot of Barail sediments indicates a cluster around shallow marine environment with a few

samples falling in deltaic (fluvial) and beach environments. It is also observed that the sediments were deposited in decreasing energy condition.

(g) Multigroup Discriminant Function Analysis

In the present study, Sahu's (1983) empirically retained discriminating Eigen's vectors V_1 and V_2 have been used. These discriminant functions may be expressed as:

$V_1 = 0.48048\ M_z + 0.62301\ \sigma_I^2 - 0.40602\ SK_I + 0.44413\ K_G$

$V_2 = 0.24523\ M_z - 0.45905\ \sigma_I^2 - 0.15715\ SK_I + 0.83931\ K_G$

Where M_z = Graphic Mean σ_I^2 = Standard Deviation

SK_I = Inclusive Graphic Skewness K_G = Graphic Kurtosis

Values of V_1 and V_2 for different samples of Barail sediments are given in Table 5.4. The bivariate plot of V_1 and V_2 with $V_1 \Lambda V_2 = 75.4^o$, after Sahu (1983) was used suitably for the differentiation of depositional environment of the Barail sediments under study. The plot (Figure 5.8) indicates in general, a shallow marine environment for the deposition of Barail sediments.

5.3 DISCUSSION AND GEOLOGICAL INTERPRETATION

Bivariate and multivariate analyses of the Barail sediments for the discrimination of depositional environments mostly show nearshore-shallow marine environments. However, some of the bivariate plots reflect diversified environments. This may be due to the fact that these plots are restricted to selective depositional environments and also do not take in account the effects of variations in sedimentation processes, grain size, tectonics, climate, and wave energy fluctuations within the depositional environments. Moreover, all the environments are not represented in one plot. It may also be emphasized here that the boundaries separating various environments in those plots are purely subjective or empirical lines of approach.

However, linear discriminant functions and log-log plot of (σ_I^2) versus (SK_G/SM_z). $S(\sigma_I^2)$ of Sahu (1964), the multigroup discrimination and plot of V_1 and V_2 with $V_1 \Lambda V_2 = 75.4°$ after Sahu (1983), the C-M patterns (Passega, 1964), and shapes of cumulative curves are applicable for distinguishing broad aspects of depositional environment of the studied Barail sediments.

On the basis of the above discussion, it may be concluded that the Oligocene Barail sediments of the study area have been deposited in a near shore-shallow marine agitated environment. Skewness values for the studied sediments being <1 also supports the above conclusion (Reineck and Singh, 1980). Many workers (Duane, 1964; Casshyap and Khan, 1982; Mahendar and Banerji, 1989; Chaudhary, 1993; Lakhar and Hazarika, 2000) have suggested that variations in textural parameters can reflect the fluctuating energy regime

during the deposition. Ghosh and Chatarjee (1994) also suggest that the variability of size parameters probably indicate changes in energy conditions, such as water depth and wave intensity. Variations in grain size both laterally and vertically also indicate a fluctuating energy regime within a shallow marine depositional set up (Srivastava and Pandey, 2008).

5.4 TEXTURAL MATURITY

Folk (1951, 1974) suggested a semi quantitative approach for determination of the textural maturity and has expressed textural maturity of the sediments based on clay matrix percentage, sorting and roundness. Both matrix rich (Jenam Formation) and matrix poor (Laisong and Renji Formations) sandstones have been encountered. Considering clay matrix variations from 1.76 to 22.92 percentages, an immature to mature character may be assigned to these sediments. On the basis of the sorting, these sediments have been found to be very well sorted to moderately sorted and hence display submature to mature character. This variation can be attributed to the fluctuating energy regimes, mixing of contrasting sediments through biogenic activities within upper shoreface environment and diagenetic processes.

Table 5.1: Ø values calculated from the cumulative curves of Barail Group of rocks

Sample No	Ø5	Ø16	Ø25	Ø50	Ø75	Ø84	Ø95
L8	0.60	0.98	1.12	1.55	1.92	2.18	2.44
L13	0.71	1.34	1.65	2.22	2.81	3.08	3.80
L15	1.50	1.81	1.98	2.38	2.72	2.91	3.31
L22	0.81	1.32	1.56	1.98	2.40	2.60	3.12
L25	0.14	0.42	0.61	1.02	1.21	1.28	2.18
L26	0.42	0.80	1.02	1.46	1.89	2.21	2.80
L28	1.41	1.83	2.06	2.42	2.79	2.98	3.35
J1	2.55	2.90	3.12	3.48	3.81	5.00	5.69
J2	2.28	2.61	2.82	3.29	3.69	3.89	5.40
J4	2.45	2.79	2.91	3.31	3.70	3.91	5.30
J6	2.62	2.91	3.08	3.39	3.68	3.83	5.09
J11	2.82	3.21	3.39	3.71	5.06	5.30	5.89
J22	2.85	3.19	3.36	3.74	5.12	5.31	5.80
J24	2.46	2.84	3.02	3.39	3.79	3.92	5.48
R6	1.91	2.35	2.58	2.99	3.45	3.71	5.10
R10	2.41	2.89	3.10	3.59	3.99	5.12	5.50
R11	2.98	3.22	3.32	3.59	3.82	3.98	5.43
R12	2.62	3.00	3.18	3.52	3.89	5.09	5.58
R14	2.38	2.71	2.91	3.32	3.79	3.99	5.48
R18	2.40	2.89	3.10	3.41	3.79	3.91	5.48
R20	2.27	2.58	2.71	3.02	3.32	3.49	3.82

Table 5.2: Grain size data and statistical measures of Barail sandstones

Sample No	M_z	σ_I	SK_I	K_G	SO_S	σ_S	σ_I Status	SK_I Status	KG Status
L8	1.57	0.58	0.01	0.94	1.84	-0.06	Moderately well sorted	Near symmetrical	Mesokurtic
L13	2.21	0.90	0.01	1.09	3.09	0.07	Moderately sorted	Near symmetrical	Mesokurtic
L15	2.37	0.55	0.00	1.00	1.81	0.05	Moderately well sorted	Near symmetrical	Mesokurtic
L22	1.97	0.67	-0.02	1.13	2.31	-0.03	Moderately well sorted	Near symmetrical	Leptokurtic
L25	0.91	0.52	-0.13	1.39	2.04	0.28	Moderately well sorted	Near symmetrical	Leptokurtic
L26	1.49	0.71	0.09	1.12	2.38	0.30	Moderately sorted	Define skewed	Leptokurtic
L28	2.41	0.58	-0.03	1.09	1.94	-0.08	Moderately well sorted	Near symmetrical	Mesokurtic
J1	3.46	0.60	0.04	1.27	2.14	0.28	Moderately well sorted	Near symmetrical	Leptokurtic
J2	3.26	0.64	-0.01	1.00	2.12	0.1	Moderately well sorted	Near symmetrical	Mesokurtic
J4	3.34	0.56	0.07	0.96	1.85	0.13	Moderately well sorted	Near symmetrical	Mesokurtic
J6	3.38	0.45	-0.05	1.00	1.47	-0.07	Well sorted	Near symmetrical	Mesokurtic
J11	3.74	0.59	0.11	1.27	2.07	0.29	Moderately well sorted	Define skewed	Leptokurtic

J22	3.75	0.58	0.05	1.05	1.95	0.17	Moderately well sorted	Near symmetrical	Mesokurtic
J24	3.38	0.58	0.03	1.08	2.02	0.16	Moderately well sorted	Near symmetrical	Mesokurtic
R6	3.02	0.67	0.04	1.03	2.19	0.03	Moderately well sorted	Near symmetrical	Mesokurtic
R10	3.53	0.62	-0.13	0.96	2.09	-0.27	Moderately well sorted	Coarse skewed	Mesokurtic
R11	3.60	0.41	0.09	1.19	1.45	0.23	Well sorted	Near symmetrical	Leptokurtic
R12	3.54	0.57	0.06	1.13	1.96	0.16	Moderately well sorted	Near symmetrical	Leptokurtic
R14	3.34	0.64	0.08	0.98	2.10	0.22	Moderately well sorted	Near symmetrical	Mesokurtic
R18	3.40	0.57	0.00	1.24	2.08	0.06	Moderately well sorted	Near symmetrical	Leptokurtic
R20	3.03	0.46	0.03	1.04	1.55	0.05	Well sorted	Near symmetrical	Mesokurtic

Table 5.3: The four discriminant functions of Barail sediments (after Sahu, 1964)

Sample No.	Y1	Y1 Status	Y2	Y2 Status	Y3	Y3 Status	Y4	Y4 Status
L8	-1.45	Beach deposition	64.54	Beach deposition	3.39	Shallow agitated marine deposition	6.20	Turbidity current deposition
L13	-1.49	Beach deposition	109.98	Shallow agitated marine processes	7.80	Shallow agitated marine deposition	7.67	Turbidity current deposition
L15	-4.20	Eolian deposition	76.10	Shallow agitated marine processes	3.39	Shallow agitated marine deposition	7.16	Turbidity current deposition
L22	-1.80	Beach deposition	82.44	Shallow agitated marine processes	4.66	Shallow agitated marine deposition	7.71	Turbidity current deposition
L25	2.39	Beach deposition	60.91	Beach deposition	3.36	Shallow agitated marine deposition	9.01	Turbidity current deposition
L26	-0.14	Beach deposition	76.78	Shallow agitated marine processes	4.47	Shallow agitated marine deposition	6.57	Turbidity current deposition
L28	-3.89	Eolian deposition	81.38	Shallow agitated marine processes	3.87	Shallow agitated marine deposition	7.87	Turbidity current deposition
J1	-7.14	Eolian deposition	101.30	Shallow agitated marine processes	4.01	Shallow agitated marine deposition	9.11	Turbidity current deposition
J2	-7.00	Eolian deposition	97.54	Shallow agitated marine processes	4.62	Shallow agitated marine deposition	7.86	Turbidity current deposition
J4	-7.90	Eolian deposition	89.96	Shallow agitated marine processes	3.40	Shallow agitated marine deposition	7.14	Turbidity current deposition
J6	-8.07	Eolian deposition	86.14	Shallow agitated marine processes	3.03	Shallow agitated marine deposition	8.14	Turbidity current deposition
J11	-8.36	Eolian deposition	103.22	Shallow agitated marine processes	3.59	Shallow agitated marine deposition	8.79	Turbidity current deposition

J22	-8.98	Eolian deposition	99.58	Shallow agitated marine processes	3.76	Shallow agitated marine deposition	8.05	Turbidity current deposition
J24	-7.56	Eolian deposition	94.78	Shallow agitated marine processes	3.78	Shallow agitated marine deposition	8.06	Turbidity current deposition
R6	-5.96	Eolian deposition	96.21	Shallow agitated marine processes	4.69	Shallow agitated marine deposition	7.57	Turbidity current deposition
R10	-7.89	Eolian deposition	101.92	Shallow agitated marine processes	5.12	Shallow agitated marine deposition	8.70	Turbidity current deposition
R11	-8.71	Eolian deposition	87.98	Shallow agitated marine processes	2.10	Shallow agitated marine deposition	8.33	Turbidity current deposition
R12	-8.03	Eolian deposition	97.10	Shallow agitated marine processes	3.59	Shallow agitated marine deposition	8.24	Turbidity current deposition
R14	-7.52	Eolian deposition	96.58	Shallow agitated marine processes	4.20	Shallow agitated marine deposition	7.24	Turbidity current deposition
R18	-7.11	Eolian deposition	98.06	Shallow agitated marine processes	3.86	Shallow agitated marine deposition	9.09	Turbidity current deposition
R20	-6.85	Eolian deposition	80.58	Shallow agitated marine processes	2.63	Shallow agitated marine deposition	7.56	Turbidity current deposition

Table 5.4: Values of V1 and V2 for different samples of Barail sediments

Sample No	V1	V2
L8	1.38	1.02
L13	2.05	1.08
L15	1.77	1.28
L22	1.73	1.23
L25	1.28	1.29
L26	1.49	1.06
L28	1.87	1.36
J1	2.44	1.74
J2	2.27	1.45
J4	2.20	1.47
J6	2.21	1.58
J11	2.53	1.80
J22	2.45	1.64
J24	2.30	1.57
R6	2.17	1.39
R10	2.42	1.52
R11	2.32	1.79
R12	2.38	1.66
R14	2.26	1.44
R18	2.38	1.72
R20	2.04	1.51

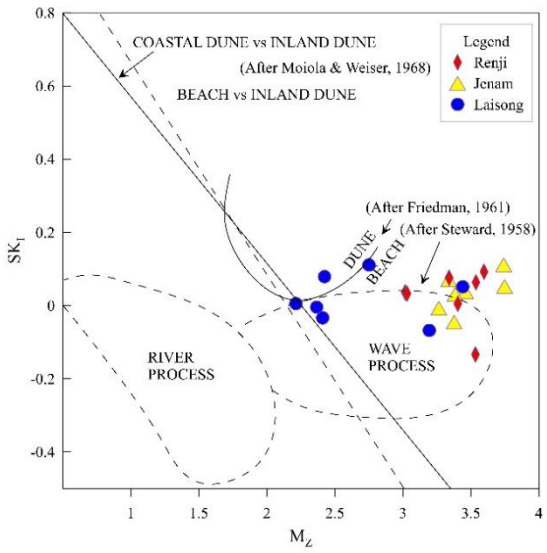

Figure 5.1: Plot of Graphic Mean (Mz) vs Inclusive Graphic Skewness (SK_I)

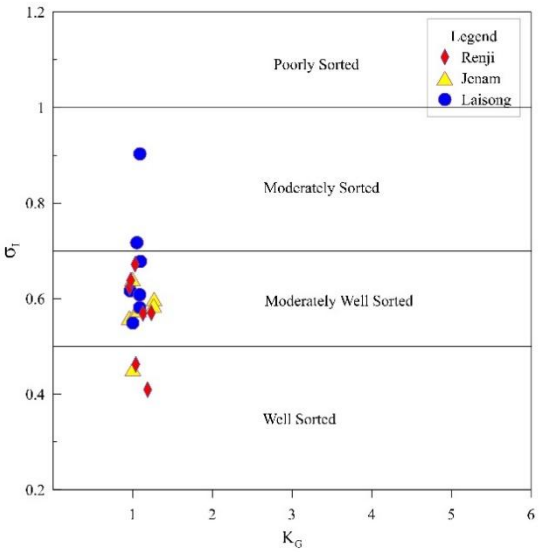

Figure 5.2: Plot of Inclusive Graphic Kurtosis (K_G) vs Inclusive Graphic Standard Deviation (σ_I)

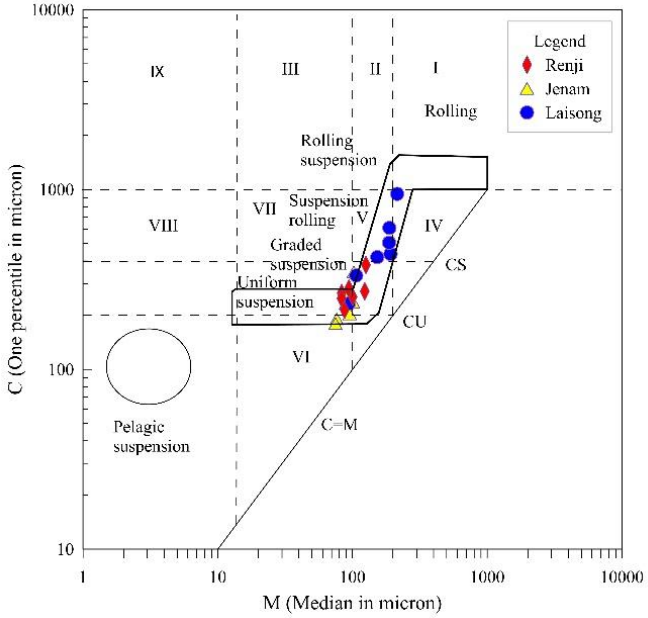

Figure 5.3: C-M diagram or pattern for the Barail sediments (after Passega, 1957)

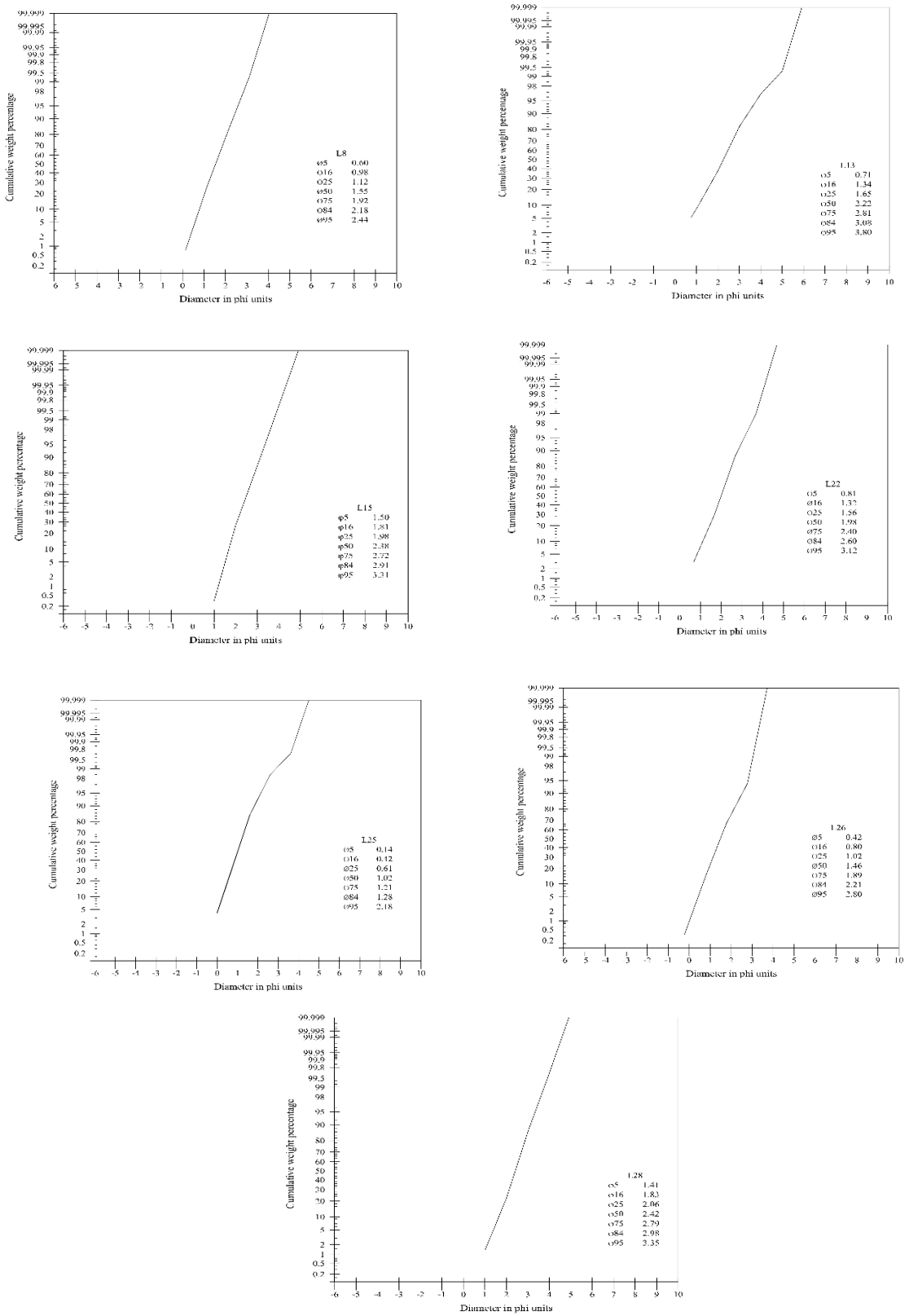

Figure 5.4: Grain size distribution curves of Laisong sandstones

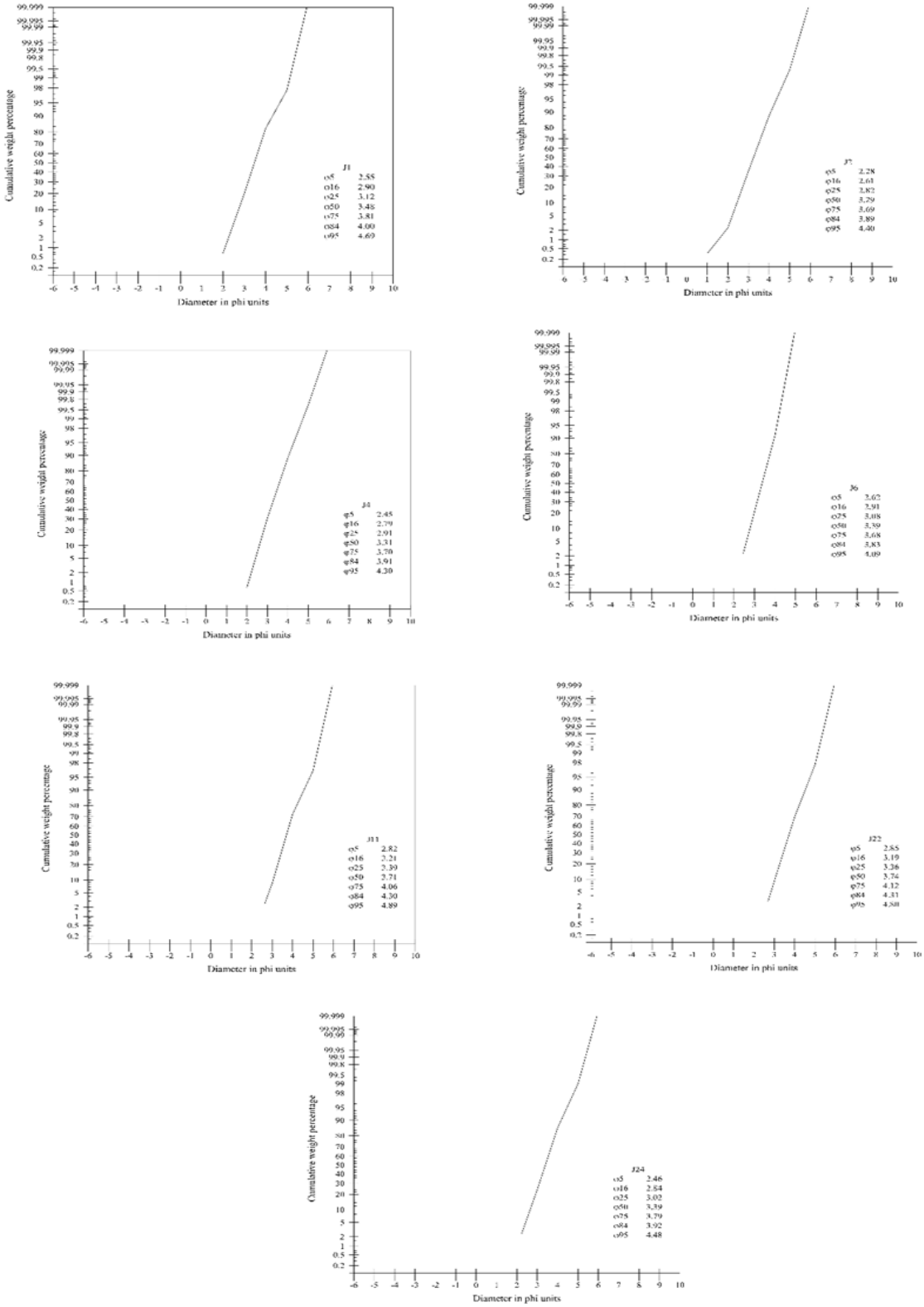

Figure 5.5: Grain size distribution curves of Jenam sandstones

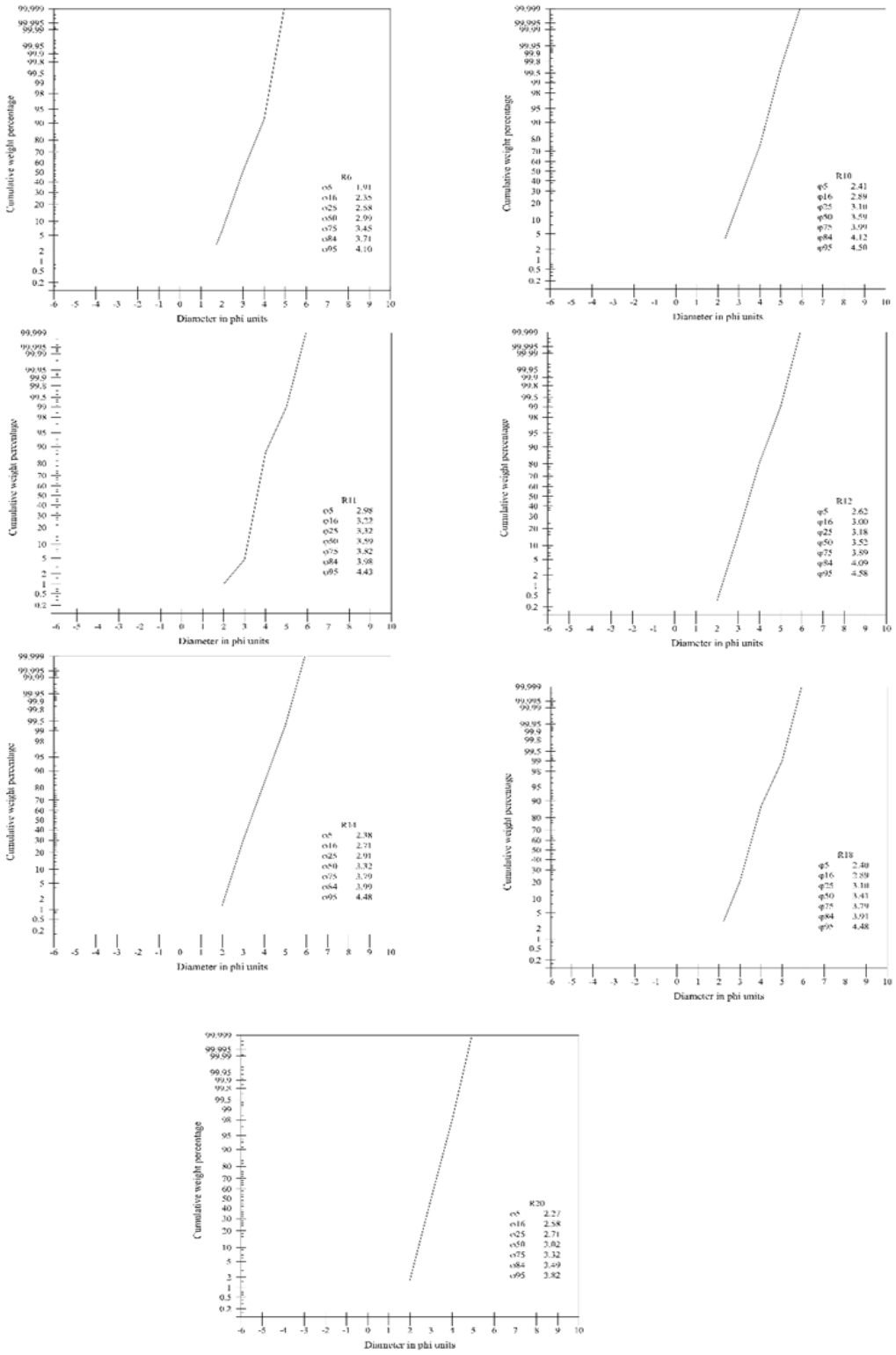

Figure 5.6: Grain size distribution curves of Renji sandstones

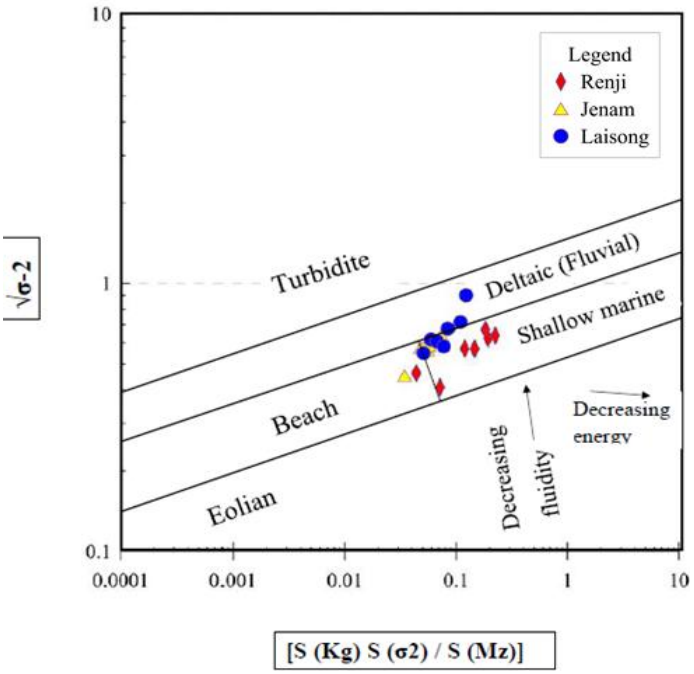

Figure 5.7: Log-log plot of mean phi deviation vs the ratio of standard deviation of kurtosis to standard deviation of mean size times the standard deviation of variance (after Sahu, 1964)

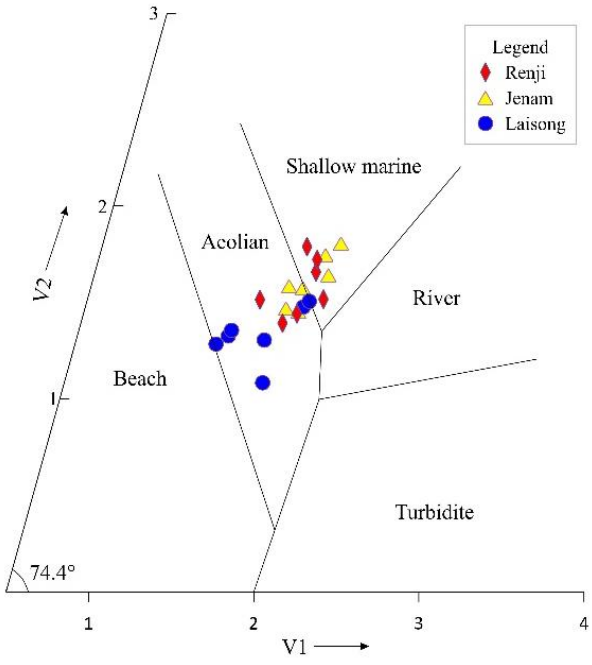

Figure 5.8: Plot of V_1 against V_2 of Barail sediments (after Sahu, 1964)

CHAPTER 6

PETROGRAPHY AND MAJOR OXIDE GEOCHEMISTRY

6.1 GENERAL

One of the most important aspects of petrographic studies of clastic rocks is to correlate the framework compositions to source rock lithology. The detail study of the framework composition help in interpreting the origin of sands and sandstones as the mineralogical composition and textures bear a direct relationship with provenance, transport history, depositional processes and diagenetic modifications of sediments (Suttner, 1974; Pettijohn, 1975). Petrographic composition of sandstone has been used by many workers for deciphering the provenance and tectonic history. Workers such as Dickinson and Rich (1972), Dickinson and Suczek (1979), Dickinson *et al.*, (1983), and Miall (1990) have correlated detrital composition of clastic rocks with the rate of source area uplift and basin subsidence. The appearance of a particular mineral suit in a stratigraphic succession has been used by many (Uddin and Lundberg, 1998 a and b; Singh *et al.*, 2004; Srivastava *et al*., 2004; Mishra and Tiwari, 2005; Srivastava and Pandey, 2011; Imchen *et al*., 2014; Srivastava and Kichu, 2021; Srivastava *et al*., 2024; Richa and Srivastava, 2024) in understanding the tectonic history responsible for determining the specific petrographic characters of a rock unit. According to Mack (1984), petrographic studies also help in understanding the climatic conditions and the relief of the source besides cementation and the diagenesis which modify the clastic grains. Mack (1984) further suggests that care must be taken while sampling for provenance evaluation on the basis of petrographic observations as locally collected data may give a distorted result.

In the present study petrographic studies on sixty (60) sandstone samples; in thin sections; for the Barail Group of rocks have been performed. Modal Analysis using grain/point counting method has been carried out for forty-five (45) samples, fifteen (15) each from Laisong, Jenam and Renji Formations respectively wherein a minimum of 250 grains have been counted.

To complement the data generated on modal composition, major oxides (thirty samples, XRFS), whole rock and clay fractions XRD (eighteen samples) and SEM-EDX analysis of three samples were also carried out.

6.2 PETROGRAPHY

The Barail sandstones of the study area display variation in colour and grain size. While the sandstones in the Jenam and Renji Formations are hard and compact in nature and range from very fine to medium sand fractions, the Laisong sandstones consists of hard, reddish brown to grey/buff color, medium to coarse grained sandstones with occasional very coarse grained sandstones.

More than 250 grains in each thin section were counted for estimation of framework grains (Table 6.1). As these three formations do not vary in their modal composition, they have been shown together. Recalculated modal composition of different formations can be read as i) Laisong sandstones (Q 76.05%, F 3.13%, RF 5.80%, Mica 3.7%, HM 5.20%, others 6.12%) ii) Jenam sandstones sandstones (Q 65.90%, F 3.51%, RF 4.7%, Mica 5.42%, HM 7.75%, others 12.82%) iii) sandstones (Q 71.48%, F 2.83%, RF 5.10%, Mica 4.76%, HM 5.72%, others 9.26%). The overall average detrital composition of Barail sandstones in the study area can be expressed as Quartz 71.14%, Feldspars 3.16%, Rock Fragments 5.19%, Mica 4.63%, 6.22% Heavies, including both opaque's and non-opaque's; and Cement 3.03%, Matrix 6.66%. Table 6.2 represents the recalculated values of detrital composition.

6.2.1 FRAMEWORK CONSTITUENTS

Quartz

Conolly, (1965) identified three basic quartz types namely, non-undulatory quartz (Figure 6.1a), undulatory quartz (Plate 6.1a, 6.4c) and polycrystalline quartz (Plate 6.1d, 6.2e, 6.3b, 6.4b), which comprise the total quartz population in a clastic rock. Monocrystalline non-undulatory quartz grains (QNU) are generally identified by their complete extinction upon a slight (less than 1°) rotation of microscope stage (Blatt and Christie, 1963), while the monocrystalline undulatory quartz grains (QU) can be distinguished by their wavy extinction. Polycrystalline quartz grains, consisting of 2 to 3 units as well as > 3 units, are generally distinguished from metaquartzite rock fragments by the presence of smooth, non-sutured boundaries between separate units (Boggs Jr., 2009).

Quartz is the most dominant framework constituent of the Barail sandstones. Mono crystalline non-undulatory quartz grain dominates over undulatory quartz in all the studied samples. They are mostly sub-angular to sub-rounded in shape. However, a few well-rounded quartz grains have also been observed (Plate 6.1a, 6.2f, 6.3c). The occurrence of polycrystalline quartz is generally very low in the studied sandstones. Presence of inclusions is a common feature of these sandstones (Plate 6.1a, 6.2a, f, 6.3c). Total quartz content varies from 54.58% to 79.84% in the overall detrital composition. Out of the total quartz content 71.14% (Qt), nearly 96.90% are monocrystalline quartz grains (Qm) while the rest 3.10% (Qp) fall under polycrystalline quartz grains.

Feldspar

Both plagioclase feldspars and K-feldspars (microcline and orthoclase) have been observed. The concentration of feldspar in the studied sandstones is significant and varies from 0.83 % to 7.52% and some of them show albitization effects (Plate 6.1b, 6.2c, d, f, 6.3d, e, 6.4a, c, e). Among the feldspar varieties, the plagioclase feldspar (78.81%) is most common and represented by sodic end member showing characteristic albite twinning. K-feldspar (21.19%) is represented by both orthoclase and microcline. Microcline (Plate 6.1c, d, 6.3c, 6.4d) and orthoclase (Plate 6.1d, 6.2b, 6.3e, 6.4c, f), both altered as well as fresh feldspar grains, were observed; the former being associated with the matrix. Microcline occurs as angular to rounded varieties in all three formations.

At places, precipitations of silica on feldspar grains have also been observed. As feldspars are more susceptible to wear and tear, their low concentration in the sandstone suggests that during surface weathering they gradually alter to clay minerals (Boggs Jr., 2012). The average feldspar to quartz ratio in present sandstones is recorded as 0.04 (average) which is linked to the amount of solution and abrasion during transport (Dickinson *et al*., 1983).

Rock Fragments

The abundance and distribution of rock fragments in the clastic sediments serve as a very important tool in interpreting the provenance of the sediment. Rock fragments are classified as igneous, metamorphic, and sedimentary rock fragments. In the studied sandstones, rock fragments occupy a significant portion of the detrital composition and are next to quartz and are identified by their composition, textural variations and a well-defined grain boundary.

The percentage of rock fragments in the studied samples ranges from 2.61% to 8.13% of the total composition with sedimentary rock fragments dominating amongst the three varieties. Sedimentary rock fragments recorded in the studied sandstones includes chert (Plate 6.3f, 6.4c), siltstones and sandstone fragments (Plate 6.1e, 6.2c, 6.3b, 6.4b). Chert is microcrystalline silica and is a distinct indicator of provenance of sedimentary origin (Sengupta, 1994). Metamorphic rock fragments (Plate 6.1f, 6.3f, 6.4f) is mostly identified as schists. Igneous and volcanic fragments are comparatively less with very sparse distribution in the studied samples (Plate 6.2a).

Mica

Micas have been observed to occur in the form of biotite, muscovite and chlorite with concentrations ranging from 1.95% to 8.17% in the overall modal composition. The highest concentration of mica has been observed in the Jenam Formation. These flaky minerals show

bending and warping features indicative of tectonic compression. (Plate 6.1b, d, 6.2e, 6.3c, d, f, 6.4b).

Cement and Matrix

Cement binds the framework grains of the sedimentary rocks and is described as a non-detrital, homogeneous component of sandstone. They are mostly formed through authigenesis i.e. precipitation within the pore spaces or formed by the dissolution of the grain boundaries. In the present study, silica (Plate 6.2d, 6.4d) and iron cement are the common cementing material. Iron cement (Plate 6.1e) is present in small amount. In addition to silica and iron cements, calcite cements (Plate 6.3b) have also been observed in the sandstones from Jenam Formation. Total cement ranges from 0.00 to 6.42%.

Pettijohn (1984) and Dickinson (1970) classified matrix into four types namely proto matrix (trapped detrital clay), epimatrix (diagenetic product of sand grains), pseudo matrix (deformed and squashed pelitic fragments) and ortho matrix (recrystallized material). Matrix content in the Barail sandstones ranges from 1.76% to 22.92%. Both matrix poor (Laisong and Renji sandstones, Plate 6.1b, c, d, 6.4d) and matrix rich sandstones (Jenam sandstones) have been observed (Plate 6.3a, d).

6.2.2 HEAVY MINERALS

Heavy minerals are defined as those with a specific gravity greater than 2.89 g/cm^3 including both chemically stable and unstable varieties. Illing (1916) was one of the earliest workers to stress on the importance of heavy mineral studies for the exploration of hydrocarbon. Heavy mineral analysis is of utmost importance in reconstructing the nature and character of source areas i.e. provenance. They serve as important indicators of sediment source rocks because different types of source rocks yield different suites of heavy minerals (Boggs Jr., 2012). The properties of heavy minerals comprehensively describe the petrological character of sediment source terrain and parent rock. Transport mechanism and weathering history of a sediment (sediment dispersal) and palaeogeographic regime can also be inferred from heavy mineral studies. The tectonic setting of a source area is also reflected by nature of heavy minerals found in the sediment (Nechev and Isohording, 1993). Mineralogical maturity of the sediments can also be inferred from the heavy mineral contents.

Heavy minerals are minor constituents in terrigenous sediments (Plate 6.3a, 6.3d, 6.4b). They are found in pre-existing rocks that can survive mechanical or chemical action as well as interstratal solution (Pettijohn, 1975). Sinha and Khan (1965) claim that sand fractions between 44 and 88 microns yield most heavy minerals. Generally, heavy minerals in sandstones constitute less than 1% of the rock (Mange and Maurer, 1992). Ultrastable heavy minerals like zircon, tourmaline and rutile are ubiquitous and are found in all the clastic

sedimentary rocks as they can survive multiple reworking. The order of persistence of heavy minerals as described by Pettijohn (1941) attributes to removal of unstable minerals by intrastratal solution serving as a major controlling factor on the survival of minerals in sediments.

In the present study heavy mineral separation methods suggested by Folk (1980) and Middleton (2003) using heavy liquid Bromoform ($CHBr_{3;}$ density 2.89 g/cm3) have been used for separation of the heavy minerals.

Altogether thirty (30) indurated sandstone samples, ten (10) from each formation, have been processed for their heavy mineral contents. Separated grains were mounted and examined under the microscope for identification. Heavy minerals concentration in the Barail sandstones were analysed with respect to their abundance and roundness to asses mineralogical maturity, source rocks and transportation history. In each grain mount a minimum of hundred (100) grains were counted.

The identified heavy mineral includes zircon, tourmaline, rutile, kyanite sillimanite, staurolite, sphene, and scapolite in the studied sediments. The opaque grains are represented by iron-oxides and are in significant proportion. Ninety percent (90%) of the heavy minerals fall under transparent variety while the opaque varieties occupy only ten percent (10%) of the total heavy mineral population (Figure 6.1a). With regard to shape, only 7% heavy mineral grains are found to be euhedral and others (93%) are rounded to well-rounded in nature (Figure 6.1b). The transparent and dominant heavy minerals in the studied sediments include zircon (L = 32%, J = 37%, R = 19%), tourmaline (L = 41%, J = 15%, R = 32%), rutile (L = 08%, J = 07%, R = 09%), sillimanite, and kyanite. Other transparent heavy minerals are represented by staurolite, sphene, and scapolite. Together kyanite, sillimanite and staurolite range between 16 to 28% (Av. 22%; L = 16%, J = 28%, R = 23%). All the three formations (Laisong, Jenam and Renji) show a very similar heavy mineral assemblage; with no significant variations in their abundance, species and shape. Kyanite is the most abundant among heavy minerals whereas rutile has the lowest concentration among the ultrastable variety.

6.2.3 DESCRIPTION OF HEAVY MINERALS

Zircon ($ZrSiO_4$)

Zircons are identified by their high refractive index, straight extinctions, high order polarization colours and non-pleochroic characters. It occurs as a common accessory mineral in igneous and metamorphic rocks and as detrital grains in sedimentary rocks. In the studied sediments zircons are mostly colourless to brown in ordinary light and show rounded to subrounded shapes (Plate 6.5 (6, 7), 6.6 (5, 6), 6.7 (5, 8)), however, prismatic, angular to subangular grains (Plate 6.5 (1-5), 6.6 (1-3, 7), 6.7 (1-4, 6, 7)) are also seen. Inclusions in

zircon and zoning are common (Plate 6.5 (6)). Few zircon grains appear to have etched and pitted marks on the surface of the grains (Plate 6.5 (5)).

Tourmaline (Ca, K, Na) (Al, Fe, Li, Mg, Mn)$_3$ (Al, Cr, Fe, V)$_6$ (Bo$_3$)$_3$ (Si, Al, B)$_6$ O$_{18}$ (OH, F)$_4$

Tourmaline is a very resistant mineral and commonly occurs as an accessory mineral in acid igneous rocks. It is also found in some schist, gneiss and phyllites. It exhibits a broad spectrum of colours like greenish yellow or pale yellow, brown, pale brown, black and green. Pleochroism is strong and distinct. The tourmaline grains are mostly well rounded (Plate 6.5 (11), 6.6 (8), 6.7 (14, 16)), sub-rounded to rounded (Plate 6.6 (11), 6.7 (15, 17)) with a few euhedral variety (Plate 6.5 (8-10), 6.6 (9, 10), 6.7 (9-13)).

Rutile (TiO_2)

They are identified by their deep-red or brownish colors. They are weakly pleochroic and show high refractive index. Rutile typically occurs as accessory mineral in plutonic igneous rocks such as granite, in metamorphic rocks such as gneiss and schist and also in sedimentary rocks. They are generally euhedral in shape (Plate 6.5 (12, 13), 6.6 (12, 13), 6.7 (18, 19)), however, sub rounded grains were also observed (Plate 6.8 (20)).

Kyanite (Al_2SiO_5)

Kyanite is abundantly found in aluminium rich metamorphic rocks and sedimentary rocks. Observed Kyanite grains are colourless and exhibits moderately rounded shapes (Plate 6.6 (17)). Angular kyanite grains are also seen (Plate 6.5 (14), 6.6 (14-16), 6.8 (21-27)). They also show step like features in order of interference colour and have inclined extinction. Almost all the grains are free from inclusions.

Sillimanite (Al_2SiO_5)

Sillimanite in the studied samples occurs as long, slender, elongated prismatic shaped grains (Plate 6.5 (15, 16)). Prism and fibrolite varieties are common. Prismatic ones are colourless while fibrous variety shows pale green to pale blue colours (Plate 6.6 (18-21), 6.8 (28, 29)). Sillimanites show distinct cleavage and display moderate to strong birefringence. Sillimanite occurs in high temperature metamorphic rocks.

Staurolite {$Fe^{2+}_2Al_9O_6$ (SiO_4)$_4$ (O, OH)$_2$}

Staurolite in sediments may be derived from medium grade metamorphic rocks. Staurolite is concentrated sparsely in the studied samples and they are represented by dark brown to blackish brown coloured varieties often with fractures. Angular and prismatic varieties are seen in the studied samples (Plate 6.5 (17), 6.6 (22, 23), 6.8 (30, 31)).

Sphene and Scapolite

It occurs as a common accessory mineral of acidic rocks and also occurs in schists and granite-gneiss and other metamorphic rocks. Most detrital sphenes are rounded or show less sphericity. Etched pits are a common feature. They show high to extreme birefringence

(Plate 6.8 (32-34)). Scapolites are found in calcium rich metamorphic rocks. Prismatic crystals are often striated (Plate 6.6 (24, 25), 6.8 (35)).

Opaques

Opaque minerals were common in all the examined samples. They are mostly composed of iron oxides. Most opaques occur as magnetites which appear brown to black in colour. Euhedral to subrounded as well as rounded grains were seen (Plate 6.5 (18-21), 6.8 (36, 37)).

6.2.4 ZIRCON TOURMALINE RUTILE (ZTR) MATURITY INDEX

The three ultrastable heavy mineral assemblage zircon, tourmaline and rutile are chemically and mechanically the most stable (Pettijohn *et al*., 1973) and on the basis of the ZTR (Zircon Tourmaline Rutile) index, mineralogical maturity of the sediments can be assessed. Hubert (1962) discusses the ZTR index as a maturity index for sandstones and describes it as the sum of their percentages among other transparent heavy minerals. The distribution of ZTR in the three formations is zircon (L = 30 J = 25, R = 15), tourmaline (L = 38, J = 10, R = 25), rutile (L = 15, J = 25, R = 7), where L is Laisong, J is Jenam and R is Renji Formations respectively. The ZTR for the samples is calculated using the equation given by Hubert (1962):

$$\text{ZTR Index} = \frac{\text{Z} + \text{T} + \text{R}}{\text{Total number of non} - \text{opaques}} \times 100$$

Sediments are considered mineralogically immature to sub-mature if the ZTR index is less than 75% and ZTR index more than 75% indicates mineralogically matured sediments (Hubert, 1962; Bassey *et al*., 2019). The ZTR index, in the present study, ranges from 64.52% to 88.24%; suggesting a sub-mature to mature characters for these sediments (Table 6.3).

6.3 CLASSIFICATION OF SANDSTONES AND MODAL ANALYSIS

Framework mineralogy forms the basis of classification of sandstones with considerations of matrix in some classifications. Several systems for classification of sandstones have been put forward by workers such as McBride (1963), Pettijohn *et al*., (1972), Friedman and Sanders (1978), Folk (1980). Sengupta (1994) modified Dott (1964) scheme which is used to classify arenites and wackes. Quartz, feldspar, rock fragments and matrix form the four criteria based on which sandstones are classified.

For classification of the Barail sandstones of the Belt of Schuppen, the scheme provided by Folk (1980), has been adopted. Folk's classification displays the three common components of sandstones *i.e.* detrital quartz (Q), feldspars (F) and rock fragment (R or L) as the end members of a ternary plot known as the QFR or QFL diagram. The relative proportions

of quartz, feldspars and rock fragments are determined by modal analysis or grain counting under a microscope which are then recalculated and plotted in the triangular diagrams.

Based on the above method, the studied sandstones have been classified as quartz arenite, sub-litharenite and sub-feldspathic arenites (Figure 6.2). However, some of the Jenam sandstones have a high matrix content and may fall into wacke category.

For interpreting the tectono-provenance various discriminatory diagrams, suggested by several workers have been adopted in the present study. The ternary plots of QtFL (total quartz-feldspar-lithic fragment; Dickinson & Suczek, 1979; Figure 6.3), QFL (quartz-feldspar-lithic fragment; Dickinson *et al*., 1983; Figure 6.4), QmFLt (quartz-feldspar-total lithic fragments; Dickinson & Suczek, 1979; Figure 6.5) and QmFLt (monocrystalline quartz-feldspar-total lithic fragments; Dickinson *et al*., 1983; Figure 6.6) suggest a recycled orogenic provenance. The QpLvLs (polycrystalline quartz-lithic volcanic-lithic sedimentary; Dickinson & Suczek, 1979; Figure 6.7) and the QmPK (mono quartz-plagioclase- potassium feldspar; Dickinson & Suczek, 1979, Figure 6.8) triangular plots suggests derivation of the sediments from a collision suture and thrust belt sources with some contribution from continental block provenance. Based on type of quartz (mono crystalline undulatory, non undulatory, polycrystalline 2-3 units and >3 units), diagrams suggested by Basu *et al*., (1975) and Tortosa *et al*., (1991) a plutonic as well as low rank metamorphic rocks have been inferred as source rocks (Figures 6.10a and b).

Suttner *et al*., (1981) plot of QFL (total quartz-feldspar-lithic fragment) suggests a metamorphic humid palaeoclimate for the source rocks. (Figure 6.9).

Palaeoclimate

According to Suttner *et al*., (1986) sandstone compositions in addition to tectonics and transportation are also influenced by palaeoclimate and sedimentation. They further suggest that the climatic signatures are preserved in sands during deposition provided they do not suffer much during transportation and sedimentary differentiation. Paleoclimate studies help in understanding the weathering processes in the provenance as well as the climatic condition of deposition. They have also suggested a bivariant log/Iog plot based on the ratios of Qp/ (F+R) and (Qm+Qp)/ (F+R) (Figure 6.11) for discriminating the climatic conditions. Based on the above plot humid climatic conditions have been inferred in the present study. Similar inferences have also been drawn from the plots QFL (Figure 6.9) suggested by Suttner *et al*., (1981).

6.4 CLAY MINERALS

Clay minerals refer to a group of hydrous alumina silicates and are composed of very fine grain size grade (<2μ). Clay minerals are natural crystalline earthy materials of fine grain size composed chemically of hydrated aluminium silicates, with magnesium,

iron, calcium, potassium or sodium present as essential constituents, organized in different fashions as superimposed alternating layers. Clay minerals are common weathering products (including weathering of feldspar) and low-temperature hydrothermal alteration products. Identification of clay minerals aid in provenance interpretation pathways and also provides information on the burial history of the sediments. X-Ray Diffraction (XRD) technique is the most efficient method for determining clay content in fine grained sediments. Tucker (1989) suggests recognition of clay minerals in thin section is possible when they have been precipitated in pore spaces in sandstones during diagenesis. Altogether eighteen (18) sandstone samples, six (6) each from Laisong, Jenam and Renji Formations were analysed for their clay and other mineral contents.

Both whole rock and clay fractions were analyzed for their clay and other mineral contents at SAIF, Gauhati University, Assam using XRD technique. The machine was set between 4° to 30° for the oriented samples while glycolated samples were run between 4° to 10°. Almost all the analysed samples record the presence of kaolinite and montmorillonite. Illite was also recorded in few samples. Diffractograms of samples L1, J1 and R1 are shown in Figure 6.12.

6.4.1 DESCRIPTION OF CLAY MINERALS

Kaolinite

In the analysed samples**,** Kaolinite is the most abundant clay mineral. Under acidic condition with a good drainage system K-feldspar produces kaolinite on alteration. Kaolinite has also been recorded in soils where extensive leaching and acidic conditions predominate under a warm humid climate.

Illite

In the present study, Illite has been observed in some of the analyzed samples. In the initial stages of weathering under alkaline conditions enriched with Ca^{2+} ions Illite is produced in the sediments by decomposition of feldspar as well as degradation of mica. The quick mixing of marine and fresh water sediments also favours the formation of illite as the marine water has high concentration of K and Mg (Grim, 1968). Under diagenetic conditions transformation of kaolinite into illite is very common.

Montmorillonite

Montimorollonites are hydrated sodium calcium aluminum magnesium silicate mineral. Montmorillonite, a member of smectite group, has been recorded in some samples. Montmorillonite, is weathering products of igneous rock such as basalts and gabbros which are rich in ferromagnesium minerals. But they can also be formed under a variety of conditions.

Chlorite

Chlorite is produced by the weathering of ferromagnesium minerals in rocks such as basalts and gabbros and has magnesium and iron in its structures. They are found in deeply buried sediments and also in low and medium rank metamorphic rocks.

6.4.2 SCANNING ELECTRON MICROSCOPY-ENERGY DISPERSIVE SPECTROSCOPY (SEM-EDX)

Scanning Electron Microscopy-Energy Dispersive Spectroscopy (SEM-EDX) is an analytical technique that provides the information about the elemental composition of the examined samples. This technique uses a focused electron beam to create high resolution images of the sample surface. When electron beam hits the sample surface it produces the X-ray emission which is unique to each element; thus allow the identification of the elemental composition of the sample. This is also a rapid method of surface and elemental analysis of the geological samples.

Scanning Electron Microscopy is useful in studying several aspects of sandstones such as detrital mineralogy, diagenesis, grain size, grain shape, sorting, angularity, cement and matrix content. SEM-EDX exhibits lower errors than optical microscopy in determining grain mineralogy, type, boundary, cement and matrix composition as it is apparently easier to differentiate the discrete entities (Worden and Utley, 2022). This technique is an intermediary between sediment mineralogy and petrology and core-based sedimentology (Armitage *et al*., 2010).

In the present study, Scanning Electron Microscope (SEM) Energy Dispersive X-ray (EDX/EDS) analysis of three (3) sandstone samples one from each formation has been carried out.

Laisong Formation

i. La: SEM-EDX of Spectrum 1 indicates peak in Ti (60.16%) and O (34.8%) and Spectrum 2 with O (35.09%) and Ti (32.76%) indicate heavy minerals such as rutile. EDX of Spectrum

3 shows dominant peaks in elemental compositions of Ca (23.56%), O (29.65%), P (10.24%) and C (9.36%), reflecting the presence of carbonates and phosphates within the detrital minerals. EDX of spectrum 4 displays peaks of O (46.25%), Si (44.52%), and Al (20.8%) which indicates the presence of clay minerals such as kaolinite. Concentration of O (38.48%), Si (21.36%) and K (5.77%) in Spectrum 6 indicates the presence of potassium silicate minerals (Plate 6.9).

ii. Lb: Dominance in concentration of Ti (61.07%), O (33.13%) and V (1.17%) in Spectrum 1 indicates that the mineral is Rutile. Presence of V in Rutile (TiO2) reflects provenance from eclogites and metamorphic rocks associated with subduction zones (Holycross & Cottrell, 2018) (Plate 6.9).

iii. Lc: EDX of Spectrum 2 shows increased concentration of S (47.99%) and Fe (34.99%) suggesting that the mineral embedded in quartz is pyrite (Plate 6.9).

iv. Ld: EDX of Spectrum 3 shows peaks in O (33.26%), Fe (25.22%), Si (15.36%), Al (10.42%) and Mg (7.38%). The chemical signature indicates that the mineral is smectite clay (Plate 6.9).

Jenam Formation

i. Ja: EDX of Spectrum 2 shows peaks in O (32.99%), Fe (37.86%), Mg (6.73%) and Ca (5.33%). High concentration of Fe and O suggests that the cement is composed of iron oxides. Presence of Ca and Mg may indicate carbonate cements. EDX of Spectrum 3 display peaks in Ti (54.86%), O (32.94%), Fe (3.44%), V (4.88%), Si (2.21%), Al (1.17%) and Mg (0.60%). High concentration of Ti and O reflects Rutile. Presence of Si, Al, Mg and O indicates the presence of clay minerals in the matrix of the sandstone (Plate 6.10).

ii. Jb: EDX of Spectrum 1 display peaks in S (45.53%), Fe (42.21%), Pb (8.78%), and O (3.76%). High concentrations of S and Fe indicates that the mineral is pyrite with minor amounts of galena (Plate 6.10).

iii. Jc: EDX of Spectrum 1 display peaks in O (33.69%), Al (27.13%), Si (17.84%), K (7.16%), Fe (5.99%), Dy (2.03%), Ti (2.42%) and Mg (0.67%). From the chemical composition, form and cleavage the mineral can be presumed as biotite. EDX of Spectrum 4 displays peaks in O (41.68%), Al (33.29%) and Si (24.92%). Chemical composition and form of the mineral reflects that the mineral is kaolinite clay (Plate 6.10).

iv. Jd: EDX of Spectrum 1 show dominance of O and Si indicating that the mineral is Quartz. Zonation in the quartz crystal is observed. EDX of Spectrum 4 shows peaks in O (41.92%), Al (17.73%), Si (16.47%), Hf (3.35%), Fe (2.50%), K (2.21%), Mg (1.13%), Na (0.67%) and Ti (0.57%). The chemical composition and presence of one set of cleavage indicates that the mineral is biotite (Severin, 2005). EDX of Spectrum 5 displays peaks in S (57.13%) and Fe (42.86%) which indicates that the mineral is pyrite (Plate 6.10).

Renji Formation

i. Ra: EDX of spectrum 2 shows peaks in O (48%), Al (19.30%), Si (13.97%), Fe (12.66%), Mg (2.12%) and K (1.10%). The elemental composition and single set of cleavage suggest that the mineral is biotite. EDX of Spectrum 4 display dominant peaks in O (56.82%), Fe (31.11%) and C (12.07%) suggesting that the minerals within the cement are iron oxides and organic matter. Spectrum 6 display peaks in O (56.20%), Si (31.80%) and Al (12%). The fine-grained morphology and elemental compositions are suggestive of kaolinite (Plate 6.11).

ii. Rb: Spectrum 7 shows peaks in O (52.79%), Si (27.77%), Al (11.3%) and Fe (8.10%). This mineral surround feldspar (spectrum 6) and is probably kaolinite which is commonly formed by the chemical weathering of feldspar. Occurrence of Fe may indicate the presence of iron oxides (Plate 6.11).

iii. Rc: Spectrum 1 shows peaks in O (57.95%) and Si (42.05%) indicating that the mineral is quartz. Zoning in quartz indicates origin of the quartz from granitic sources (Vernon, 2000; Müller *et al*., 2005; Matthews *et al*., 2012). Spectrum 2 and Spectrum 4 shows dominant peaks in O (67.83%) and Fe (32.22%) indicating that the mineral is iron oxide (Plate 6.11).

iv. Rd: Spectrum 3 shows peaks in Si (50.92%), O (47.93%), Fe (0.83%) and Al (0.32%). The elemental composition and single set of cleavage indicates chlorite. Spectrum 4 exhibits peaks in O (50.79%), Si (24.04%), Al (21.88%) and Fe (3.29%). Spectrum 6 exhibits peaks in O (52.50%), Si (25.27%), Al (21.43%) and Fe (0.80%). Elemental compositions from Spectrum 4 and 6 indicates the presence of kaolinite clay minerals (Plate 6.12).

v. Re: EDX of Spectrum 2 shows peaks in S (49.12%), Fe (40.4%) and O (10.48%) suggesting that the mineral is pyrite. Pyrites can be found as replacement minerals in fossils. The form of the mineral appears to be similar to that of a microfossil. Therefore, Spectrum 2 is presumably a microfossil which has been replaced by pyrite (Plate 6.12).

vi. Rf: EDX characterization of Spectrum 3 exhibits dominant peaks of Zn (49.93%), S (26.49%), O (14.78%) and Si (5.33%) with traces of Fe (2.85%) and Ti (0.63%) which indicates the mineral is sphalerite with probable traces of iron oxides and rutile. Spectrum 4 display peaks in O (36.89%), Fe (28.54%), Si (14.37%), Al (12.06%) indicating the presence of clay minerals (Plate 6.12).

vii. Rg: EDX of Spectrum 1 exhibits dominant peaks in Ce (30.20%), La (13.34%), O (24.98%), P (16.90%) indicating that the mineral is monazite (Plate 6.12).

viii. Rh: Spectrum 4 shows peaks in O (57.46%), Al (19.65%) and Si (22.90%) indicating the presence of kaolinite clay (Plate 6.12).

Based on the elemental compositions, following minerals/materials have been identified in the Barail sandstones.

1. Clay minerals such as Kaolinite and smectite (montmorillonite) have been reported in all the formations. Chlorite has been reported from Renji sandstones

2. Zircon and rutile have been reported from all the formations. In Laisong sandstones vanadium bearing rutile has been observed
3. Quartz Zonings have also been reported from Renji and Jenam Formations
4. Pyrite has been reported from Jenam and Renji Formations only
5. Biotite has been identified by its composition and cleavage
6. In addition to that SEM-EDX also suggests the presence of monazite and pyroxenes
7. Carbonate cements from Jenam and Laisong sandstones only
8. Iron oxide and organic matter have been reported from Jenam and Renji Formations

6.5 DIAGENESIS

Diagenesis in the broadest sense encompasses all of the processes that act to modify sediments after deposition (Boggs Jr., 2012). According to Blatt *et al*., (1980), diagenetic changes occur near the surface and at deeper levels and depend on burial time, temperature and subsurface water chemistry. Sengupta (1994) referred to diagenesis as those changes which the sediment undergoes between deposition and lithification under normal temperature and pressure conditions. Rock porosity, mineralogy, and chemical composition may all be altered or changed to various degrees during burial diagenesis. The generally accepted depth range and temperature where diagenesis begins is 4 to 7 km and 120° to 220°C.

Sedimentation rate and its duration are direct functions of degree of diagenetic alterations in sedimentary deposits (Nazarkin, 1979). Petroleum and Groundwater Geologists take keen interest in diagenesis because of its economic significance as it can adversely affect the ability of siliciclastic rocks to store and transmit fluids (Stonecipher, 2000). Many workers (Pitman, 1972; Krinsley and Doornkamp, 1973; Ingersoll, 1974; Marzolf, 1976; Kichu and Srivastava, 2018) have suggested that the appearance of diagenetic signatures within sediments is co-relatable with increasing depth. Diagenetic zones discriminated by depth range include near surface (*telogenetic*), shallow depth (*eogenetic*) and deeper level (*mesogenetic*) zones (Burley *et* al., 1985).

Petrographic examination remains the mainstay of diagenetic study; however, other instrumental analysis like Scanning Electron Microscopy (SEM), X-Ray Diffraction (XRD) analysis, Cathodo-luminescence (CL) petrography and Electron Probe Micro Analyser (EPMA) enhance the petrographic data and has been extensively used in recent years. To unveil the diagenetic history of the Barail sediments, petrographic approach, SEM-EDX and XRD methods have been applied in the present study.

6.5.1 EFFECTS OF DIAGENESIS

Various diagenetic features observed in the Barail sandstones include compaction, cementation and authigenesis. Different degree of compaction stages are observed in the samples. An increase in the depth of burial increases the compaction rate, thereby leading to

the emergence of long or straight contacts (Plate 6.1e, 6.2a, and 6.4f), concavo-convex contacts (Plate 6.2a, b, and 6.2c) within the framework grains. With further increase in depth, the grain contacts become sutured (Plate 6.1c, 6.3b, 6.4a, d, e) reflecting deep burial diagenesis. The intense compaction leads to the decrease in the primary porosity of the rocks. Warping of micaceous minerals (Plate 6.2e, 6.4b) around detrital quartz and presence of penetrative contacts/sutured contacts suggest the deep burial conditions. These two features are attributed to the compaction processes which are the result of pressure created by piling of sediments as well subsidence of the basin.

Silica cements (Plate 6.2d, 6.4d) occur commonly in the studied samples. Ferruginous (iron) cements (Plate 6.1e) and calcite cements (Plate 6.3b) have also been observed in the Barail sandstones. Walker (1974) suggested that a major source of iron cements may be the weathering of iron rich minerals. Grain boundaries have been dissolved either by the cementing material or reaction with the matrix at various places (Plate 6.2f, 6.3a, b, c, 6.4a, d, e).

Overgrowth generally begins with the restoration of the edges (Carozzi, 1960; Heald and Lorese, 1974) (Plate 6.1f, 6.2d). Presence of authigenic quartz in these sediments indicate the early diagenetic modification under eogenetic marine conditions (Burley *et al*., 1985).

Albitization represents authigenesis where the chemistry of sea water plays an important role. Albitization may occur at temperatures 100-150°C (Boles, 1982; Surdam *et al*., 1989) and also at temperatures as low as 70-100°C (Morad *et al*., 1990). Presence of authigenic feldspar in the studied samples suggests increasing pressure and temperature (>100°C) in response to burial and thermal history (Plate 6.4e, albitized feldspar displaying chessboard fabric or pattern).

6.5.2 PRESSURE, TEMPERATURE AND DEPTH REGIME

Silica cementation not only requires water saturated with silica but also circulation of large volume of silica saturated water. Probably during eodiagenesis silica cementation takes place. According to Dutton and Diggs (1990) silica may precipitate between 55-75^{0}C temperature and a burial depth ranging from 1 to 1.5 km. However, Sudram *et al*., (1989) opined that the quartz overgrowth can take place under early mesodiagenetic as well as late mesodiagenetic stages. While working with the sandstones from Norway offshore Walderhaug (1990) suggests a temperature range of 90 to 118^0 C. Boggs Jr., (2012) suggests that pH has little effect on silica precipitation during normal diagenetic conditions.

In sedimentary environment albitization of feldspar in the sandstones is a common phenomenon. Albitization may take place by direct precipitation or it may have an intermediate stage which involves the replacement of feldspar by calcite anhydrite followed by albitization. Many workers (Boles, 1982; Sudram *et al.*, 1989) have suggested that

albitization may take place between a temperature ranges of 110 to 150^0 C with the depth being between 2.5 to 3.0 km. However, Morad *et al*., (1990) suggest a temperature range of 70-100^0C. According to various workers Boles (1982), Sudram *et al.*, (1989), and Boggs Jr., (2012), permeability, temperature, dissolution of parent material and Na^+/K^+ ratio are the factors which affect the albitization of K-feldspar. They also suggest that most of the Na for albitization come either from pore water or from the transformation of clay minerals. Milliken (1992) suggests that approximately 56-68 % of K-feldapar are albitized following dissolution-precipitation mechanism. Albitization also suggests increasing pressure, temperature, burial and thermal history.

Diagenetic signatures persevered in the studied sediments may be grouped into early and late diagenesis. Silica overgrowth and precipitation of calcite and iron cements suggest an early diagenetic regime whereas crushing, bending, fracturing and warping of micaceous minerals around quartz grains suggest the increasing pressure temperature, pressure and depth of burial i.e. late diagenesis (Sengupta, 1994, Singh and Singh, 1994).

Dapples (1962) proposed three stages of diagenesis based on the geochemical characteristic:

Stage (1) *redoxomorphic* where reduction and oxidation form the basis for this stage. Occurs during deposition and early burial diagenesis

Stage (2) *locomorphic* stage is categorized precipitation of mineral matter into pore spaces and replacement reactions. Such reactions are typical of the early burial stage and are an important part of the process of lithification

Stage (3) *phyllomorphic* follows the principal locomorphic replacements and involves development of micas, principally from clays

In the studied sandstones silica overgrowth, modified grain to grain contacts and alteration of feldspar represent the locomorphic stage (Borac and Friedman, 1981) whereas precipitation of iron oxide precipitation represents the redoxomorphic stage (Bjorkum and Gjelvik, 1988). Formation of authigenic mica in the studied sandstones is represented by phyllomorphic stage though not very common.

6.5.3 SOURCE OF CEMENTS

Silica cement

One of the most common cements in sandstones is silica; however, their source is still being debated as silica for cementation may come from both sandstones and shale within the depositional basin. Silica can also be supplied by the deeply buried rocks undergoing low-grade metamorphism. Pressure solution as a major source of silica cement has been suggested by various workers (Einsele, 2000). According to Prothero and Schwab (2004) about one third of the silica needed for cementation comes from pressure solution processes. Einsele (2000)

further suggests that on reaction with water volcanic glass, K-feldspar and mafic minerals also release silica along with formation of clay minerals including illite.

On the basis of the above three possible sources can be envisaged for supply of silica for cementation in the Barail sandstones.

(a) devitrification of volcanic glass (Surdam and Boles, 1979)

(b) diagenetic transformation of silicates including clay minerals (Towe, 1962) and

(c) pressure solution effects (Dapples, 1979)

Carbonate Cement

The carbonate cements have been reported both in Laisong as well as in Jenam Formations through SEM-EDX, however, in thin section it is observed only in the Jenam Formation. Most of the carbonates are in micritic phase only. Detrital limestone, on dissolution liberate sufficient Ca^{+} and CO_3^{-} ions to the migrating pore water, which under a controlled Eh and pH conditions may precipitate excess carbonate as pure calcite (Dapples, 1972). Precipitation takes place in a carbonate saturated system only when the solubility of calcium carbonate in pore water decreases. Decrease in the solubility is the result of increase in the concentration of calcium rise in temperature and also decrease in $\Sigma\ CO_2$. According to Boggs Jr., (2012) if there is decrease in total CO_2, pH will increase which causes the carbonate precipitation. Presence of Eocene limestones in the vicinity of the basin could be considered as the probable source for supply of carbonate for cementation.

Ferruginous cement

Iron oxide cement occurs as shapeless void fillers and also as coating on framework grains. Walker (1974) has considered in place weathering of iron rich minerals as a major source of iron cement. Presence of oxidized meteoric water enhances the dissolution of iron–rich silicates and precipitation of ferruginous cement. Ferrous iron for precipitation as cement can be supplied by the dissolution of iron bearing accessory minerals of igneous and metamorphic rock fragments and also some of the phyllosilicates.

6.6 MAJOR OXIDE GEOCHEMISTRY

The origin, tectonics, environmental, and ecological evolution of clastic sedimentary rocks are recorded in the geochemical components (Yan *et al*., 2007). Distribution of elements in sediments are controlled by a number of physical, chemical and biological factors, therefore study of geochemical attributes of the sediments would provide information on their source and environment of deposition. According to Kakul (1968) concentration of TiO_2, Fe_2O_3, Na_2O and K_2O in sediments are good chemical indicators their petrographic composition. The association and interrelation between chemical composition, framework mineralogy,

provenance type and tectonic setting of sedimentary basins has been studied upon and interpreted by many workers (Garrels and Mckenzie, 1971; Engel *et al*., 1974; Potter, 1978; Dickinson and Suczek, 1979; Bhatia, 1983; Herron, 1988; Nesbitt *et al*., 1996).

In the present study to support the petrographic data, X-Ray Fluorescence Spectrometer (XRFS) analysis of the Barail sandstones have also been carried out for their geochemical properties. The major oxides composition and variation in sandstones help in understanding the provenance type and weathering conditions, which are controlled by the tectonic setting of a basin (Bhatia, 1983). Thirty (30) Barail sandstone samples, ten (10) each from Laisong, Jenam and Renji Formations have been analysed by X-Ray Fluorescence Spectrometer (XRFS) for their major elemental composition (Table 6.4). The studied samples show high concentration of SiO_2 in all the three formations. The average concentration of the major oxides for the Barail Group of rocks in the Belt of Schuppen is as SiO_2 78.55%, Al_2O_3 11.77%, Fe_2O_3 33.96%, MnO 0.00%, MgO 1.00%, CaO 0.57%, Na_2O 0.90%, K_2O 1.50%, TiO_2 0.81% and P_2O_5 0.10%.

6.6.1 TECTONIC SETTING AND CLASSIFICATION

Based on the chemical composition, the plot of log (Fe_2O_3/K_2O) vs log (SiO_2/Al_2O_3) (Figure 6.13) after Herron (1988) shows that most samples fall in litharenite sandstone category with a few in the wacke type as well as arkose sandstones. Various bivariate plots (Fe_2O_3 (Total) + MgO vs K_2O/ Na_2O; Fe_2O_3 (Total) + MgO vs Al_2O_3/SiO_2 and Fe_2O_3 (Total) + MgO vs TiO_2 suggested by Bhatia (1983; Figures 6.14, 6.15, and 6.16), have been utilized and a transitional tectonic setting has been inferred for these sandstones. Roser and Korsch's (1986) discriminatory diagram using log (K_2O/Na_2O) vs SiO_2 (Figure 6.17) also suggests the same. This is further corroborated by the inferences drawn from ternary plots CaO-Na_2O-K_2O (Figure 6.18) and Fe_2O_3-MgO-TiO_2 (Figure 6.19) after LeMaitre (1976) and Condie (1967), which indicate granitic and granodioritic sources for the Barail sandstones.

The SiO_2 composition is relatively high in sandstones of all the three formations. The high ratio of SiO_2/Al_2O_3 (avg 78.55/11.77, Table 6.4) indicates the influence of recycling, weathering and transportation processes. The high Al_2O_3/TiO_2 ratio, in the (avg 11.77/0.81) sediments; point towards a continental source for these sediments (Fyffe and Pickerill, 1993).

From the bivariate plot of Al_2O_3+K_2O+Na_2O vs SiO_2, after Suttner and Dutta (1986), the paleoclimatic condition of the Oligocene sediments appears to be largely humid (Figure 6.20).

6.6.2 PALAEOCLIMATIC CONDITIONS

Weathering indices aids in deciphering the weathering conditions of the past. The chemical and mineralogical composition of clastic rocks and changes in these components is the result of chemical weathering in the source area (Nesbitt *et al*., 1996). In the present study, common weathering indices such as Chemical Index of Alteration (CIA; Nesbitt and Young, 1982) and Index of Chemical Variability (ICV; Cox *et al*., 1995) have been used to decipher the paleoclimatic conditions. The Chemical Index of Alteration (CIA) is a tool to calculate the weathering intensity to determine the sediment source rocks (Nesbitt and Young, 1982). The CIA and ICV can be expressed as follows;

$CIA^{\#} = [Al_2O_3/ (Al_2O_3 + CaO^* + Na_2O + K_2O)] *100$

$ICV^{\wedge} = [\{Fe_2O_3 + K_2O + Na_2O + CaO^* + MgO + MnO + TiO_2\}/Al_2O_3]$

where CaO* indicates Ca incorporated from the silicate bearing minerals; # indicates by using Molecular Proportions and ^ indicates by using Weight Percentage.

Table 6.5 shows the values of various weathering indices of the studied sandstones. The relatively high CIA values for the Barail sandstones (60.16 to 87.15; Avg. 79.76) suggesting intense weathering conditions.

Cox *et al*., (1995) have suggested ICV range for different minerals between 0.6 to 1.0 for feldspar, illite and muscovite. They also suggest the ICV range between 0 to 0.3 for clay minerals and 0.3 to 1.0 for feldspars based on the ratio of $K2O/Al_2O_3$. The Barail sandstones show an average Index of Chemical Variability (ICV) = 0.75 and K_2O/Al_2O_3 ratio = 0.13. The plot of CIA vs ICV proposed by Long *et al*., (2012) represents the maturity and weathering nature of clastic sediments (Figure 6.21). Based on the plot, the Oligocene Barail sediments are mature sediments that have undergone intense weathering under humid type of climate.

Table 6.1: Detrital composition of Barail sediments in the study area

Serial Number	Sample ID	Total Quartz %	Total Feldspar %	Total RF %	Mica %	Heavy Mineral %	Cem %	Mat %
1	L1	77.67	3.40	5.34	2.91	4.37	1.46	4.85
2	L5	76.31	4.02	5.62	2.81	3.61	1.61	6.02
3	L8	71.71	1.99	4.78	3.19	7.57	1.59	9.16
4	L11	76.96	2.94	6.37	3.43	4.41	3.43	2.45
5	L13	79.42	2.47	6.58	3.29	3.29	2.88	2.06
6	L14	73.68	2.63	3.51	3.95	5.26	2.19	8.77
7	L15	78.18	3.18	6.82	4.09	4.55	1.36	1.82
8	L16	75.45	1.34	5.36	2.23	4.02	2.23	9.38
9	L17	79.22	2.60	5.63	3.46	4.33	2.60	2.16
10	L18	77.97	1.76	4.85	3.96	6.61	3.08	1.76
11	L20	73.68	7.52	7.52	2.26	5.64	1.13	2.26
12	L21	79.84	2.06	5.35	4.53	3.70	2.47	2.06
13	L22	68.94	1.28	7.66	7.66	10.64	1.28	2.55
14	L24	78.33	5.33	4.33	3.67	4.00	1.67	2.67
15	L28	73.39	4.44	7.26	4.03	6.05	1.61	3.23
16	J1	66.28	1.94	2.71	4.65	9.69	3.10	11.63
17	J2	66.37	2.69	4.48	7.62	5.83	2.24	10.76
18	J4	63.81	2.61	2.61	7.84	7.84	2.61	12.69
19	J6	64.13	1.81	4.35	6.52	6.88	2.90	13.41
20	J10	54.58	5.00	5.00	7.92	4.58	0.00	22.92
21	J11	63.30	4.59	4.13	6.88	6.88	4.13	10.09
22	J12	68.53	3.85	2.80	4.20	12.24	3.15	5.24
23	J13	63.59	4.82	5.62	8.17	9.24	3.21	6.43
24	J19	69.51	3.25	8.13	4.88	7.72	2.44	4.07
25	J20	60.07	5.13	5.13	2.93	10.99	2.93	12.82
26	J21	60.16	6.64	4.69	1.95	10.55	4.30	11.72
27	J22	74.12	2.63	4.82	3.07	5.26	3.51	6.58
28	J23	66.67	3.89	5.56	5.00	5.56	5.56	7.78
29	J24	75.22	2.21	4.87	3.98	5.31	3.10	5.31
30	J25	72.06	1.62	5.26	5.67	7.69	3.24	4.45
31	R1	74.14	2.59	3.45	4.31	8.62	2.59	4.31

32	R6	73.49	2.33	5.12	5.12	4.65	3.26	6.05
33	R8	74.53	3.30	7.08	3.77	3.77	3.77	3.77
34	R10	72.71	2.88	2.88	5.17	4.33	0.00	12.02
35	R12	71.01	4.35	6.28	5.80	5.31	4.35	2.90
36	R13	66.39	4.15	6.22	3.73	3.32	2.90	13.28
37	R14	75.79	2.38	3.97	3.57	6.35	3.97	3.97
38	R15	69.19	4.27	3.79	3.79	7.58	4.27	7.11
39	R19	66.67	2.90	5.31	5.31	10.14	4.35	5.31
40	R20	74.79	0.83	4.55	4.13	5.37	3.72	6.61
41	R21	68.89	2.22	7.22	5.00	6.67	4.44	5.56
42	R22	75.55	2.62	4.80	3.49	4.37	3.93	5.24
43	R23	74.42	2.33	4.65	5.12	4.19	5.12	4.19
44	R24	69.52	2.67	5.88	5.35	4.81	6.42	5.35
45	R30	65.10	2.60	5.21	7.81	6.25	6.25	6.77

Table 6.2: Recalculated values of detrital composition

Sl No.	**Sample ID**	**Recalculated Quartz %**				**Recalculated Feldspar %**		**Recalculated Rock Fragment %**		
		2 to 3 Units	**> 3 Units**	**Undu-latory**	**Non-undu latory**	**K-feldspar**	**Plagio clase**	**Sedimen-tary**	**Meta-morphic**	**Igneous**
1	L1	2.34	0	5.62	81.46	1.12	2.81	4.49	1.12	0.56
2	L5	1.02	0.51	3.27	84.11	0.93	3.74	4.21	1.4	0.93
3	L8	2.84	0	3.05	85.79	0.51	2.03	4.57	1.02	0.51
4	L11	0.93	0.47	4.55	82.95	0.57	2.84	6.82	0.57	0
5	L13	1.65	0.55	6.98	80.93	0.47	2.33	5.12	1.4	0.93
6	L14	3.09	1.03	8.79	79.12	1.1	2.2	3.3	1.1	0
7	L15	1.09	0.54	4.64	82.47	1.03	2.58	5.15	1.55	1.03
8	L16	3.96	0.99	3.26	83.15	0	1.63	4.89	1.09	0.54
9	L17	2.6	0	1.49	86.63	0.5	2.48	3.96	2.48	0
10	L18	2.97	1.27	7.81	79.17	0	2.08	2.6	2.08	1.04
11	L20	5.19	1.89	6.78	69.92	0.85	7.63	5.51	2.54	0.42
12	L21	1.09	0	6.13	84.43	0.47	1.89	3.77	1.42	0.94
13	L22	1.14	0	3.83	83.06	0	1.64	6.56	2.73	0.55
14	L24	3.79	1.9	4.92	79.55	1.14	4.92	3.41	1.52	0

15	L28	2.73	0.55	4.27	79.15	2.37	2.84	6.16	1.9	0.47
16	J1	2.44	0	5.46	85.79	0.55	2.19	2.19	1.64	0
17	J2	1.08	0	3.66	85.37	1.22	2.44	3.66	1.22	1.22
18	J4	0.52	0	10.81	81.08	0	3.78	2.7	1.08	0
19	J6	1.29	0	7.73	82.47	0	2.58	3.09	2.06	1.03
20	J10	1.91	0.64	10.97	70.97	1.94	5.81	4.52	1.94	1.29
21	J11	0.47	1.4	6.37	78.98	0.64	5.73	2.55	1.91	1.27
22	J12	2.73	1.64	6.05	81.4	0.47	4.65	2.33	0.93	0.47
23	J13	1.51	0.5	10.93	72.68	2.19	4.37	4.37	1.64	1.64
24	J19	1.56	0.52	3.52	80.4	3.02	1.01	6.03	2.01	2.01
25	J20	1.64	1.09	4.17	78.65	0.52	6.77	5.73	1.04	0.52
26	J21	2.69	1.08	5.46	74.86	3.28	6.01	3.28	2.19	1.09
27	J22	1.46	0	7.53	82.26	1.08	2.15	4.3	1.08	0.54
28	J23	1.61	1.08	10.95	72.99	0.73	4.38	5.11	2.19	0
29	J24	2.05	0	3.23	86.02	0	2.69	3.76	2.15	0
30	J25	1.08	0.54	7.69	82.05	0	2.05	4.62	1.54	0.51
31	R1	1.15	0.57	5.38	85.48	1.61	1.61	3.76	0.54	0
32	R6	7.78	1.11	6.9	74.71	1.15	1.72	4.6	1.72	0
33	R8	3.18	1.91	5	78.33	1.67	2.22	5	2.22	1.11
34	R10	2.37	1.18	7.01	81.53	1.27	2.55	1.91	1.27	0.64
35	R12	1.08	0	5.92	79.88	0.59	4.73	2.96	3.55	1.18
36	R13	0.48	0	4.86	81.08	0	5.41	4.32	2.7	1.08
37	R14	2.45	0	4.83	85.51	0.48	2.42	2.42	0.97	1.45
38	R15	1.29	0	7.36	80.98	1.23	4.29	1.84	1.84	1.23
39	R19	2.06	0	9.03	77.42	1.29	2.58	4.52	1.29	1.29
40	R20	3.55	0.71	4.12	86.08	0	1.03	3.09	2.06	0.52
41	R21	2.11	0	7.09	78.01	0	2.84	5.67	2.13	1.42
42	R22	1.71	0.57	2.11	86.84	0.53	2.63	4.21	1.05	0.53
43	R23	0.68	2.05	3.43	85.71	0.57	2.29	3.43	1.71	0.57
44	R24	3.57	1.43	2.74	81.51	1.37	2.05	4.79	1.37	1.37
45	R30	3.77	1.89	9.29	75.71	0	3.57	5.71	0.71	0.71

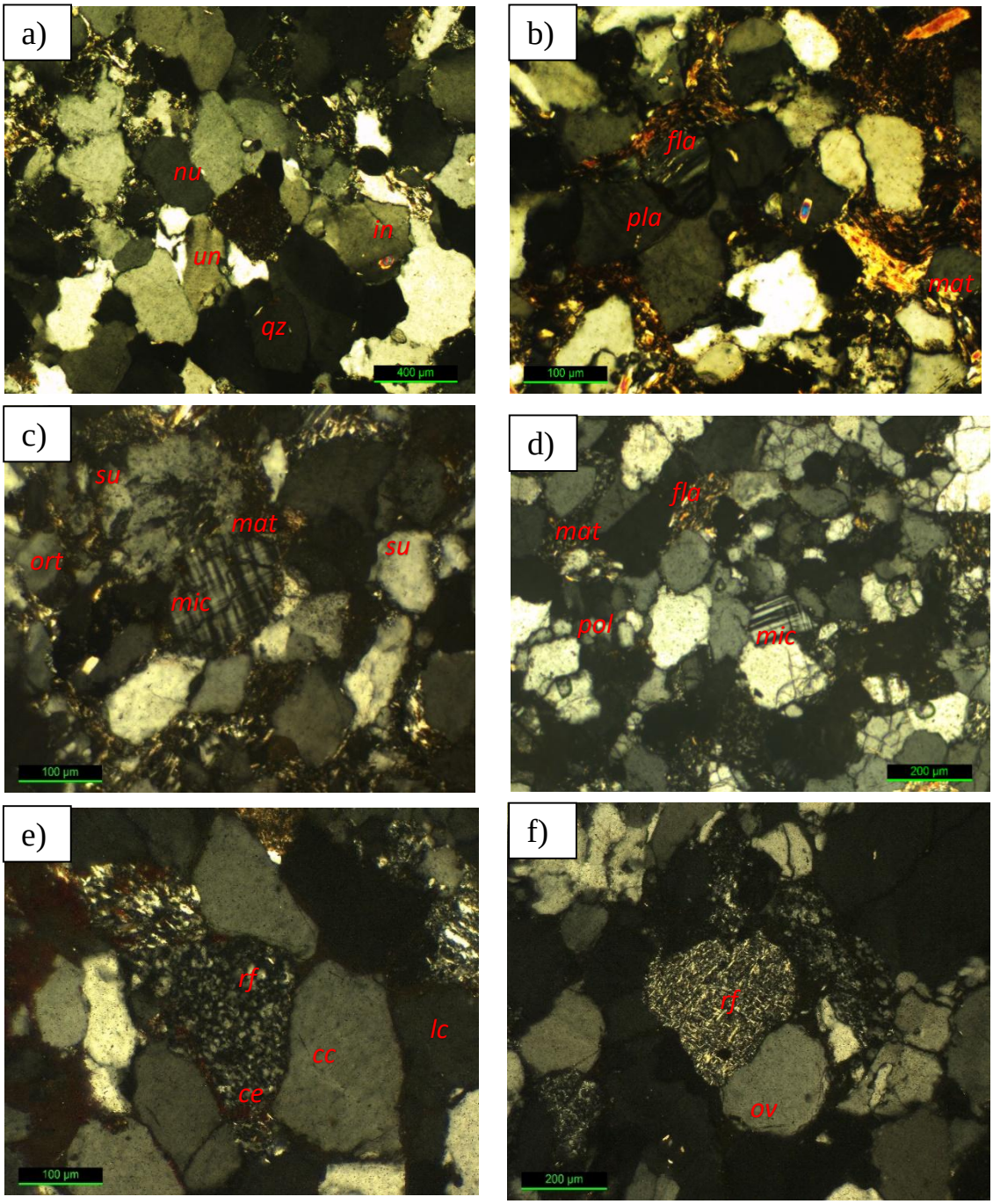

Plate 6.1: Photomicrographs of Laisong sandstones a) non-undulatory quartz (*nu*); undulatory quartz (*un*); rounded quartz (*qz*); inclusion in quartz (*inc*) b) bending of mica (*fla*); albitized feldspar (*pla*); matrix (*mat*) c) microcline (*mic*); orthoclase (*ort*); matrix (*mat*); sutured contact (*su*) d) matrix (*mat*); microcline (*mic*); bending of mica (*fla*); polyscrystalline quartz (*pol*) e) sedimentary rock fragment (*rf*); iron cement (*cem*); long contact (*lc*); concavo-convex contact (*cc*) f) metamorphic rock fragment (*rf*); overgrowth (ov)

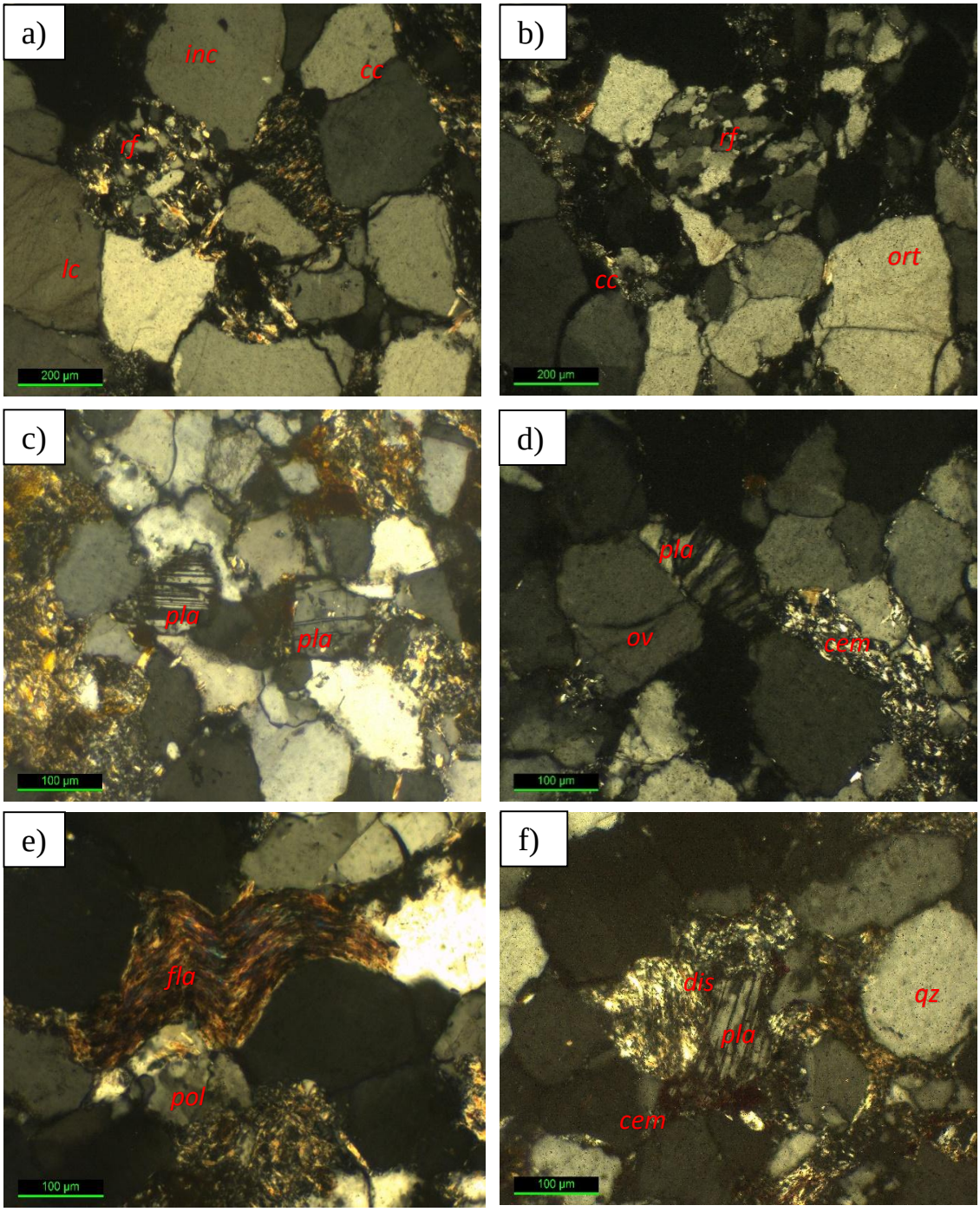

Plate 6.2: Photomicrographs of Laisong sandstones showing a) igneous rock fragment (*rf*); concavo-convex contact (*cc*); inclusion in quartz (*inc*); long contact (*lc*) b) sedimentary rock fragment (*rf*); orthoclase (*ort*); concavo-convex contact (*cc*) c) albitized feldspar (*pla*) d) albitized feldspar (*pla*); silica cement (*cem*); overgrowth (*ov*) e) bending of mica (*fla*); polyscrystalline quartz (*pol*) f) dissolved grain boundary (*dis*) albitized feldspar (*pla*); rounded quartz (*qz*); ferruginous cement (*cem*)

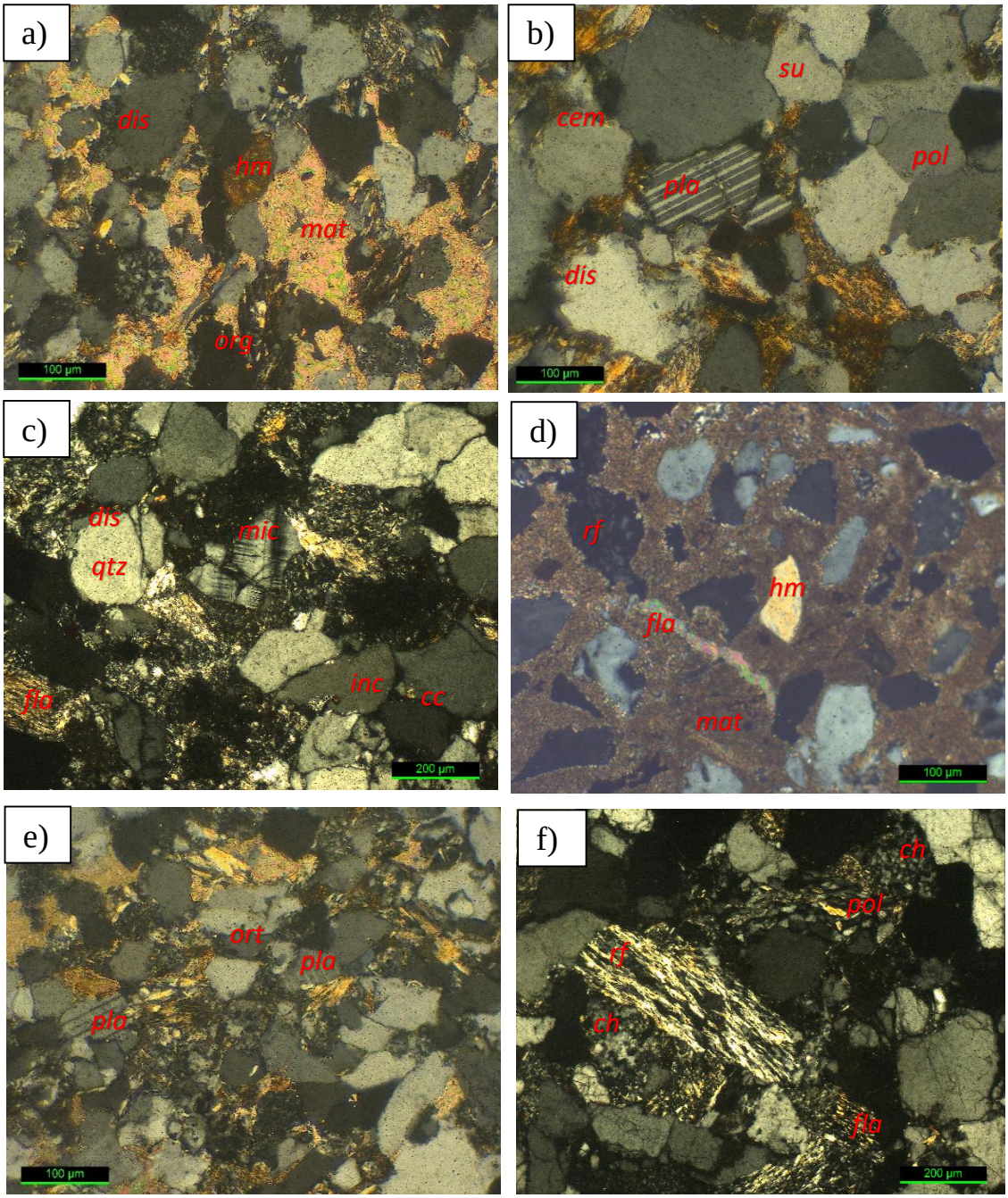

Plate 6.3: Photomicrographs of Jenam sandstones a) chlorite matrix (*mat*); dissolved grain boundary (*dis*); heavy mineral (*hm*); organic matter (*org*) b) plagioclase feldspar (*pla*); dissolved grain boundary (*dis*); polycrystalline quartz (*pol*); calcite cement (*cem*); sutured contact (*su*) c) microcline (*mic*); rounded quartz (*qtz*); inclusion in quartz (*inc*); concavo-convex contact (*cc*); mica (*fla*) d) matrix (*mat*); heavy mineral (*hm*); rock fragment (*rf*); mica (*fla*) e) plagioclase feldspar (*pla*); orthoclase (*ort*) f) polycrystalline quartz (*pol*); metamorphic rock fragment (*rf*); chert (*ch*); mica (*fla)*

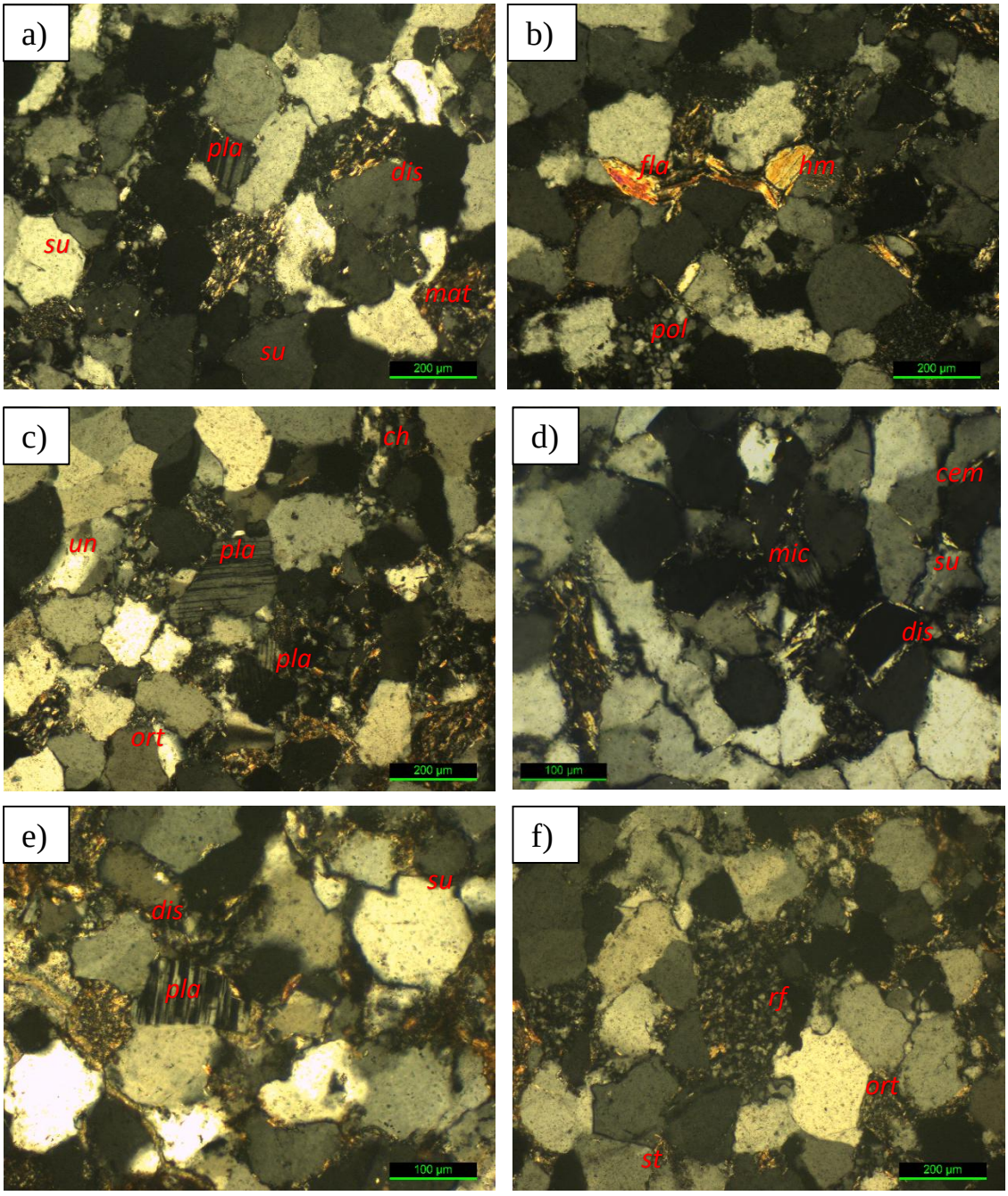

Plate 6.4: Photomicrographs of Renji sandstones a) plagioclase feldspar (*pla*); dissolved grain boundary (*dis*); matrix (*mat*); sutured contact (*su*) b) bending of mica (*fla*); polycrystalline quartz (*pol*); heavy mineral (*hm*) c) plagioclase feldspar (*pla*); orthoclase (ort); chert (*ch*); undulatory quartz (*un*) d) microcline (*mic*); sutured contact (*su*); dissolved grain boundary (*dis*); silica cement (*cem*) e) sutured contact (*su*); plagioclase feldspar (*pla*) displaying chessboard pattern; dissolved grain boundary (*dis*) f) metamorphic rock fragment (*rf*); orthoclase (ort); straight contact (*st*)

Table 6.3: ZTR index calculated from the % of ZTR in the three formations

Heavy Mineral	**Laisong**	**Jenam**	**Renji**
Zircon	30	25	15
Tourmaline	38	10	25
Rutile	7	5	7
Total no. of ZTR	75	40	47
Total no. of non opaques	85	62	70
ZTR Index (%)	**88.24**	**64.52**	**67.14**

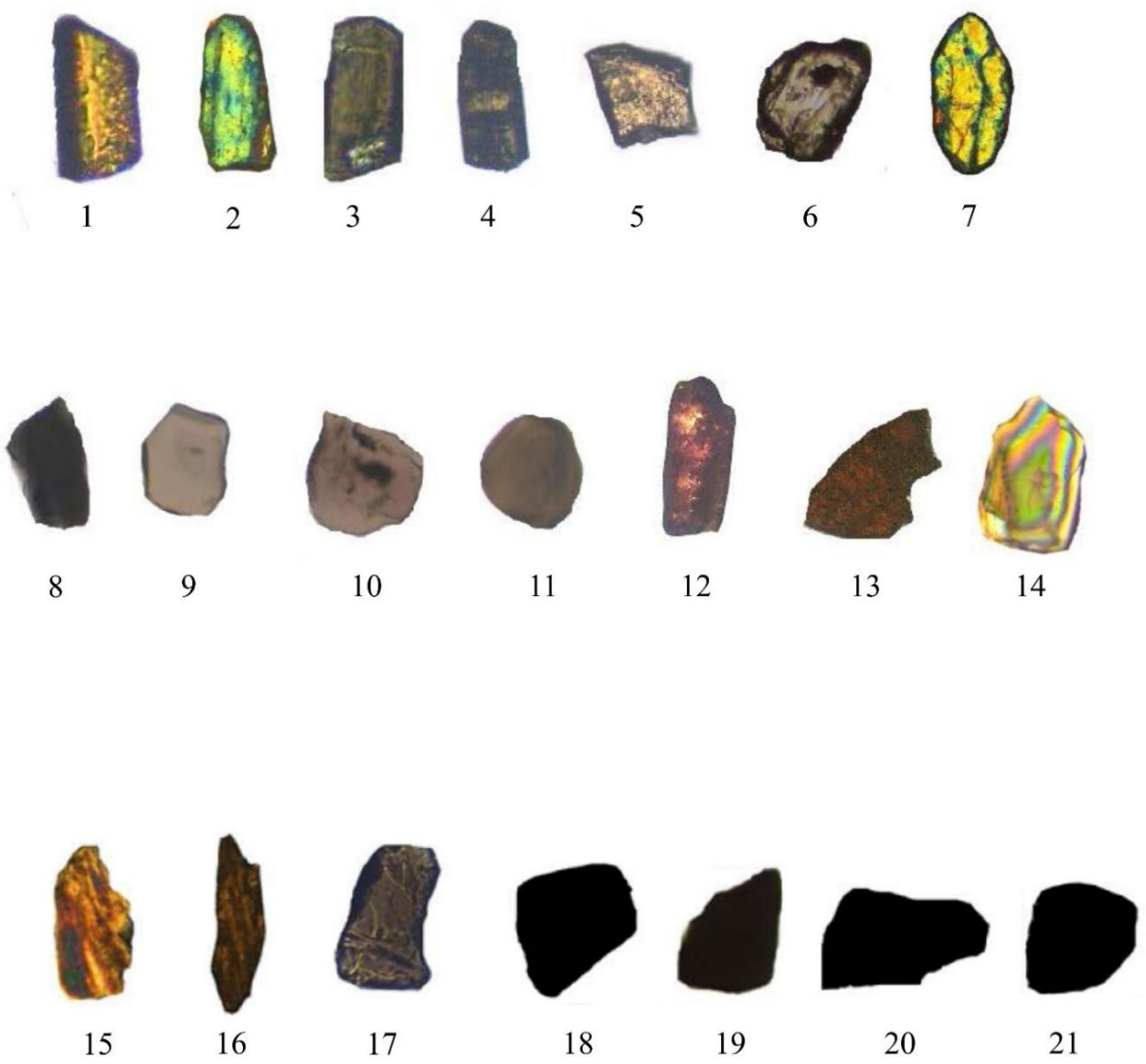

Plate 6.5: Photomicrographs showing Heavy Minerals of Laisong sandstones. Zircon 1-7; Tourmaline 8-11; Rutile 12, 13; Kyanite 14; Sillimanite 15, 16; Staurolite 17; Opaques 18-21

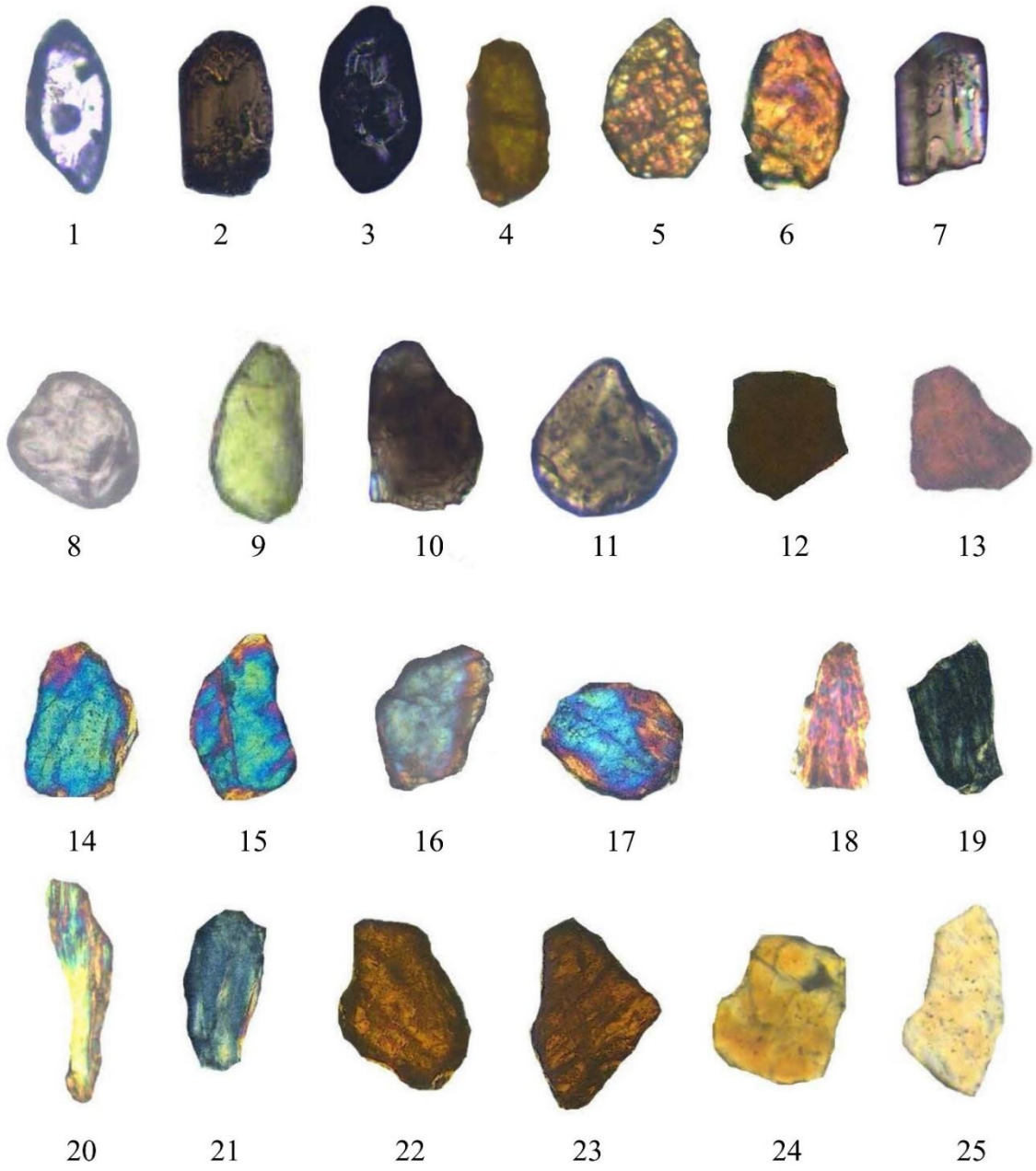

Plate 6.6: Photomicrographs showing Heavy Minerals of Jenam sandstones. Zircon 1-7; Tourmaline 8-11; Rutile 12, 13; Kyanite 14-17; Sillimanite 18-21; Staurolite 22, 23; Scapolite 24, 25

Plate 6.7: Photomicrographs showing Heavy Minerals of Renji sandstones. Zircon 1-8; Tourmaline 9-17; Rutile18-19

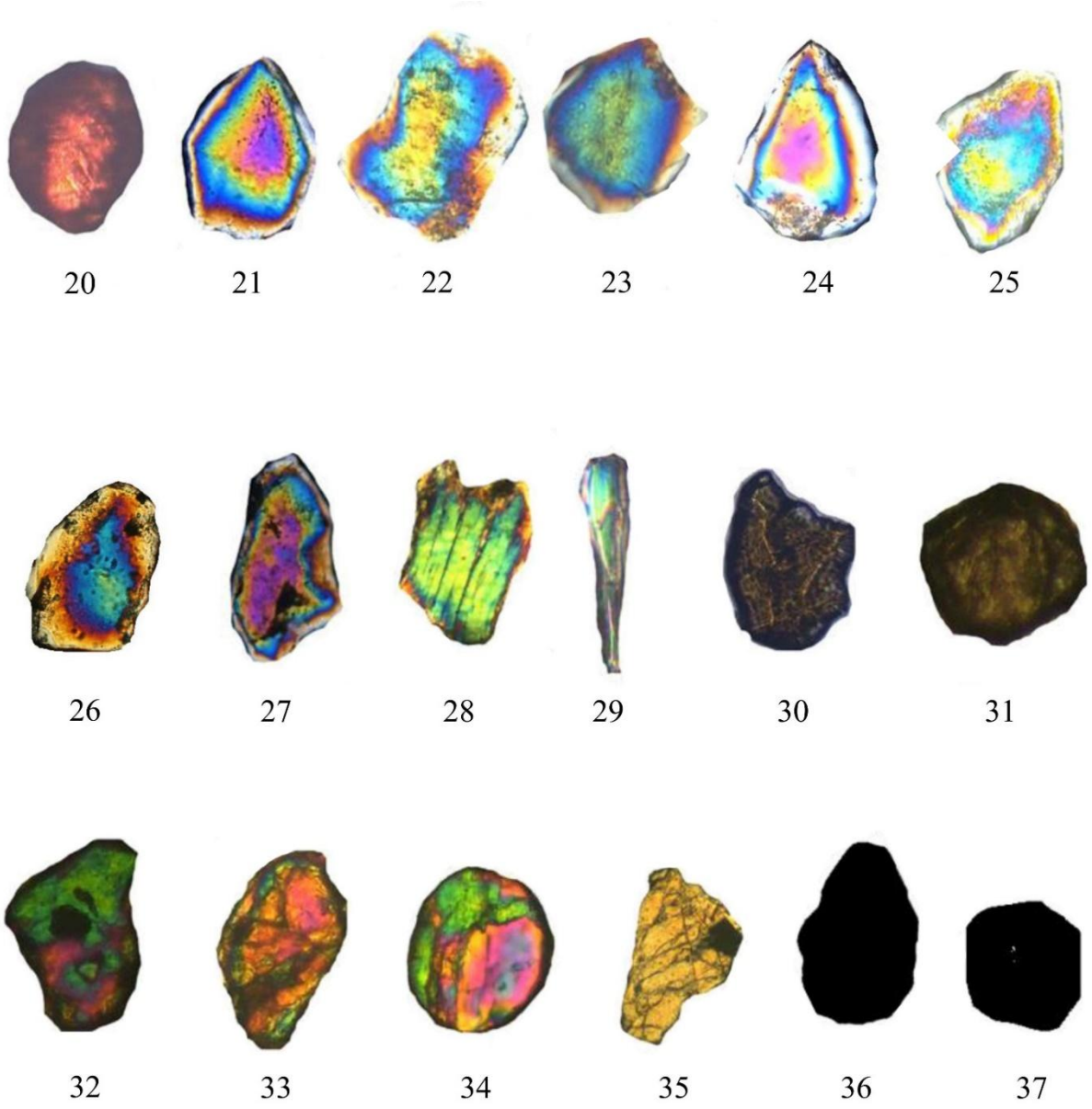

Plate 6.8: Photomicrographs showing Heavy Minerals of Renji sandstones. Rutile 20; Kyanite 21-27; Sillimanite 28, 29; Staurolite 30, 31; Sphene 32-34; Scapolite 35; Opaques 36, 37

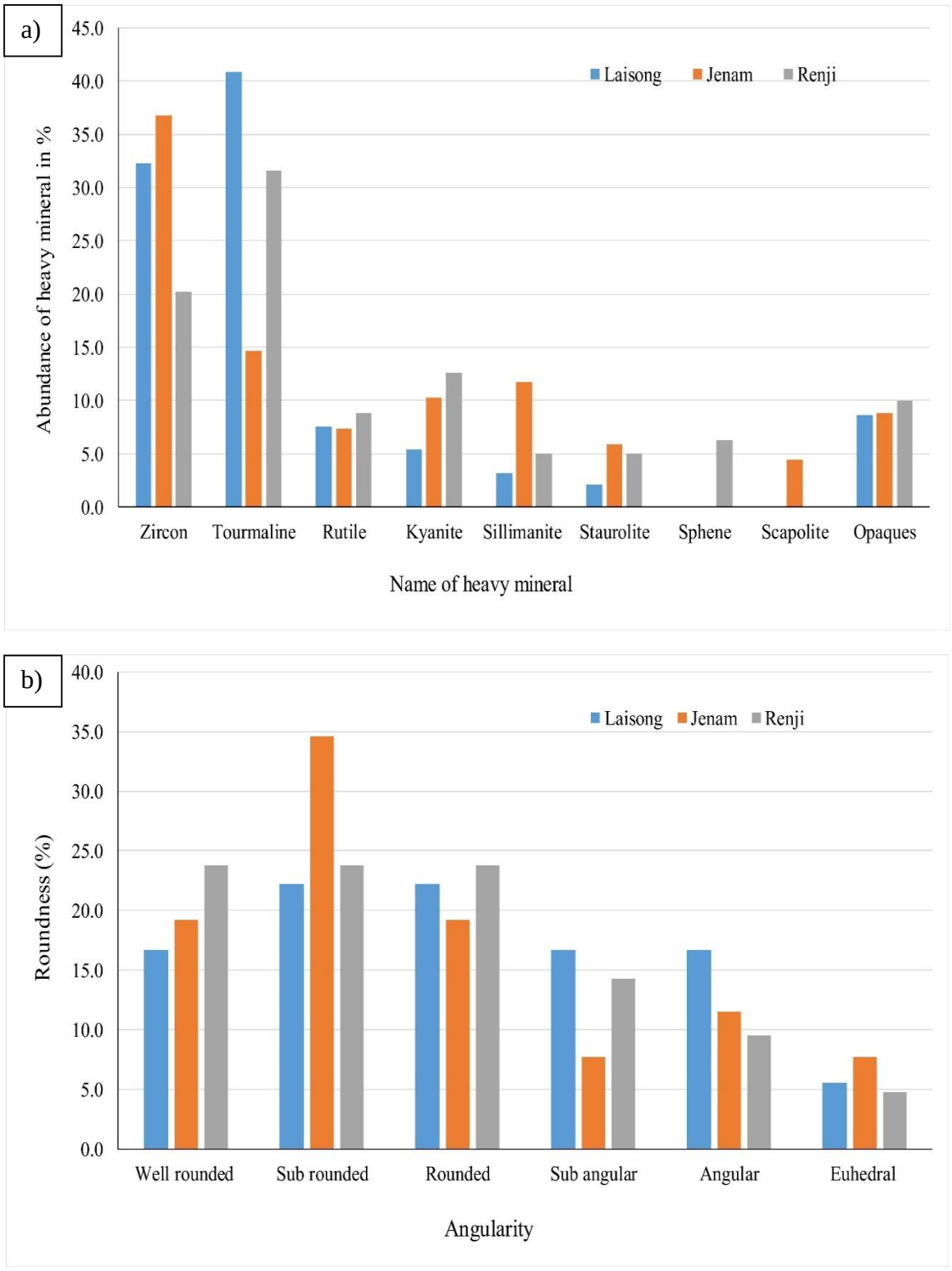

Figure 6.1: Bar graph representing (a) abundance of heavy minerals and (b) roundness of Barail sediments

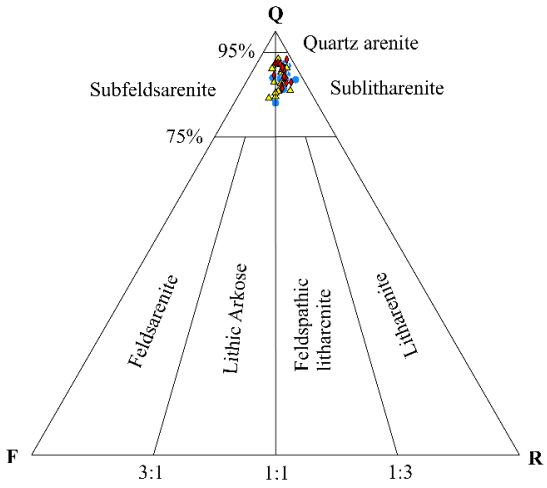

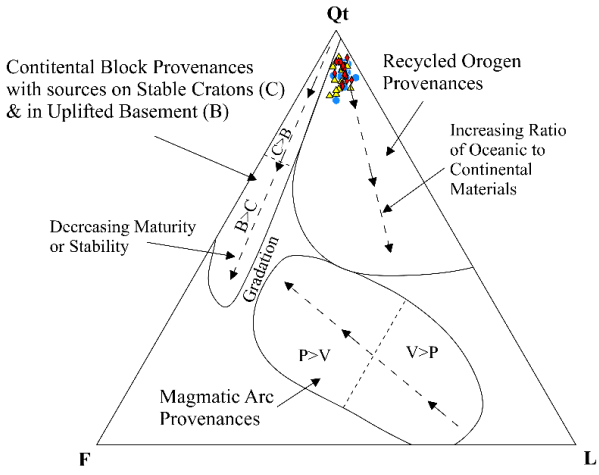

Figure 6.3: Ternary plot of total quartz, feldspar and lithic fragments (after Dickinson & Suczek, 1979)

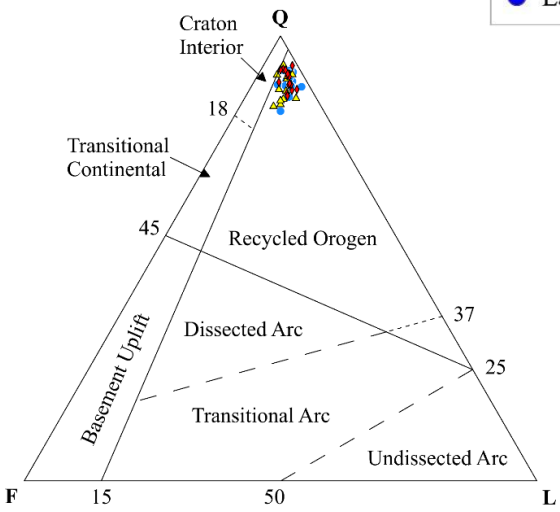

Figure 6.4: Ternary plot of total quartz, feldspar and lithic fragments (after Dickinson *et al*., 1983)

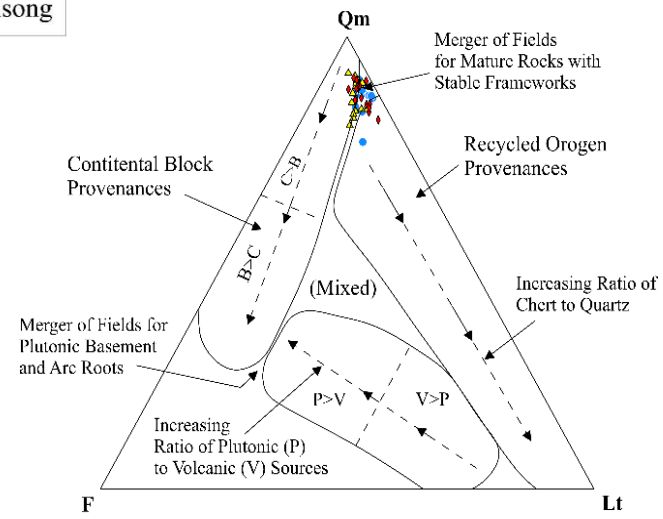

Figure 6.5: Ternary plot of quartz (mono), feldspar and lithic fragments (after Dickinson & Suczek, 1979)

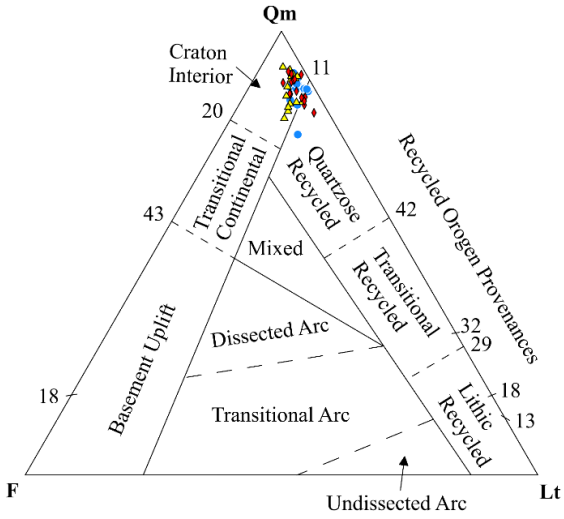

Figure 6.6: Ternary plot of quartz (mono), feldspar and lithic fragments (after Dickinson *et al*., 1983)

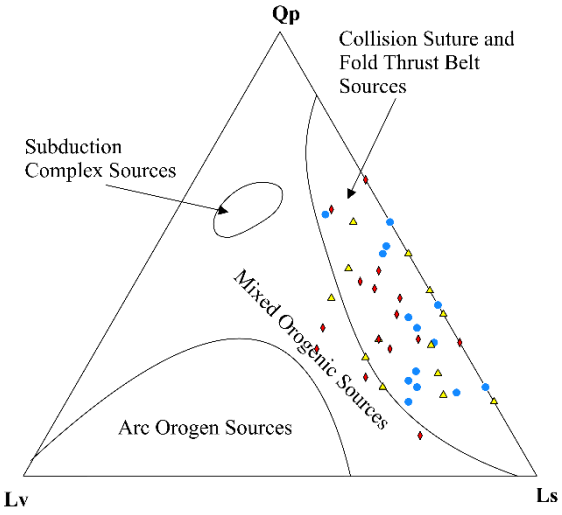

Figure 6.7: Ternary plot of quartz (poly), lithic (volcanic) and lithic (sedimentary) (after Dickinson & Suczek, 1979)

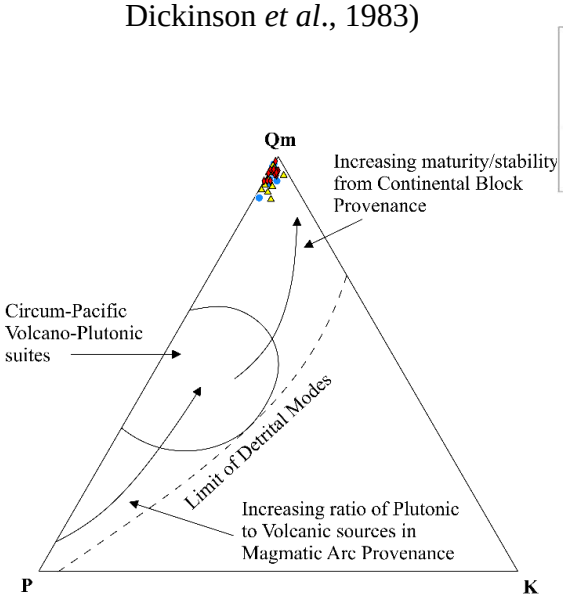

Figure 6.8: Ternary plot of quartz (mono), feldspar (sodic) and feldspar (potash) (after Dickinson & Suczek, 1979)

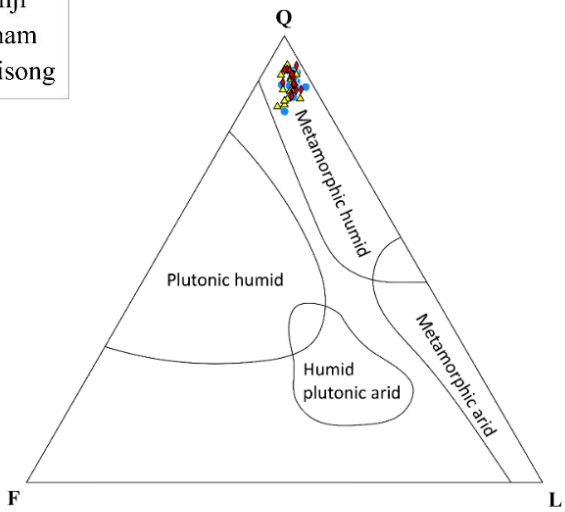

Figure 6.9: Ternary plot of total quartz, feldspar and lithic fragments (after Suttner *et al*., 1981)

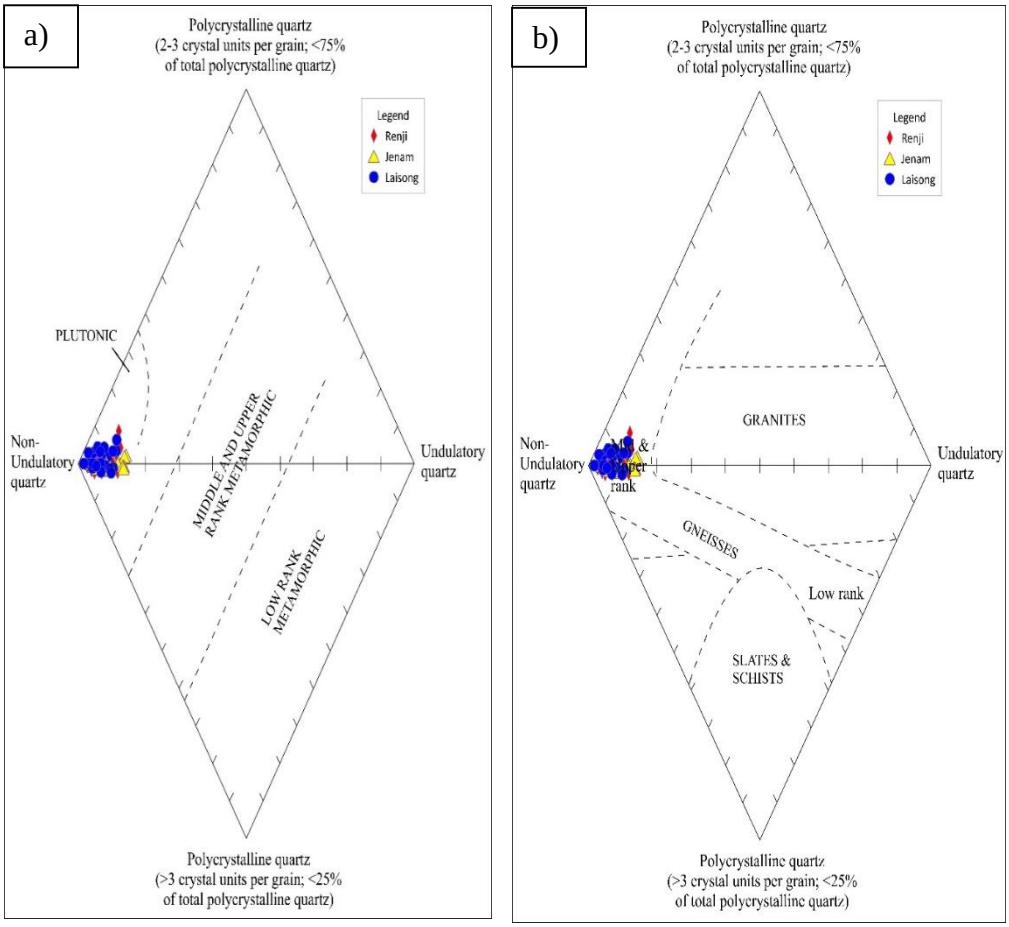

Figure 6.10: Diamond plot of non-undulatory quartz, undulatory quartz, polycrystalline quartz (2-3 units and polycrystalline quartz (> 3 units) after a) Basu *et al*., (1975) and b) Tortosa *et al*., (1991)

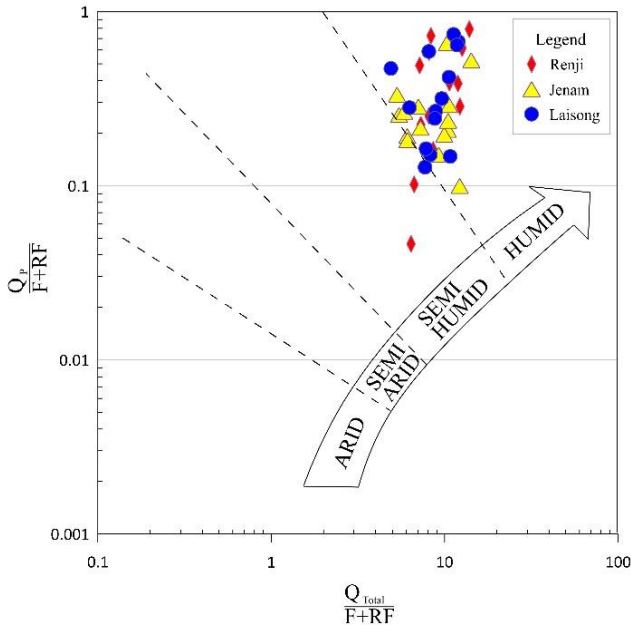

Figure 6.11: Bivariant log/log plot based on the ratios of Qp/ (F+R) and (Qm+Qp)/ (F+R) after Suttner *et al*., (1986)

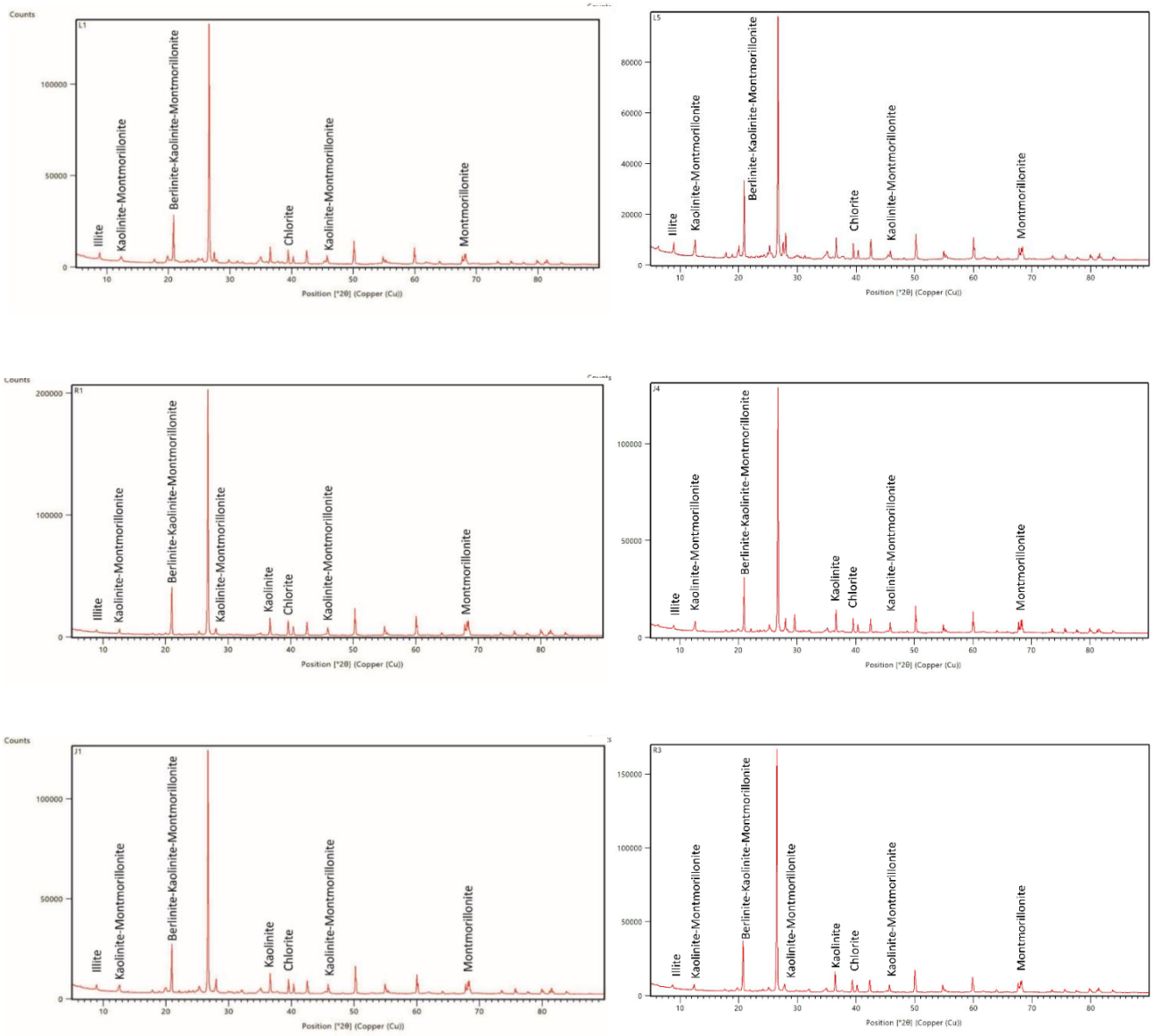

Figure 6.12: Representative XRD curves (diffractograms) showing peaks of various clay minerals

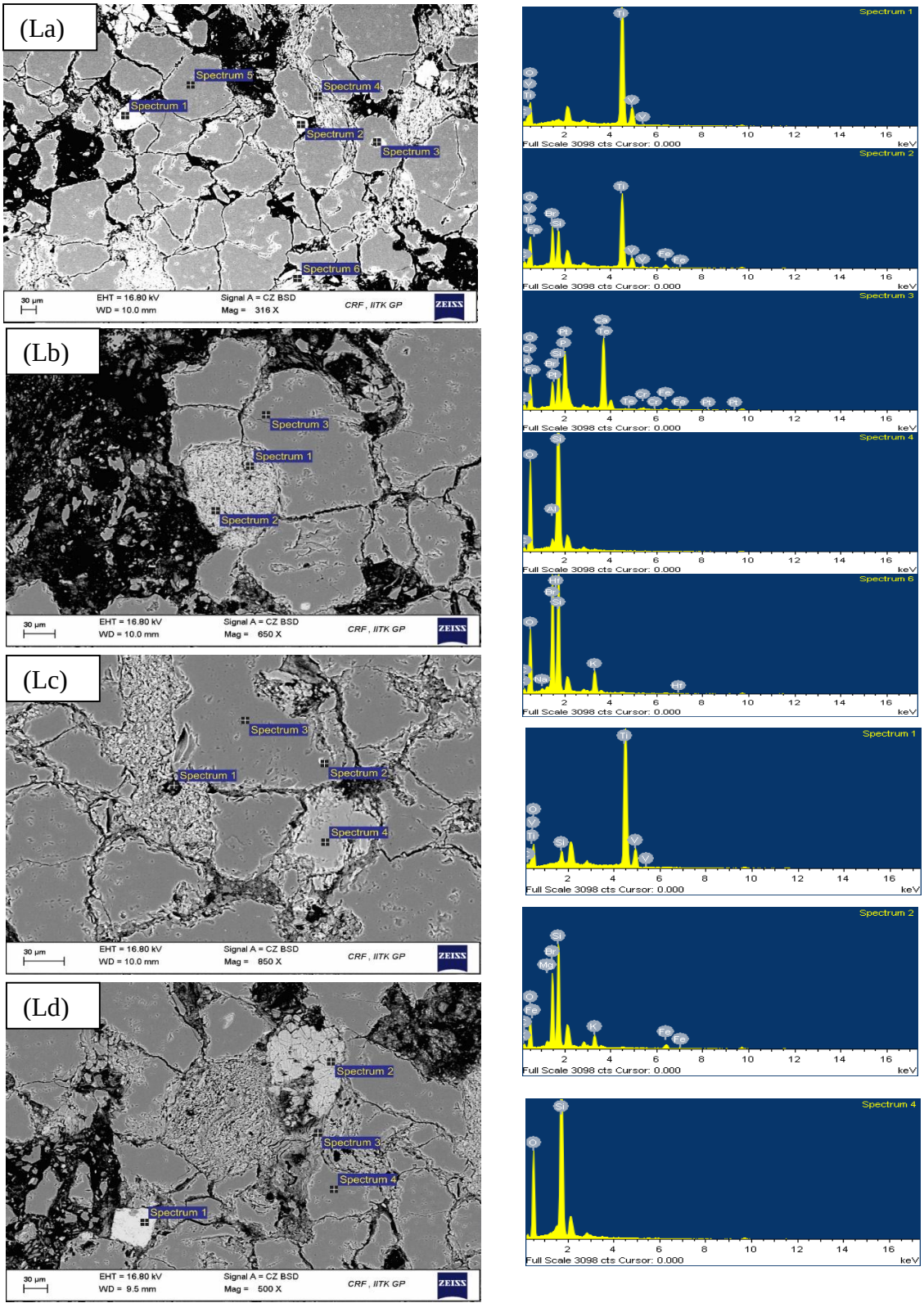

Plate 6.9: SEM and EDX of La, Lb, Lc and Ld

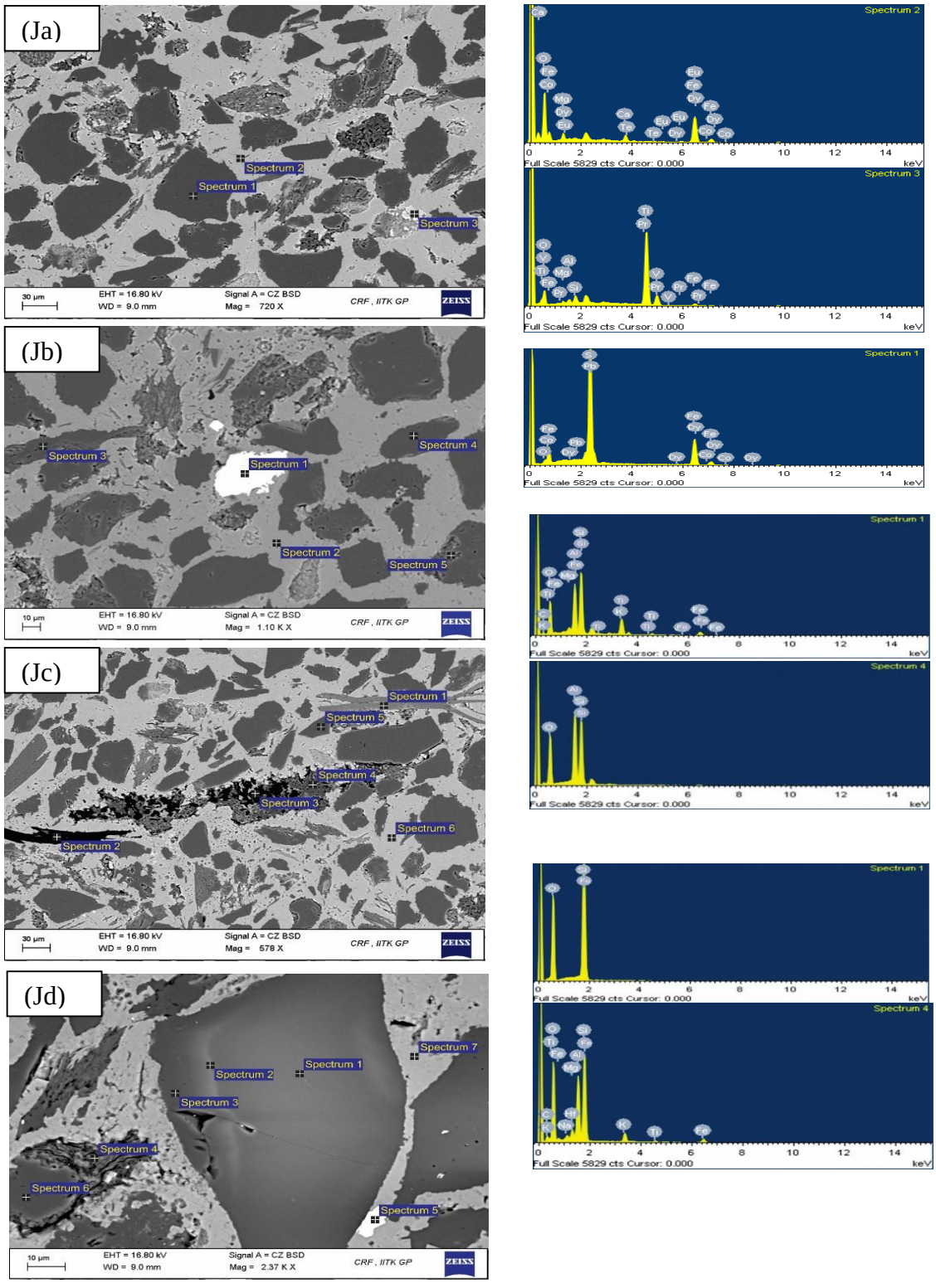

Figure 6.10: SEM and EDX of Ja, Jb, Jc, and Jd

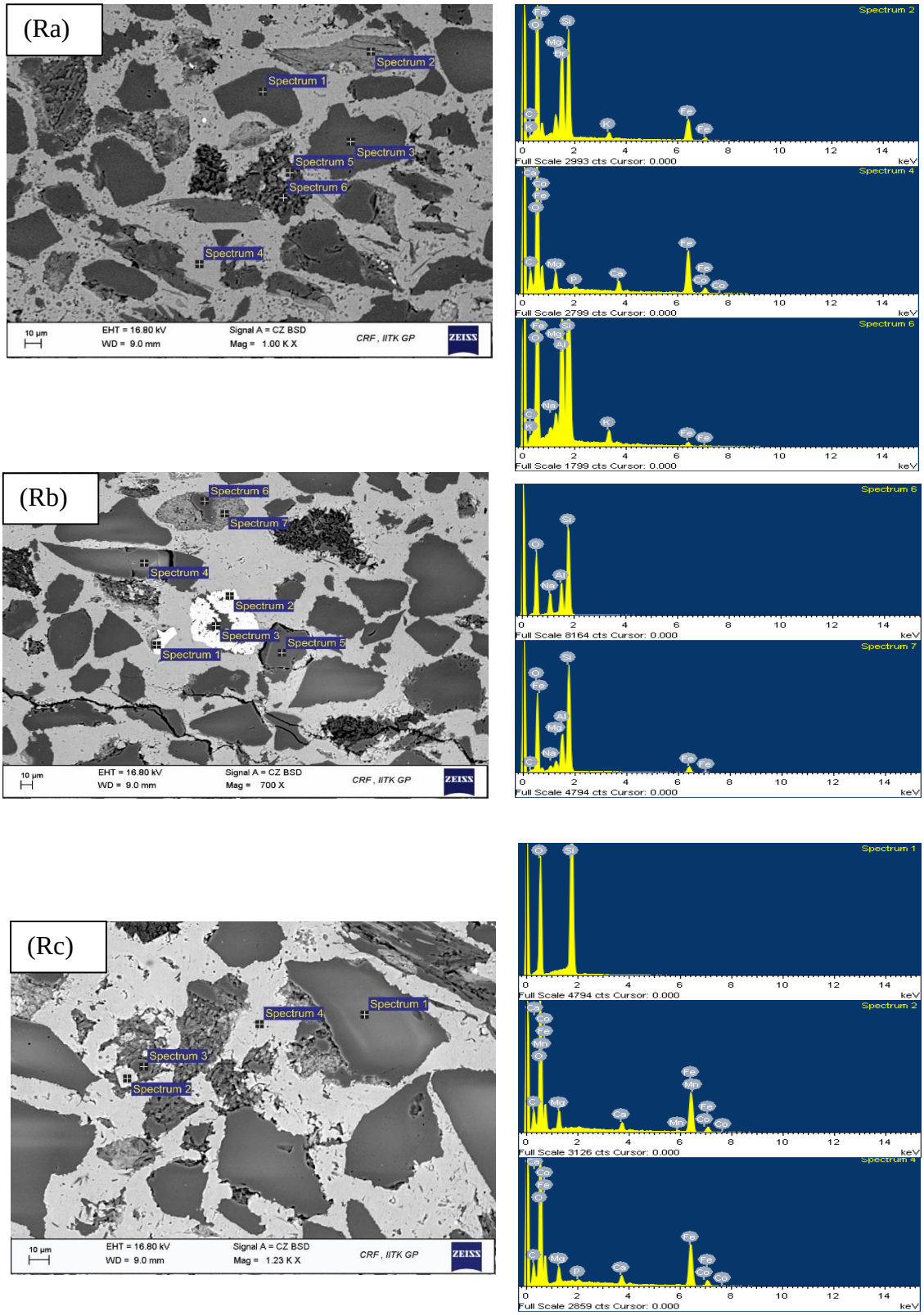

Figure 6.11: SEM and EDX of Ra, Rb, and Rc

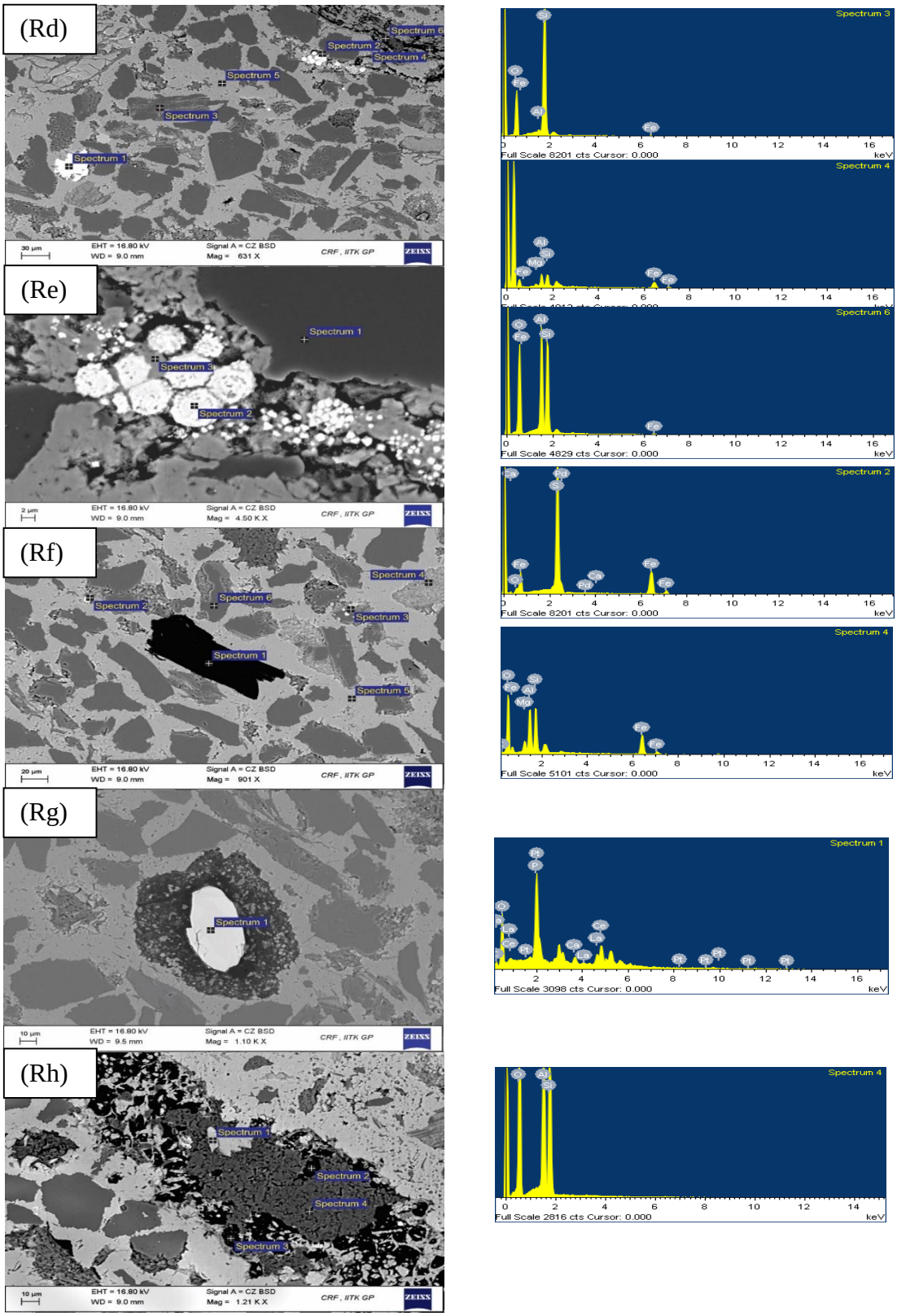

Figure 6.12: SEM and EDX of Rd, Re, Rf, Rg, and Rh

Table 6.4: Percentage of major oxides in the sandstone samples

Sample No.	SiO_2	Al_2O_3	Fe_2O_3 (T)	MnO	MgO	CaO	Na_2O	K_2O	TiO_2	P_2O_5
L1	80.1	14.31	1.79	0.001	0.62	0.13	0.49	1.72	0.65	0
L5	76.91	13.71	3.61	0.001	1.34	0.17	0.66	2.14	0.74	0.13
L8	84.13	10.95	1.44	0.001	0.41	0.19	0.47	1.32	0.89	0
L11	87.59	6.85	1.81	0.001	0.49	0.17	0.39	0.97	0.58	0
L14	75.88	18.79	0.77	0.005	0.48	0	0.62	2.21	0.95	0
L15	69.06	20.07	3.75	0.002	1.55	0	0.68	2.61	1.18	0
L17	83.34	13.02	0.52	0.007	0.34	0.16	0.45	1.31	0.67	0
L22	86.67	9.23	0.74	0.005	0.35	0.21	0.4	1.1	1.07	0
L23	94.52	2.78	0.73	0.001	0.25	0.3	0.44	0.3	0.24	0
L24	82.07	10.41	2.74	0.002	1.01	0.21	0.6	1.64	0.58	0.12
J1	68.74	16.58	7.84	0.004	1.42	0.34	1.15	2.08	1.08	0.17
J2	71.24	13.98	8.33	0.005	1.31	0.44	1.16	1.76	0.91	0.18
J4	67.91	12.88	7.3	0.007	1.69	5.6	1.42	1.51	0.97	0.16
J6	63.92	14.13	10.12	0.004	2.28	1.53	1.18	1.49	0.85	0.15
J10	70	12.95	6.65	0.001	1.22	0.14	1.33	1.52	0.87	0.16
J12	83.23	8.89	3.28	0.001	0.96	0.13	1.22	1.07	0.77	0.11
J16	64.53	18.22	9.67	0.005	1.98	0.47	1.22	1.99	1.17	0.18
J17	81.95	10.39	3.44	0.001	0.92	0	0.97	1.21	0.68	0.18
J19	80.76	11.07	4.15	0.002	0.81	0.14	0.64	1.31	0.75	0.13
J21	68.95	16.07	7.24	0.006	1.5	1.28	1.37	1.97	1.11	0.19
R1	90.41	4.83	1.72	0.001	0.56	0.27	0.67	0.72	0.48	0
R3	79.11	10.85	4.58	0.006	1.16	0.27	1.01	1.68	0.72	0.15
R6	78.7	11.57	4.17	0.003	0.98	0.65	1.25	1.56	0.75	0.11
R8	83.66	8.96	2.56	0.002	0.91	0.22	0.9	1.43	0.63	0.12
R10	78.59	11.52	4.11	0.001	1.11	0.22	1.19	1.6	1.02	0.16
R12	80.36	11.13	3.04	0.001	1.09	0.25	1.24	1.62	0.9	0.15
R17	73.73	12.03	5.02	0.002	1.04	0.32	1.38	1.68	1.13	0.2
R18	75.04	11.4	4.68	0.004	1.35	2.93	1.26	1.41	0.84	0.12
R23	89.83	6.93	0.97	0	0.27	0.21	0.31	0.83	0.43	0
R30	85.58	8.47	1.94	0.001	0.74	0.24	0.84	1.25	0.69	0

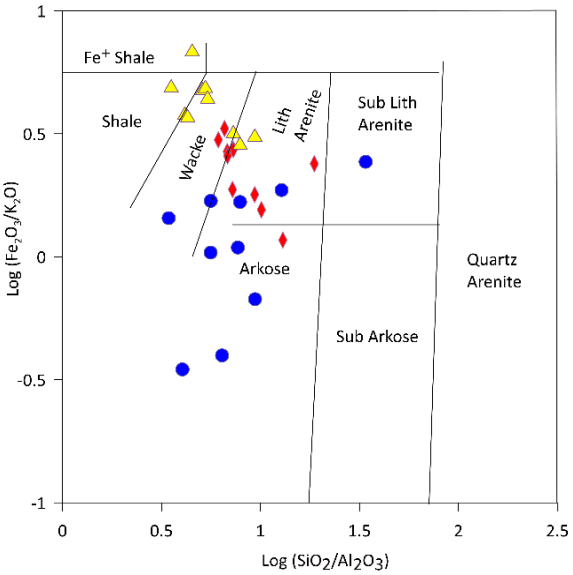

Figure 6.13: [log (Fe_2O_3/K_2O) vs log (SiO_2/Al_2O_3)] (after Herron, 1988)

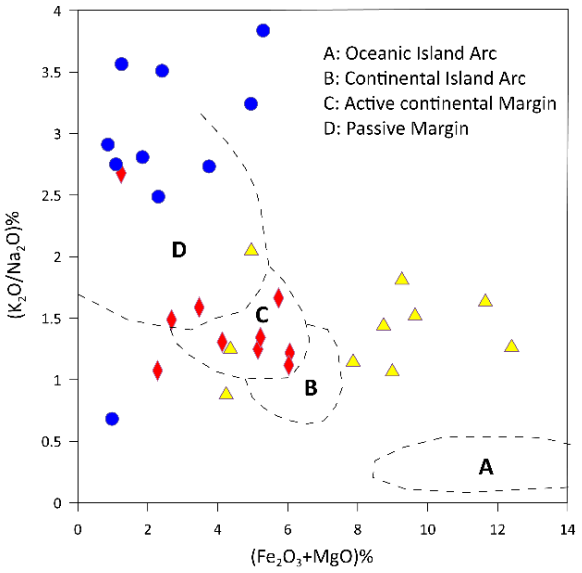

Figure 6.14: (K_2O/Na_2O vs Fe_2O_3/MgO) (after Bhatia, 1983)

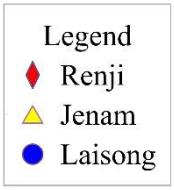

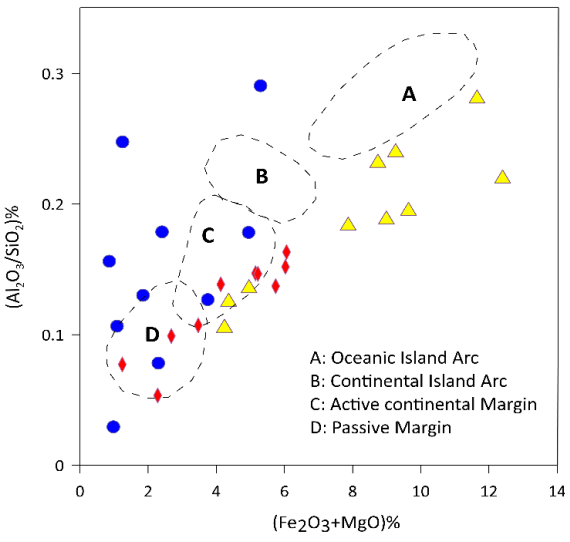

Figure 6.15: (Al_2O_3/SiO_2 vs Fe_2O_3/MgO) (after Bhatia, 1983)

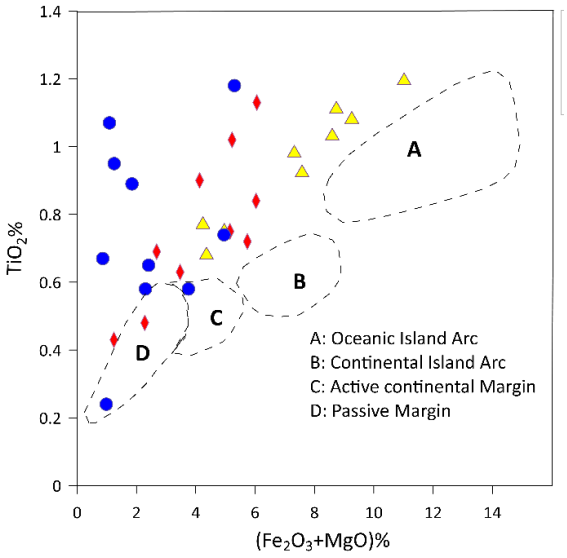

Figure 6.16: (TiO_2 vs Fe_2O_3/MgO) (after Bhatia, 1983)

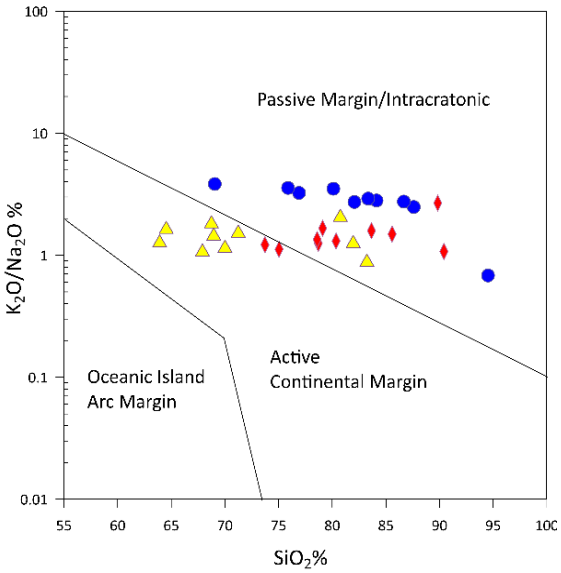

Figure 6.17: (K_2O/Na_2O) vs (SiO_2) (after Roser & Korsch, 1986)

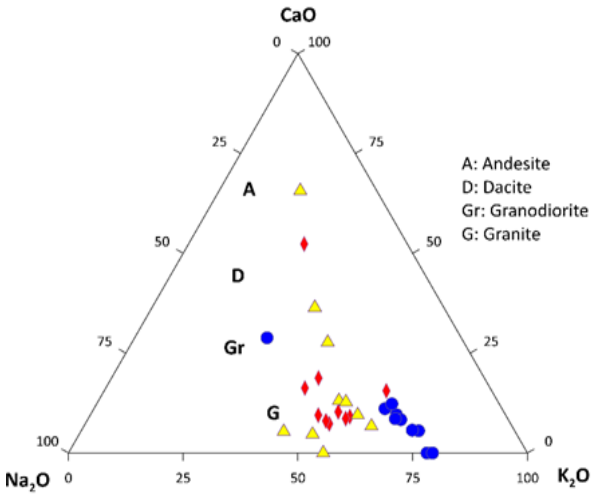

Figure 6.18: Ternary Plot of CaO-Na_2O- K_2O (after Le Maitre, 1976)

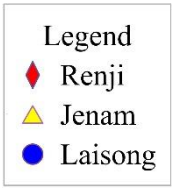

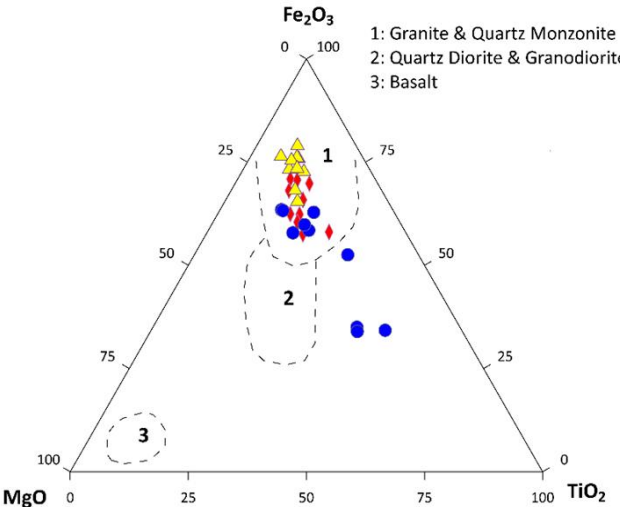

Figure 6.19: Ternary Plot of Fe_2O_3-MgO-TiO_2 (after Condie, 1967)

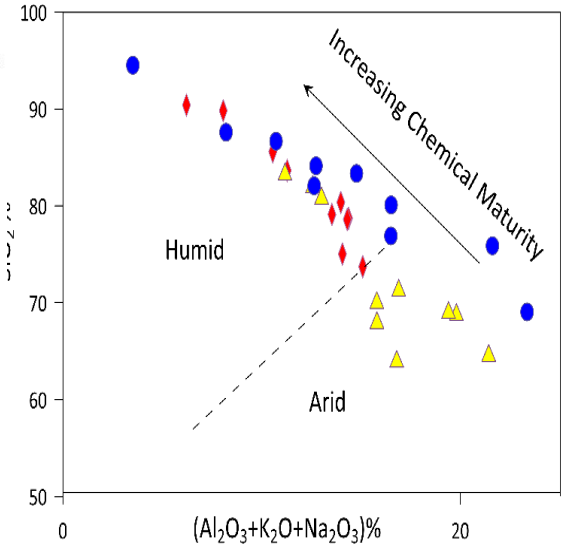

Figure 6.20: (SiO_2) vs (Al_2O_3+K_2O+Na_2O) (after Suttner & Dutta, 1986)

Table 6.5: Geochemical weathering parameters of Barail sandstones (where, CIA: Chemical Index of Alteration after Nesbitt and Young (1982); PIA: Plagioclase Index of Alteration after Fedo *et al*., (1995); CIW: Chemical Index of Weathering after Harnois (1988); ICV: Index of Chemical Variability after Cox *et al*., (1995)

Sample No.	CIA	PIA	CIW	ICV
L1	85.95	95.31	95.85	0.38
L5	82.19	93.31	94.29	0.63
L8	84.69	93.59	94.32	0.43
L11	81.74	91.30	92.44	0.64
L14	86.91	96.40	96.81	0.27
L15	85.92	96.25	96.72	0.49
L17	87.15	95.05	95.52	0.27
L22	84.37	93.02	93.80	0.42
L23	72.77	77.02	78.98	0.81
L24	80.95	91.54	92.78	0.65
J1	82.28	90.68	91.75	0.84
J2	80.62	88.42	89.73	1.00
J4	60.16	61.83	64.72	1.44
J6	77.09	82.35	83.91	1.24
J10	81.24	88.60	89.81	0.91
J12	78.60	85.28	86.82	0.84
J16	83.20	90.57	91.51	0.91
J17	82.66	90.44	91.46	0.69
J19	84.12	92.60	93.42	0.70
J21	77.67	84.18	85.84	0.90
R1	74.42	81.39	83.71	0.92
R3	78.57	87.75	89.45	0.87
R6	76.98	84.05	85.89	0.81
R8	77.85	87.05	88.89	0.74
R10	79.28	87.56	89.10	0.80
R12	78.16	86.45	88.19	0.73
R17	78.07	85.89	87.62	0.88
R18	67.06	70.45	73.12	1.09
R23	83.70	92.15	93.02	0.44
R30	78.43	86.99	88.69	0.67

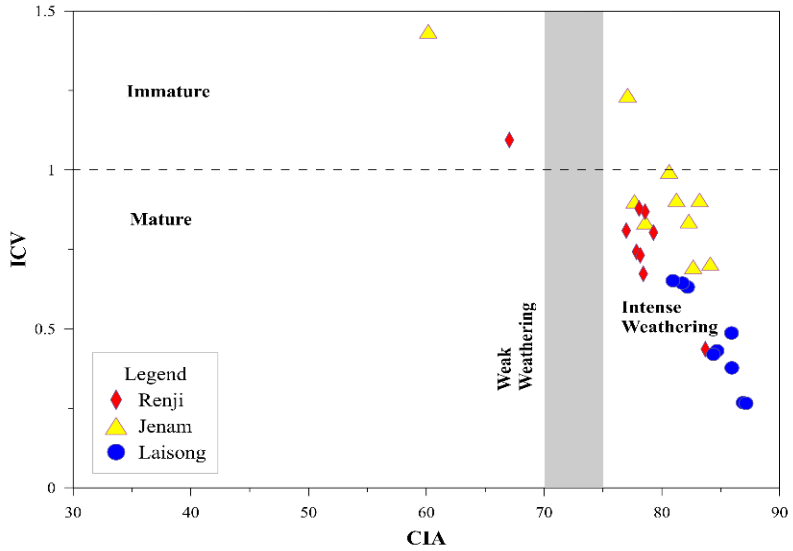

Figure 6.21: Binary plot of CIA vs ICV after Long *et al*., (2012) representing maturity and weathering nature of Barail sandstones

CHAPTER 7
DEPOSITIONAL ENVIRONMENT AND TECTONO PROVENANCE

7.1 RECONSTRUCTION OF PALAEOENVIRONMENTS

A sedimentary environment is characterized by a set of physical, biological and chemical processes operating at a specified rate and intensity. Different sedimentary environments may have a lot of commonalities but each of them have their own unique characteristics. It is the study of modern sediments (Johnson and Stride, 1969; Swift, 1969; Swift *et al*., 1971; Hubert and Hyde, 1982; Reading, 1986) which has helped in understanding the environment of the past. Such studies also help interpret the ancient products in terms of catastrophic and normal processes and their resultant facies mosaic in space and time. The normal sedimentary processes persisting for longer duration include, pelagic sedimentation, organic growth, climatic changes, tidal and fluvial currents and diagenetic modifications. The catastrophic processes which occur instantaneously include floods, storm surges, earthquakes, tectonic impulses and volcanism. According to Goldring (1965), preservation potential of the depositional environment controls the development of the depositional facies. On the basis of lithology including grain size, geometry, sedimentary structures, palaeocurrents, fossils and facies associations a regional framework sequence can be developed for the ancient sediments. This help in the reconstructions of depositional environment and development of a suitable conceptual model.

The present study suggests that the Oligocene Barail sediments were deposited in a marginal marine environment (Boggs Jr., 2012)/ mesotidal coastal complex (Hayes, 1975) with fluctuating energy regime. It's a zone characterized by fluvial and sea processes including waves and tides. The main depositional system of the marginal marine environment/mesotidal coastal complex includes deltas, beaches, barrier islands, tides and shoreface. Estuaries and lagoons are also part of the marginal marine environments. However, they are characteristic of a transgressive coast whereas deltas are features of regressive coasts (Boggs Jr., 2012).

The Laisong and Renji Formations are dominantly arenaceous in composition whereas Jenam Formation shows a mixed sand-shale lithology. Such lithological variations through time among the Barail sediments may be explained as the result of the tectonically controlled fluctuation in the sea level. The fluctuations of the sea level could be either due to glacial activities or changes in the basin geometry or high sedimentation rate and tectonic movement. Local tectonic subsidence or uplift can also affect the shore line significantly.

The study area presents dominantly coarsening upward sequences suggesting a regressive phase of the sea level. However, within dominantly coarsening upward sequences a few fining upward trends have also been observed. According to Leeder (1982), such environmental setup may be explained as progradation of the shoreface towards offshore

which have been crisscrossed by the fining upward tidal-inlet channel deposits. The tectonic impulses and fluctuating energy regimes are responsible for the fining upward sequences.

In the present study altogether ten (10) lithofacies have been identified and are interpreted for their depositional environments/sub environments. The description of various depositional environments/sub environments responsible for development of different lithofacies in the Barail Group of rocks is given below:

7.1.1 MESOTIDAL SHOREFACE ENVIRONMENT

The main barrier separates mesotidal shoreface region from lagoons and tidal flats of the back of the barrier. This is a highly dynamic system. Along the shoreface various features are formed by the waves and tides. Shoreface begins where the base of a wave first meets the bottom approximately 10-20 m depending upon the size of it (Prothero and Schwab, 2004). The upper shoreface (surf zone) is influenced by plunging waves and wave driven offshore currents. Plane laminations, fine cross lamination, ripple marks and vertical trace fossils are the main features of the upper shoreface. During the unusual high energy waves, as during storm, the upper shoreface is susceptible to weathering. Based on the various depositional features barrier islands are subdivided into several sub environment (Prothero and Schwab, 2004).

Laisong Formation

In the present study, on the basis of the above descriptions and following features, the lithofacies *Sm*/ *Sw*/ *Sr* and *Sx* of Laisong Formation are considered to represent the high energy upper shoreface environment (beach face, inter-tidal channel, sub aqueous levees and inter distributary bay) within a mesostidal coastal complexes (Reading, 1991; Prothero and Schwab, 2004; Srivastava and Pandey, 2005; Reinick and Singh, 1980; Kichu *et al*., 2018; Ozukum *et al*., 2022; Srivastava and Kesen, 2018).

i. Presence of fine to medium sand, low angle cross lamination and vertical burrows of *Skolithos*, *Monocraterion*, *Laevicyclus* and *Ophiomorpha* in the Laisong Formation, with an overall linear or shoe string type bed geometry and also the presence of medium grained channeled sandstones.
ii. Presence of asymmetrical, symmetrical and interference ripples in fine to medium sand lithologies (*Sr* facies).
iii. Presence of wavy laminations and lenticular bedding, ripple laminations, both large and small scale channels in the medium to coarse grained wavy laminated sandstone facies (*Sw* facies).
iv. Presences of fine cross lamination with occasional wave ripple cross laminations within the fine to medium sandstones (*Sx* facies).

v. Presence of well sorted thickly bedded massive medium to coarse grained sandstone facies (*Sm* facies) also suggests an upper shoreface high energy environment.
vi. Presence of coal streak/beds associated with fine grained sand-silt mud unit.
vii. Occurrences of overall a coarsening and thickening upward sequences with a few fining upward patterns.
viii. Presence of moderately to moderately well sorted mature to super mature sandstones having characteristics of tidal channels, channel margin bars and levees.
ix. Laterally extensive and/ or elongate sand body geometry paralleling the palaeoshore.

7.1.2. BARRIER ISLAND-MESOTIDAL SHORELINE ENVIRONMENT

According to Elliot (1986), Prothero and Schwab (2004), and Singh (2012) on mesotidal coasts, short barrier islands are dissected by many tidal channels having a tide range of 2 to 4 meters and they are generally found on passive continental margins. Depending upon the sea level variations barrier island may also migrate. Barrier island deposits typically show laterally extensive sand geometry and constitute a significant part of transgressive and regressive shoreline deposits. Presence of heterolithic facies in association with current formed sedimentary structures is a typical characteristic of barrier island- mesotidal shoreline complex.

On the basis of the above features and field evidences a barrier island mesotidal shoreline complex environments has been interpreted for the deposition of the Jenam Formation.

Jenam Formation

i. Presence of heterolithic facies comprising of sand shale units (*Ss* facies) and fine laminated silt-shale lithologies (*Fl* facies) in association with bidirectional cross laminations/form ripples.
ii. Occurrences of wavy laminations/lenticular bedding with small sands lenses showing fine cross laminations,
iii. Presence of carbonaceous and micaceous material within the Jenam Formation.
iv. Presence of coal streaks/beds in association with carbonaceous shale.
v. Occasional presence of channelled sandstones and small crested asymmetrical ripples within *Sch* facies.
vi. Occurrences of horizontally disposed trace fossils of *Planolites beverleyensis* and *Thalassinoides horizontalis* in the fine sediments of *low* energy environment.

vii. Presence of horizontally disposed *Nerites* ichnofacies also suggest the same as it has been reported from many environments including lagoonal to deltaic to deep marine environments (Rinsberg, 1994; Uchman, 1995).

viii. Colour variations in adjacent beds, and presence of plane/parallel laminations, horizontal traces and coal streaks in very fine to fine sand.

ix. Presence of moderately to moderately well sorted mature to super mature sandstones having characteristics of tidal channels, channel margin bars and levees.

x. Laterally extensive and/ or elongate sand body showing shoestring geometry paralleling the palaeoshore.

7.1.3 DELTA FRONT SUB-ENVIRONMENT

Deltas are formed where rate of supply of the sediments is more than the rate of marine erosion. Deltas are formed on a passive margin coast and are seldom formed on active continental margins. They experience a complex combination of fluvial and marine processes and hence a variety of sub environments. There are three sub environments within a deltaic environment; the delta plane, delta front and the prodelta. Coarsening and thickening upward sequence suggest a tide dominated delta. Tidal distributary channels are less prone to switching and abandonment but can migrate laterally. A wide range of grain sizes are found within the deltaic environment. Depending upon the current strength a variety of structures are produced including ripples, lenticular beds, cross and plane laminations. Coal and organic matter can also be locally found associated with deltaic sediments.

On the basis of the above features and field evidences a delta front sub environments has been envisaged for the deposition of the Renji Formation.

Renji Formation

i. Presence of channels in the fine to medium sandstone facies showing lateral migration in the *Sch* facies also suggests delta front sub environment.

ii. Deltaic environment is also suggested by the presence of fine to medium grained sandstones showing colour variations in the adjacent beds, ripple, plane lamination and coal streak/deposit within *Sl* facies.

iii. Presence of wavy or lenticular bedding, cross laminated sand lenses within fine to medium sandstones alongwith carbonaceous shales in *Sw* facies suggest a delta front environment.

iv. Overall coarsening and thickening upward pattern within Renji sediments.

v. Presence of trace fossil *Palaeophycus striatus* in the *Sl* facies also suggests a transitional environment.

vi. Presence of organic matter and coal streak/deposits also points towards a deltaic environment.

7.2 DEPOSITIONAL HISTORY

Sedimentological studies involving lithofacies analysis, textural, mineralogical and provenance of the Barail sediments indicate the deposition was mainly controlled by tectonics of the region during late Eocene-Oligocene period. This tectonic phase during the evolution of Indo-Myanmar Ranges (IMR) has been characterized by the presence of an epiric sea along passive margin. Acharyya (1990, 2007), suggests that a collision of Naga-Chin-Arakan island with the central Myanmar continental block; took place during early middle Eocene period within the oceanic domain of India. The Eocene-Oligocene uninterrupted sedimentation continued and kept pace with tectonics of the region. The reorganization of the drainage and shifting of the depocenter with fluctuation in the sea level resulted from the subduction of the Indian plate below the Myanmar plate. Naik (1998) and Kumar and Naik (2006) have called this as retrogradation phase resulting in soft collision between the northeastern edge of the Indian plate and the Sinian plate, and transforming the eastern passive margin of India into a collisional belt. According to them, this is a classic example of the transformation of a passive margin into an active margin setting. This soft collision was also responsible for the evolution of Northeast- Southwest trending foreland basin through time as a result of continuously changing plate interaction.

Based on the various features of the studied sediments a deltaic- mesotidal- barrier island-shoreface environments where both tidal and wave processes play important role; has been inferred. A low preservation potential in the upper shoreface regions has been indicated by the presence of gently dipping cross/parallel laminations in the sandstone of the study area. Fining upward sequence within a broad coarsening and thickening sequences reflect the effects of the tidal ebb current.

The conceptual model (Figure 7.1) developed for the Barail sedimentation, shows the distribution of various lithofacies for marginal marine/upper shoreface environmental setup. Distribution of various lithofacies suggests a decrease in the energy conditions across the shelf in response to increasing water depth and decreasing intensity of the waves.

7.3 EVIDENCES FROM ICHNO FOSSILS

Environmental parameters such as oxygen, salinity substrate and energy conditions, controlled the occurrence and distribution of trace fossils. According to Seilacher (1967) a clear relationship between distribution pattern, bathymetry and hydrodynamic condition exits. All the trace fossils recorded from the Barail sediments are dominantly marine in nature except *Palaeophycus striatus* which has been reported from varied environments including flood

plains and extremely shallow water. In the study area, concentrations of traces are relatively low and they mostly belong to *Skolithos, Cruziana* and *Nerites* ichnoassemblages. *Skolithos* ichnofacies is represented by *Skolithos verticalis, Monocraterion* isp and *Laevicyclus* isp, whereas *Cruziana* ichnofacies i.e. represented by *Chondrites, Planolites beverleyensis, Palaeophycus striatus,* and *Thalassinoides horizontalis*. Another ichnofacies recorded from the studied sediments is represented by *Nerites* isp.

Skolithos ichnofacies are generally found in well sorted, clean, and shifting particulate substrates which is present in relatively high level of current or wave energy. According to MacEachern *et al.*, (2007) such conditions are common in the shoreface and sheltered foreshore though they are found in wide range of high energy shallow water environment. Both Frey *et al.*, (1990) and MacEachern *et al*., (2007) have suggested that *Skolithos* ichnofacies generally grades seaward into *Cruziana* ichnofacies for an idealized shoreface models for trace fossils. Frequent high energy events and changes in sedimentation rate are found to be associated with *Skolithos* ichnofacies (Walker and James, 1992; Singh *et al.*, 2008). Unconsolidated substrate and relatively moderate to low energy conditions is suggested by the presence of *Planolites* (Tiwari *et al.*, 2011). *Cruziana* ichnofacies favours the area where current action is less intense and food settles on the surface. This zone is dominated by tracks, trails and tunnels. The *Cruziana* assemblage is generally found in a shallow marine setting with moderate energy and uniform salinity (Pemberton *et al*., 1992; Sudan *et al*., 2002; MacEachern *et al*., 2007; Singh *et al*., 2008; Khalo and Pandey, 2018; Kichu *et al*., 2018; Ozukum *et al*., 2022). Presence of horizontally disposed traces indicates a reduced energy conditions similar to lower shoreface-offshore marine/ barrier island settings. *Nerites* ichnofacies has been reported from diverse environments including lagoonal to deltaic to deep marine environments (Rinsberg, 1994; Uchman, 1998). Presence of horizontal trace of *Palaeophycus striatus* also suggest low energy environments/ deltaic sequences (Wenger *et al*., 2025).

Occurrences of mixed ichnoassemblages and their distribution suggests a fluctuating environmental regime with moderate to strong energy conditions within barrier island mesotidal -shoreface complex.

7.4 TECTONO PROVENANCE

Many workers (Dickinson and Suczek, 1979; Ingersoll and Suczek, 1979; Dickinson and Valloni, 1980; Dickinson, 1982; Suczek and Ingersoll, 1985 and Korsch, 1984) have attempted to correlate the framework composition of sandstones with tectonic provenance, basin settings and also the plate interaction in the geologic past. Later Uddin and Lundberg (1998a), Singh *et al.,* (2004), Srivastava *et al.,* (2004), Allen *et al.,* (2008), Srivastava and

Pandey (2011) and Richa and Srivastava (2024) have also made similar attempts to correlate the proportion of the framework constituents to that of tectonic settings.

However, Mack (1984) suggests that some sandstone deposited during transitional tectonic regimes, sandstones containing detrital carbonate and some of the quartzose sandstone may introduce some error population and accurate provenance may not be interpreted.

Mack (1984) also suggests that such categories of sandstone are anomalous in composition and exceptions to the plate tectonic regimes. He also suggested that the while applying sandstone petrography as an indicator of plate tectonic settings; processes and conditions under which the sandstones were deposited should be taken into interpretation.

Table 6.2 presents the recalculated modal data of the Barail sandstones. Based on the observations made on Barail sandstones through the present work, it may be envisaged that the basin received sediments from mixed provenance. The presence of sedimentary, metamorphic and igneous rock fragments and the dominance of monocrystalline non-undulatory quartz grains, also supports a mixed provenance. Blatt *et al*., (1980), illustrated that the dominance of monocrystalline non-undulatory quartz in the sandstones points towards pre-existing sedimentary rocks, fine-grained schists, phyllites and slates and volcanic and hypabyssal igneous rocks within a tectonically active setup. Also the presence of non-undulatory quartz, less polycrystalline quartz and sedimentary rock fragments suggest a sedimentary source (Blatt and Christies, 1963). Different types of quartz as provenance indicator is represented below.

Type	Provenance	Reference
1. Quartz undulatory	Undulose extinction > ~ 5 degrees: metamorphic rocks	Krynine (1940), Folk (1974)
2. Quartz nonundulatory	Igneous rocks	Basu *et al*., (1975)
3. Polycrystalline quartz	Metamorphic origin, plutonic rocks	Basu *et al*., (1975)
4. Zoned quartz	Volcanic and plutonic rocks, hydrothermal veins	Boggs and Krinsley (2006)
5. Quartz with inclusions	Hydrothermal veins	Folk (1974)

Based on the framework composition it may also be suggested that the sediments were supplied by igneous, metamorphic and sedimentary sources mainly from the lesser Himalaya (north) the Indian craton (west), and the Ophiolites/Naga Metamorphics (east). Also, the presence of the well-rounded framework grains also point towards supply from the earlier tectonic regimes. Study further suggests that these sediments were derived from a collision suture and fold-thrust belt sources with increased sediment maturity from continental block

provenance. The presence of euhedral, sub-rounded, subhedral to well-rounded zircon, tourmaline, rutile, staurolite, sillimanite, kyanite, sphene, scapolite with some opaques also suggests the same. Similar inferences may also be drawn from the cosmopolitan nature of heavy mineral accumulations in the studied sediments. It can be suggested that the sediments were mainly supplied by a recycled orogen with minor contributions from the craton interior. In addition to that, presence of K-feldspar and plagioclase feldspar in all the three formations point towards a continuous supply from granitic, metamorphic and volcanic sources. Preservation of otherwise susceptible minerals also suggests nearness of the source and short transportation facilitating the preservation of such minerals. This also points towards the drainage reorganization, in the source area in response to the tectonics of the region; thereby bringing sediments from different directions.

Based on the observations made on various discriminatory diagrams, it may be inferred that the Barail sediments had received its detritus mainly from a recycled orogen with some sediment supply from the craton interior. Continued interactions between Indian and Myanmar plates would have brought the Indian craton closer to the basin. Presence of mixed detritus also points towards a transitional and/or active tectonic regime for Barail sedimentation, keeping pace with the changing plate interaction.

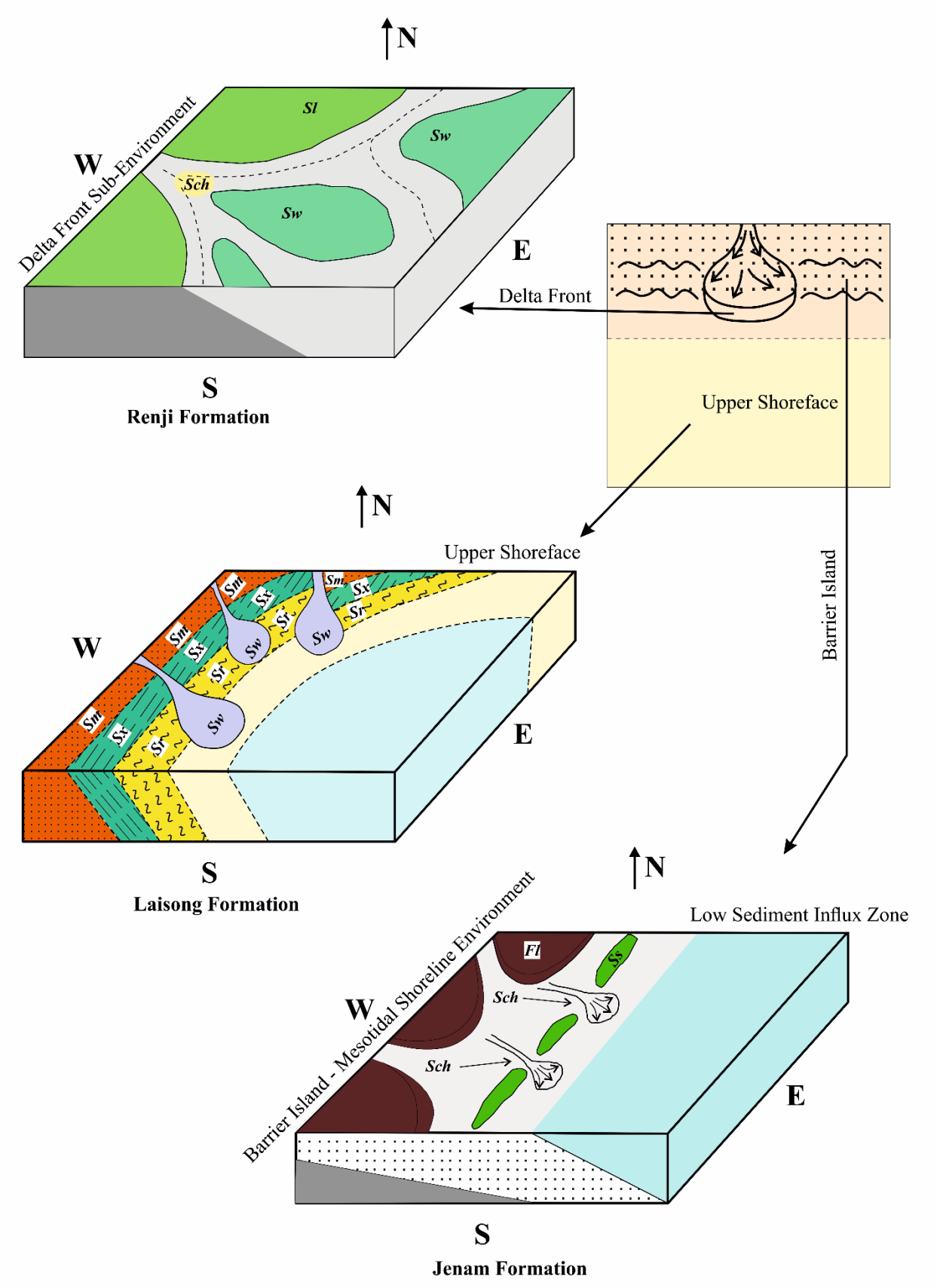

Figure 7.1: Conceptual model for the Barail sediments in the study area

CHAPTER 8

SUMMARY AND CONCLUSION

The study area, located between Piphema and Medziphema towns, is a part of the Belt of Schuppen, where the Oligocene Barail Group of rocks are exposed along Kohima Dimapur National Highway 29 (AH-1). The investigated area forms a part of the Survey of India Toposheet no. 83 G/13 and G/14 and is bounded between N 25°44′50" and N 25°47′00" latitudes and E 93°53′00" and E 93°58′00" longitudes. It provides a unique opportunity to examine their evolution with respect to time and tectonics of the region. In the Belt of Schuppen, Barail sediments are confined within the Disang and Sanis-Chongliyimsen Thrusts and have been divided into Laisong, Jenam and Renji Formations. Laisong Formation, the oldest litho-unit, is medium to coarse grained occasionally very coarse-grained, well-bedded sandstones consisting of hard, reddish brown to grey/buff colour sand. At places it alternates with hard silty and sandy shales. The Jenam Formation, overlying the Laisong Formation in the east of Pherima village, occurs between Disang and Piphema Thrusts, and is represented by well-bedded, dark grey to grey shale, siltstone and fine grained sandstone units. The Renji Formation, the topmost formation of the Barail Group is represented by well bedded medium to coarse-grained, hard and compact sandstones with alternating beds of siltstone and shale. Plane, small scale cross laminations, ripples, wavy laminations and occurrences of coal streaks and trace fossils have been observed in all the three formations.

Through the present work, an attempt has been made to interpret the depositional environment and also to search for provenance using facies analysis techniques, and the petrographic and geochemical attributes.

To achieve the above objectives, twenty one (21) sandstone samples were examined for their grain size attributes and forty five (45) representative sandstones samples were studied for their modal composition. In addition to that, thirty (30) sandstone samples were also analyzed for their major oxide composition (XRFS). XRD (18 samples) and SEM-EDX (3 samples) studies have also been performed on the sandstone samples for clay mineral contents and also for post depositional changes in the Barail sandstones. More than 150 representative samples were collected from various locations of the study area in time and space. Total ten (10) vertical profile sections were meticulously constructed and carefully examined at suitable locations in the field. Sedimentary structures, including biogenic, were also recorded and photographed to supplement the field data.

To simplify and to generalize the observations made in the field for reconstruction of the depositional environments a lithofacies scheme has been developed on the basis of observations made through the study of vertical profile sections. Based on the facies parameters (lithology, grain size, primary sedimentary and biogenic structures and bed geometry) altogether 10 lithofacies have been identified; four (4) in Laisong sediments and

three (3) each from Jenam and Renji Formations. Lithofacies identified in the different formations of Barail Group of sediments are *Sm*, *Sw*, *Sr*, *Sx*, *Ss*, *Fl*, *Sch*, *Sw*, *Sl*, and *Sch* respectively.

Using various bivariate statistical and textural parameters of grain size properties of the Barail sediments attempt has been made for the discrimination of the depositional environments. For discriminating among the broad aspects of the depositional environment, the linear discriminant function and log-log plot of (σ_I^2) versus (SK_G/SM_z).*S* (σ_I^2) and multigroup discrimination and plot of V_1 and V_2 with $V_1 \Lambda V_2 = 74.4°$ (Sahu, 1964; 1983), have also been employed and a nearshore-shallow marine environment has been interpreted for the deposition of Barail sediments. The C-M plot for the sediments corresponds to generally Class IV and V suggesting that studied sediments have been transported by both graded and uniform suspension with some sediment transported as bed load. The average values for CU and CS for Barail sediments correspond to 210 and 420 microns, respectively. Using Passega's (1964) Cs-C depth diagram a depth range of very shallow to 60/70 m has been estimated within a shallow marine environmental conditions for the deposition of the Barail sediments.

Lithofacies analysis of the sediments of the study area suggests a tectonically controlled uninterrupted deposition of Barail sediments in the Belt of Schuppen. Study further suggests that during the Barail sedimentation, a wide range of sub environments prevailed within a Delta-barrier island-mesotidal shoreface coastal complex. Presence of a heterolithic facies comprising of laterally extensive sand-silt-shale units with coal deposits and horizontal traces (Jenam Formation) between two dominantly arenaceous facies (Laisong and Renji Formations) is a unique feature of Barail sedimentation. This unique sediment built-up could be explained as the result of sea level fluctuations in response to the tectonics of the region, anti-clock wise movement of the Indian plate, rapid sinking/subsidence, progressive shallowing of the basin and subsequent uplift.

Three distinct depositional sub-environments for the three formations of the Barail Group interpreted on the basis of the lithofacies analysis include; high energy shoreface environments (Laisong Formation), the barrier island-mesotidal shoreline environment (Jenam Formation) and the delta front sub-environment (Renji Formation). Distribution of various lithofacies of the Barail sediments within the study area also suggests that the deposition of Barail sediments had been influenced by the fluctuating sea level in response to changing plate interaction during upper Eocene-Oligocene period. Study suggests that the Barail sediments have been deposited during a dominantly regressive phase. The changing plate interactions during upper Eocene-Oligocene time had reorganized the drainage in the vicinity which in turn had brought sediments form different directions.

The average modal composition of the sediments may be seen in Table 6.1. The sandstones in the study area are quartz arenite, sub-litharenite and sub-feldspathic arenites in composition. They show signatures of both early and deep burial diagenesis. Heavy mineral assemblage coupled with framework grains indicate a mixed provenance with substantial contribution coming from igneous source. Based on the quartz types; contributions from plutonic as well as metamorphic sources have also been inferred. Presence of zoned quartz in these sediments also suggests supply from plutonic as well as volcanic sources. Similar inferences have also been drawn from geochemical analysis. Compositionally, the sediments in the study area are moderately mature to mature. A dominantly humid climate has been envisaged for the weathering and erosion of sediments.

Ternary plots of QFL, Q_mFL_t, Q_mPK and $Q_pL_vL_s$ (Dickinson and Suczek, 1979) and Q_mFL_t (Dickinson *et al*., 1983) suggest that Barail sediments were largely supplied by recycled orogen, collision suture and fold thrust belt sources with contributions also coming from cratonic sources. Presence of both potash (orthoclase and microcline) and plagioclase feldspar, various lithic fragments and cosmopolitan nature of heavy minerals also support the above view. Based on the location of the basin and time of deposition it may be suggested that the sediments were supplied most probably by the Indian craton lying in the West, the lesser Himalaya in the North, the Ophiolites and Naga Metamorphics in the east and also from the sediments formed under earlier tectonic regimes.

Presence of otherwise susceptible mineral such as orthoclase and microcline in the studied sediments also suggest that not only the source was lying close to the basin, but also basin was undulatory in nature thereby restricting long transportation and preservation of such minerals. High rate of sediment supply and quick burial can also help in the preservation of susceptible minerals. Continuously changing plate interaction through time had resulted in the deposition of such a mixed detritus where sediments formed under earlier tectonic regimes had also contributed to the basin. Geochemical analysis (major oxides) of these sediments also supports the above views and confirms the inferences drawn from petrographic studies.

On the basis of distribution of the various lithofacies within the study area, a conceptual model for their origin has been envisaged. The depositional model represents a marginal marine depositional setup of Delta-barrier island - mesotidal coastal complex where appreciable tidal currents played important role. On the basis of lithofacies distributions, a progressive decrease in the energy of the medium across the shelf in response to increasing water depth and decreasing intensity of wave disturbances has been visualized. A summary of characteristic features of all the lithofacies has been presented below in Table 8.1.

The Barail Group of rocks in the study area have undergone diagenesis till the mesogenetic stage. A flow chart representing the regimes of diagenesis and the processes involved has been shown in Figure 8.1.

Table 8.1: Summary of all the characteristics features of the Barail sediments

Formation	Lithofacies	Sedimentary features	Framework grains	Heavy minerals	Ichnofossil	Depositional Environment
LAISONG	*Sm*, *Sw*, *Sr*, *Sx*	Massive sandstone, thickly bedded, plane and cross lamination, lenticular/wavy laminations, asymmetrical ripples, symmetrical ripples, moderate bioturbation, coal streaks, cross bedding	Q 76.05%, F 3.13%, RF 5.80%, mica 3.70%, HM 5.20%, cem 2.04%, matrix 4.08%	Zircon, Tourmaline, Rutile, Kyanite, Sillimanite, Staurolite, Sphene, Scapolite, Opaques ZTR Index 88.24%	*Laevicyclus*, *Skolithos*, *Moncraterion*, *Chondrite* isp	Intertidal, shallow marine upper shoreface environment
JENAM	*Ss*, *Fl*, *Sch*	Bidirectional cross laminations, lenticular beddings, ripples and ripple cross laminations	Q 65.89%, F 3.51%, RF 4.68%, HM 5.42%, mica 7.75%, cem 3.09%, matrix 9.73%	Zircon, Tourmaline, Rutile, Sillimanite, Kyanite, Sphene, Scapolite, Staurolite, Opaques ZTR Index 64.52%	*Thallasinoides horizontalis*	Barrier island-shoreline mesotidal complex
RENJI	*Sw*, *Sl*, *Sch*	Symmetrical and asymmetrical ripples, Wavy laminations, coal streaks/beds, Channels	Q 71.48%, F 2.83%, RF 5.09%, HM 4.76%, mica 5.72%, cem 3.96%, matrix 6.16%	Tourmaline, Zircon, Kyanite, Scapolite, Staurolite, Sillimanite, Sphene, Rutile, Opaques ZTR Index 67.14%	*Palaeophycus striatus*	Delta front sub environments

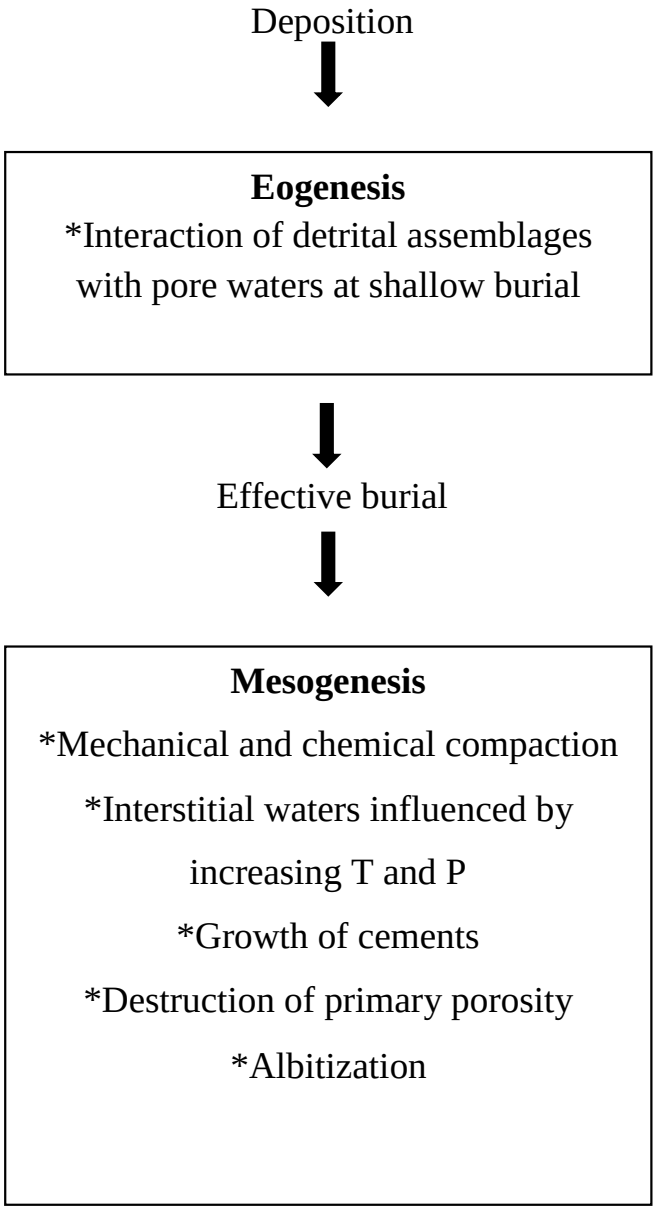

Figure 8.1: Flow chart showing the diagenetic regimes (after S. Boggs Jr, 2009)

REFERENCES

Acharyya, S. (1982). Structural framework and tectonic evolution of the Eastern Himalaya. *Himalayan Geology*, v.10, pp.412-439.

Acharyya, S. (1990). Pan-Indian Gondwana Plate break up and evolution of the northern and eastern collision margins of the Indian Plate. *Jour. Him. Geol.*, v.1, pp.75-91.

Acharyya, S. (2007). Evolution of the Himalayan Palaeogene foreland basins, influence of its litho-packet on the formation of thrust related domes and windows in the Eastern Himalayas − A review, *Jour. Asian Earth Sci.* 31. pp.1-17.

Agrawal, O. P. and Kacker, R. N. (1979). Nagaland ophiolites-a subduction zone ophiolite complex in a Tethyan orogenic belt. In (Panayioutou. A. ed). *Proceedings, International Ophiolite Symposeum, Cyprus*, pp.455-461.

Agarwal, O.P. and Ghose, N.C. (1986). Geology and stratigraphy of Naga Ophiolite between Meluri and Awankho, Phek District, Nagaland, India. In. *Ophiolites and Indian Plate Margins* (*Ed*s. N.C. Ghose and S. Vardharajan), pp.163-195.

Aier, I., Luirei, K., Bhakuni, S.S., Thong, G.T. and Kothyari, G.C. (2011). Geomorphic evolution of Medziphema intermontane basin and Quaternary deformation in the schuppen belt, Nagaland, NE India. *Zeit. für Geo*., v. 55, pp.247-265.

Allen, J.R.L. (1966). Note on the use of plaster of Paris in flow visualization and some geological applications, *Journal of Fluid Mechanics*. 25. pp.331-335.

Allen, J.R.L. (1967). Depth indicators of clastic sequences, *Marine Geology*. 5. pp.429-446.

Allen, J.R.L. (1982). Simple models for the shape and symmetry of tidal sand waves. Dynamically stable symmetrical equilibrium forms, *Marine Geology*. 48. pp.51-73.

Allen, R., Najman, Y., Carter, A., Barfod, D., Bickle, M.J., Chapman, H.J., Garzanti, E., Vezzoli, G., Ando, S., and Parrish, R.R. (2008). Provenance of the Tertiary sedimentary rocks of the Indo-Burman Ranges, Burma-Burma arc or Himalayan derived? *Jour. Geol. Soc. London*, v.165, pp.1045-1057.

Anderton, R. (1985). Clastic facies models and facies analysis. *Geological Society, London, Special Publications*, *18*(1), pp.31-47.

Armitage, P. J., Worden, R. H., Faulkner, D. R., Aplin, A. C., Butcher, A. R., and Iliffe, J. (2010). Diagenetic and sedimentary controls on porosity in Lower Carboniferous fine-grained lithologies, Krechba field, Algeria. A petrological study of a caprock to a carbon capture site. *Marine and Petroleum Geology*, *27*(7), pp.1395-1410.

Armitage, P. J., Worden, R. H., Faulkner, D. R., Aplin, A. C., Butcher, A. R., and Espie, A. A. (2013). Mercia Mudstone Formation caprock to carbon capture and storage sites. Petrology and petrophysical characteristics. *Journal of the Geological Society*, 170 (1), pp.119–132.

Bassey, C. E., Ite, A. E., Asuaiko, E. R., and Aidoko, E. E. (2019). Textural and Heavy Minerals Characterization of Coastal Sediments in Ibeno and Eastern Obolo Local Government Areas of Akwa Ibom State–Nigeria. *Jour. Geosciences, 7*(4), pp.191-200.

Bastia, R., Nail, G.C., and Mohapatra P. (1993). Hydrocarbon Prospects of Schuppen Belt, Assam Arakan Basin. Proc. Sec. Seminar on Petro. Basins of India, *Indian Petroleum Publishers, Dehradun, India*, v.1, pp.493-509.

Basu, A., Young, S.W., Suttner, L.J., James, W.C., and Mack, G.H. (1975). Re-evaluation of the use of undulatory extinction and poly-crystallinity in detrital quartz for provenance interpretation. *Jour. Sed. Petrol.*, v.45, pp.873-882.

Bezbaruah, D., Kashyap, K., and Boruah, M. P. (2016). Field geology and morphometric evidences supporting active tectonics of Amguri-Tuli-Merangkong area in the Assam-Nagaland border, India. *South East Asian Journal of Sedimentary Basin Research*, 2-3-4(1), pp.37-46.

Bhatia, M.R. (1983). Plate tectonics and geochemical composition of sandstones. *The Jour. of Geol.*, v.91 (6), pp.611-627.

Billings, E. (1862). New species of fossils from different parts of the Lower, Middle and Upper Silurian rocks of Canada. In. *Palaeozoic Fossils, Geological Survey of Canada Adv Sheet*, v.1 (1861–65), pp.96–168.

Bjorkum, P.A. and Gjelsvik, N. (1988). An isochemical model for formation of authigenic kaolinite, K- feldspar and illite in sediments, *Journal of Sedimentary Petrology*. 58. pp.506-511.

Blatt, H. and Christie, J.M. (1963). Undulatory extinction in quartz of igneous and metamprphic rocks and its significance in provenance studies of sedimentary rocks. *Jour. Sed. Research*, v.33 (3), pp.559-579.

Blatt, H., Middleton, G., and Murray, R. (1980). Origin of Sedimentary Rocks. *Prentice Hall Inc., Englewood Cliffs, New Jersey*. 782p.

Boggs, S., Jr. and D. Krinsley. (2006). Application of Cathodoluminescence Imaging to the Study of Sedimentary Rocks. *Cambridge University Press, Cambridge*.

Boggs, S., Jr. (2009). Petrology of Sedimentary Rocks. 2nd Edition, *Cambridge University Press, New York*. 600p.

Boggs, S., Jr. (2012). Petrography of Sedimentary Rocks, 5th Edition, *Cambridge University Press*. 600p.

Boles, J.R. (1982). Active albitization of plagioclase, Gulf Coast Tertiary, *Amer. Jour. Sci.* 282. pp.165-180.

Borak, B. and Friedman, G.M. (1981). Textures of sandstones and carbonate rocks in the world's deepest wells (in excess of 30,000 ft. or 9.1 km). Anadarko Basin, Oklahoma, *Sedimentary Geology*. 29. pp.133-151.

Borgohain, P., Bezbaruah, D., Gogoi, M. P., Gogoi, Y. K., Phukan, P. P., and Bhuyan, D. (2021). Petrography and diagenetic evolution of the Barail sandstones of Naga Schuppen belt, North East India. *Current Science*, *121*(8), pp.1107-1113.

Bromley, R.G., (1996). Trace Fossils. Biology, Taphonomy and Applications. *Chapman and Hall, London,* 361p.

Brunnschweiler, R. (1966). On the geology of Indo-Burman Ranges. *Jour. Geol. Soc. Australia*, v.13, pp.137-194.

Burley, S.D., Kantorowicz, J.D., and Waugh, B. (1985). Clastic diagenesis. *In*. Sedimentology. Recent and Applied Aspects (*Eds*. P. Brenchley and B.P.B. Williams). *Spec. Publ. Geol. Soc. London, Blackwell Scientific Publications, Oxford*. 18. pp.189–226.

Campbell, N. (1967). Tectonics, reefs, and stratiform lead-zinc deposits of the Pine Point area, Canada. *ECON. GEOL. MON.* 3, pp.59-70.

Carozzi, A.V. (1960). Microscopic Sedimentary Petrography. *Wiley, New York-London,* 485p.

Casshyap, S.M. and Khan, Z.A. (1982). Paleohydrology of Permian Gondwana streams in Bokaro basin, Bihar, *J. Geol. Soc. India.* 23. pp.419–430.

Chakradhar, M. and Gaur, M.P. (1985). Geological mapping around Jaluke, Kohima district, Nagaland. *Geol. Surv. Ind. Progress Report (Unpublished),* Field Season pp.1984-1985.

Chakravarti, D.K. and Banerjee, R.M. (1988). Evolution of Kohima Synclinorium − A reappraisal, *GSI*. 115 pts 2 and 4.

Chappell, J. (1967). Recognizing fossil strand lines from grain-size analysis, *Journal of Sedimentary Research*. 37(1). pp.157–165.

Chaudhary, A.R. (1993). Textural parameters of the Nagthat sediments of the Chakarata Hills, Kumaun Himalayas, *Ind. Jour. Earth Sci*. 20(3and4). pp.119-125.

Collinson, J.D. and Thompson, D.B. (1994). Sedimentary Structures, *CBS Publishers, New Delhi*. 198p.

Collinson, J. W., Hammer, W. R., Askin, R. A., and Elliot, D. H. (2006). Permian-Triassic boundary in the central transantarctic Mountains, Antarctica. *Geological Society of America Bulletin*, *118*(5-6), pp.747-763.

Condie, K.C. (1967). Geochemistry of early Precambrian Greywacke from Wyoming, *Geochim. Cosmochim. Acta*. 321. pp.2136-2147.

Conner, C.W. and Frem, J.C. (1966). Precision on linear and aerial measurements in estimating grain size. *Jour. Sediment. Petro.* v.36, pp.397-402.

Conolly, J.R. (1965). The occurrence of polycrystallinity and undulatory extinction in quartz in sandstones. *Jour. Sediment. Petrol.*, v.35, pp.116-135.

Corps, E. V. (1949). Digboi oil field, Assam. *AAPG Bulletin*, *33*(1), pp.1-21.

Cox, R., Lowe, D. R., and Cullers, R. L. (1995). The influence of sediment recycling and basement composition on evolution of mudrock chemistry in the southwestern United States. *Geochimica et Cosmochimca Acta*, 59, pp.2919-2940.

Dapples, E. C. (1962). Stages of diagenesis in the development of sandstones. *Geological Society of America Bulletin*, *73*(8), pp.913-934.

Dapples, E. C., (1972). Some concepts of cementation and lithification of sandstones. *Bulletin of American Association of Petroleum Geologists*, 46, pp.3-25.

Dapples, E.C. (1979). Diagenesis of sandstones. In. *Diagenesis in Sediments and Sedimentary Rocks* (*Eds*. G. Larsen and G.V. Chilingar), *Elsevier*, pp.31-97.

Dasgupta, A. (1977). Geology of Assam-Arakan Region. Quart. J. *Geol. Mini. Min. Soc. Ind*., v. 49, pp.20-36.

Dasgupta, P.K., Chakraborty, P.K., and Dutta, D. (1991) Basinward migrating submarine fan environments from the Barail Group in the North Cachar Hills, Assam-Arakan Orogen, India. In. A.H. Bouma and R.M. Carter (Eds.), Facies Models in Exploration and Development of Hydrocarbon and Ore Deposits. *VSP*, *Utrecht*, *The Netherlands*, 254p

Desikachar, S.V. (1974). A review of the tectonic and geologic history of the Eastern India in terms of Plate Tectonic Theory. *Jour. Geol. Soc. India*, v.15 (2), pp.137-149.

Devdas, V. and Gandhi, P. (1985). Report on Systematic Geological Mapping in (I) Pangti-Oldars area, Wokha District and (ii) Ungma-Longsa Area, and (iii) Anaki-Tuli-Asangma Area, Mokokchung District. *Geol. Surv. Ind. Progress Report (Unpublished).*

Dickinson, W.R. (1970). Interpreting detrital modes of greywacke and arkose. *Jour. Sed. Petrol.*, v.40, pp.695-707.

Dickinson, W.R. and Rich, E.I. (1972). Petrologic intervals and petrofacies in the Great Valley sequence, Sacramento Valley, California. *Geol. Soc. Amer. Bull.*, v.83, pp.3007-3024.

Dickinson, W.R. and Suczek, C.A. (1979). Plate tectonics and sandstone composition. *Amer. Assoc. Petrol. Geol. Bull.*, v.63, pp.2164-2182.

Dickinson, W.R. and Valloni, R. (1980). Plate settings and provenance of sands in modern ocean basins. *Geology*, v.8, pp.82-86.

Dickinson, W.R. (1982). Composition of sandstones in circumpacific subduction complexes and fore arc basins. *AAPG Bull.*, v.66, pp.121-137.

Dickinson, W.R., Beard, L.S., Brakenridge, G.R., Erjave, J.L., Ferguson, R.C., Inman, K.F., Knepp, R.A., Lindberg, F.A., and Ryberg, P.P. (1983). Provenance of North American Phanerozoic sandstones in relation to tectonic setting, *Geol. Soc. Am. Bull*. 94. pp.222-235.

Dilek, Y. (2015). Structure and Petrology of the Nagaland-Manipur Hill Ophiolite Melange Zone, NE India. A Fossil Tethyan Subduction Channel at the India–Burma Plate Boundary. *Episodes*, *38*(4), pp.298-314.

Directorate of Geology and Mining (1978). Status of Geological Work and Mineral Discoveries in Nagaland, *Miscellaneous Report (Unpublished).*

Dott, R.H. Jr. (1964). Wacke, graywacke and matrix- what approach to immature sandstone classification? *Journal of Sedimentary Petrology*, v.34 (3), pp.625-632.

Duane, D. B. (1964). Significance of skewness in recent sediments, western Pamlico Sound, North Carolina, *Journal of Sedimentary Petrology*. 34(4). pp.864–874.

Dutton, S.P. and Diggs, T.N. (1990). Of quartz cementation in the Lower Cretaceous Travis Peak Formation, East Texas History, *Journal of Sedimentary Petrology*. 60. pp.191-202.

Einsele, G. (2000), Sedimentary basins. Evolution, facies, and sediment budget, 2nd ed. *Springer-Verlag, Berlin*, 792p.

Ekdale, A.A., Bromley, R.G. and Pemberton, G.S. (1984). Ichnology. The Use of Trace Fossils in Sedimentology and Stratigraphy, *Short Courses 15, Society of Economic Paleontologists and Mineralogists*.

Elliott, T. (1986). Deltas, in Reading, H. G. (ed.). Sedimentary environments and fades, 2nd ed., *Blackwell Scientific Pub., Oxford*, pp.113-154.

Engel, A. E., Itson, S. P., Engel, C. G., Stickney, D. M., and Cray JR, E. J. (1974). Crustal evolution and global tectonics. a petrogenic view. *Geological Society of America Bulletin*, *85*(6), pp.843-858.

Evans, P. (1932). Tertiary succession in Assam. *Trans. Min. Geol. Inst.*, v. 27(3), pp.155-260.

Folk, R.L. (1951). Stages of textural maturity in sedimentary rocks. *Jour. Sediment. Petrol*. 21. pp.127-130.

Folk, R.L. and Ward, W.C. (1957). Brazos River bar. A study in the significance of grain size parameters, *Jour. Sediment. Petrol*. 27. pp.3-26.

Folk, R.L. (1966). A review of grain size parameters, *Sedimentology*. 6. pp.73-93.

Folk, R.L. (1974). Petrology of Sedimentary Rocks. *Hemphill Publishing Co., Austin, Texas*, 170p.

Folk, R.L. (1980). Petrology of Sedimentary Rock. *Hemphill Publishing Co., Austin, Texas*. 182p.

Frey, R. W. and Pemberton, S. G. (1985). Biogenic structures in outcrops and cores. I. Approaches to ichnology. *Bulletin of Canadian Petroleum Geology, 33*(1), pp.72-115.

Frey, R.W., Pemberton, S.G., and Saunders, T.D.A. (1990). Ichnofacies and bathymetry. A passive relationship. *Jour. Paleon.*, v.64, pp.155-158.

Friedman, G.M. (1961). Distinction between dune, beach and river sands from textural characteristics, *Jour. Sediment. Petrol*. 36. pp.514-529.

Friedman, G.M. (1962). On sorting, sorting coefficient and the log normality of the grain size distribution of sandstones. *Jour. Geol.*, v.70, pp.737-753.

Friedman, G.M. (1967). Dynamic processes and statistical parameters compared for size frequency distribution of beach and river sands, *Jour. Sediment. Petrol*. 37. pp.327-354.

Friedman, G.M. and Sanders, J.E. (1978). Principles of Sedimentology, *Wiley, New York*, 792p.

Fyffe, L. R. and Pickerill, R. K. (1993). Geochemistry of Upper Cambrian-Lower Ordovician black shale along a northeastern Appalachian transect. *Geological Society of America Bulletin*, *105*(7), pp.897-910.

Ganju, J. L. and Khar, B. M. (1985). Structure, tectonics and hydrocarbon prospects of Naga Hills based on integrated remotely sensed data. Petrol. *Asia Jour*, *8*(2), pp.142-151.

Ganju, J. L., Khar, B. M., and Chaturvedi, J. G. (1986). Geology and Hydrocarbon prospects of Naga Hill, south of 27 degree latitude. *Bulletin. Oil and Natural Gas Commission*, v.23 (2), pp.129-145.

Garrels, R. M. and F. T. McKenzie. (1971), Evolution of sedimentary rocks. *W.W. Norton, New York*, 397p.

Gazzi, P. (1966). Le arenarie del flysch sopracretaceo dell'Appennio modenese. correlazioni con il flysch di Monghidero. *Mineralogica et Petrographica Acta*, *12*, pp.69-97.

Geological Survey of India. (1975). *Progress Report for Field Session 1974-75 (Unpublished).*

Geological Survey of India. (1981). Systematic geological mapping around Tuli Merangkong and Changtongya area, Mokokchung district, Nagaland. *Progress Report (Field Season 1977-78).*

Geological Survey of India. (1983). Systematic Geological Mapping of Medziphema-Khonoma-Pulomi Area, Kohima District, Nagaland, *Progress Report for The F. S. 1981-82.*

Geological Survey of India. (2011). Geology and Mineral resources of Manipur, Mizoram, Nagaland and Tripura. Geological Survey of India, *Miscellaneous Publication*, No. 30, Part IV, v.1, (Part-2).

Ghose, N.C., Agrawal, O.P., and Chatterjee, N. (2010). Geological and mineralogical study of eclogite and glaucophane schists in the Naga Hills Ophiolite, Northeast India. *Island Arc*, v. 19, pp.336-356.

Ghosh, S.K. and Chatterjee, B.K. (1994). Depositional mechanism as revealed from grain size measures of the Palaeoproterozoic Kolhan siliclastics, Keonjhar district, Orissa, India, *Sediment. Geol.* 89. pp.181-196.

Goldring, R. (1965). Sediments into rock. *New Scientist*, v.26, pp.863-865.

Goswami, D.N.D. (1960). Geology of Assam. *Dept. Publ*., University of Guwahati.

Grim, R.E. (1968). Clay Mineralogy, *2nd Edition, McGraw-Hill, New York*. 596p.

Hall, J. (1843). Geology of New York, Part 4. Survey of the Fourth Geological District. *Carroll and Cook, Albany*. 525p.

Hall, J. (1852). Paleontology of New York. Volume 2. C. *Van Benthuysen, Albany, New York*. 362 p.

Harris, S.A. (1958). Differentiation of various Egyptian aeolian microenvironments by mechanical composition, *Jour. Sed. Petrol*. 28. pp.164-174.

Hayden, H.H. (1910). Some coalfields in Northeastern Assam. *Geological Survey of India Records*, v.40, No. 4, pp.283-319.

Hayes, M.O. (1975). Morphology of sand accumulation in estuaries - an introduction to the symposium. In. *Estuarine Research v.II, Geol. and Engg*. (*Ed*. L.E. Cronin), *Academic Press, London*, pp.3-22.

Heald, M.T. and Lorese, R.E. (1974). Inference of coating on quartz cementation, *Jour. Sed. Pet.* 44. pp.1269-1274.

Herron, M.M. (1988). Geochemical classification of terrigenous sands and shales from core or log data. *Jour. Sed. Petrol.*, v.58, pp.820-829.

Holycross, M., Cottrell, E. (2018). Rutile Controls on Vanadium During Eclogite Partial Melting. *American Geophysical Union, Fall Meeting 2018, abstract #V33C-0247.*

Howard, J.D. (1972). Trace fossils as criteria for recognizing shorelines in stratigraphic record. In. *Recognition of Sedimentary Environments* (*Eds*. J. K. Rigby and W. M. K. Hambil), *Society of Economic Palaeontologists and Mineralogists Spec. Publ. No.* 16, pp.215–25.

Hubert, J. F. (1962). A Zircon-Tourmaline-Rutile maturity index and independence of heavy mineral assemblage with gross composition and texture of sandstones. *Journal of Sedimentary Petrology*, v.32 (3), pp.440-450.

Hubert, J.F. and Hyde, M.G. (1982). Sheet flow deposits of graded beds and mudstones on an alluvial sandflat playa system, Upper Triassic Blomidon Red Beds, St. Mary's Bay, Nova Scotia. *Sedimentology*, v.29, pp.437-475.

Illing, V.C. (1916). The Oilfields of Trinidad. Proc. *Geol. Assoc.,* Vol.27, 115p.

Imchen, W., Thong, G.T., and Pongen, T. (2014). Provenance, tectonic setting and age of the sediments of the Upper Disang Formation in Phek District, Nagaland. *Jour. Asian Earth Sciences*, v.88, pp.11-27.

Ingersoll, R.V. (1974). Surface textures of first cycle quartz sand grains. *Jour. Sediment. Petrol.*, v.44, pp.151-157.

Ingersoll, R.V. and Suczek, C.A. (1979). Petrology and provenance of Neogene sand from Nicobar and Bengal fans, DSDP sites 211 and 218. *Jour. Sediment. Petrol.*, v.49, pp.1217-1228.

James, W.C. and Oaks, R.Q. Jr. (1977). Petrology of the Kinnikinic quartzite (Middle Ordovician), East Central Idaho, *Jour. Sediment. Petrol*. 47. pp.1491-1511.

Johnson, M.A. and Stride, A.H. (1969). Geological significance of North Sea and transport rates. *Nature*, v.224, pp.1016-1017.

Kakul, Z. (1968). Origin, development and chemical classification of early Palaeozoic sandstone of central Bohemia. *Proc. Int. Geo. Cong.*, pp.61-72.

Kent, W.N., Hickman, R.G., and Dasgupta, U. (2002). Application of a ramp/flat fault model to interpretation of the Naga thrust and possible implications for petroleum exploration along the Naga thrust front. *Am. Assoc. Pet. Geol. Bull.* 86, pp.2023– 2045.

Khalo, A. and Pandey, N. (2018). Palaeoenvironmental significance of ichnofossils assemblages from the Palaeogene sediments of Inner Fold Belt, Naga Hills, NE India. *Jour. Geo. Soc. India*, v.91, pp.201-208.

Kichu, A.M., Srivastava, S.K., and Khesoh, K. (2018). Trace fossils from Oligocene Barail Sediments in and around Jotsoma, Kohima, Nagaland - implications of palaeoenvironment. *Jour. Palaen. Soc. India*, v.63(2), pp.197-202.

Korsch, R.J. (1984). Sandstone composition from the New England orogen, Eastern Australia - implications for tectonic settings. *Jour. Sed. Petrol.*, v.51, pp.212-220.

Krinsley, D.H. and Doornkamp, J.C. (1973). Atlas of Quartz Sand Surface Textures, *Cambridge University Press*. 90p.

Krumbein, W.C. and Pettijohn, F.J. (1938). Manual of Sedimentary Petrology, *Appleton- Century Crofts, New York.*

Krynine, P. D. (1940). Petrology and Genesis of the Third Bradford Sand. *Pennsylvania State College Mineral Industries Experimental Station, Bulletin 27*.

Kumar, R. and Naik, G.C. (2006). Late Eocene to early Oligocene depositional system in Assam Shelf, *6th International Conference and Exposition on Petroleum Geophysics, Kolkata, 2006*, pp.904-910.

Kunte, S. V. (1988). Geomorphic analysis of upper Assam plains and adjoining areas for hydrocarbon exploration. *Journal of the Indian Society of Remote Sensing*, *16*, pp.15-28.

Lakhar, A.C. and Hazarika, I.M. (2000). Significance of grain size parameters in environmental interpretation of the Tipam Sandstones, Jaipur area, Dibrugarh District, Assam, *Jour. Ind. Assoc. Sedimentologists*. 19(1-2). pp.69-78.

Leeder, M.R. (1982). Sedimentology, *George Allen and Unwin, London*. 344p.

LeMaitre, R.W. (1976). The chemical variability of some common igneous rocks, *Jour. Petrol.* 17. pp.589-637.

Long, X., Yuan, C., Sun, M., Safonova, I., Xiao, W., and Wang, Y. (2012). Geochemistry and U Pb detrital zircon dating of Paleozoic graywackes in East Junggar, NW China. Insights into subduction accretion processes in the southern Central Asian Orogenic Belt, Gondwana Re., 21, pp.637-653.

Longkumer, L., Luirei, K., Moiya, J. N., and Thong, G. T. (2019). Morphotectonics and neotectonic activity of the Schuppen Belt of Mokokchung, Nagaland, India. *Journal of Asian Earth Sciences*, *170*, pp.138-154.

Lundgren, S.A.B. (1891). Studier Öfver fossilförande lösa block, *Geol. Fören. Stockholm, Forhandl.* 13. pp.111-121.

MacEachern, J.A., Pemberton, S.G., Gingras, M.K., and Bann, K.L. (2007). The ichnofacies paradigm. A fifty year retrospective. *In*. Trace Fossils. Concepts, Problems, Prospects (*Ed*. W. Miller), Elsevier, Amsterdam, pp.52-77.

Mack G.H. (1984). Exceptions to the relationship between plate tectonics and sandstone composition. *Journal Sedimentary Petrology,* v.54, pp.212-220

Mahendar, K. and Banerji, R.K. (1989). Textural study and depositional environment of sand grains from rocks of Jaisalmer Formation, Jaisalmer District, Rajasthan, India, *Jour. Geol. Soc. India*. 33(3). pp.228-242.

Mallet, F.R. (1876). On the coal fields of Naga Hills bordering the Lakhimpur and Sibsagar Distict, Assam. *Geol. Survey of India*. 12(2).286p.

Mange, M. A. and Maurer, H. F. W. (1992). Heavy Minerals in Colour, *Chapman and Hall, New York*, 147p.

Marzolf, J.E. (1976). Sand grain frosting and quartz overgrowth examined by SEM - the Najavo Sandstone, Utah. *Jour. Sediment. Petrol*., v.46, pp.906-912.

Matthews, N. E., Pyle, D. M., Smith, V. C., Wilson, C. J. N., Huber, C., and Van Hinsberg, V. (2012). Quartz zoning and the pre-eruptive evolution of the~ 340-ka Whakamaru magma systems, New Zealand. *Contributions to Mineralogy and Petrology*, *163*, pp.87-107.

Mason, C.C. and Folk, R.L. (1958). Differentiation of beach, dune and eolian flat environments by size analysis, Mustang Islands, Texas, *Jour. Sediments. Petrol*. 28. pp.211-226.

Mathur, L.P. and Evans, P. (1964). Oil in India, *22nd session*, *Int. Geol. Congress, New Delhi, India*. 85p.

McBride, E. F. (1963). A classification of common sandstones. *Journal of Sedimentary Research*, v.33 (3), pp.664–669.

McLennan, S.M., Hemming, S., McDaniel, D.K., and Hanson, G.N. (1993). Geochemical approaches to sedimentation, provenance and tectonics, *Geol. Soc. Amer. Spl. Paper*. 284. pp.21-40.

Miall, A.D. (1990). Hierarchies of architectural units in clastic rocks and their relationships to sedimentation rate. In. *The Three Dimensional Facies Architecture of Terrigenous Clastic Sediments* (*Eds*. A.D. Miall and Tyler), *Soc. Econ. Palalo. and Mineralogist*.

Middleton, G. V. (1973). Johannes Walther's law of the correlation of facies. *Geological Society of America Bulletin*, *84*(3), pp.979-988.

Middleton, G.V. (1976). Hydraulic interpretation of sand size distributions, *Jour. Geol*. 84. pp.405-426.

Middleton, G. V. (2003). *Encyclopedia of sediments and sedimentary rocks*, Springerp. 821p.

Milliken, K. L. (1992). Chemical behavior of detrital feldspars in mudrocks versus sandstones, Frio Formation (Oligocene), South Texas. *Journal of Sedimentary Research, 62*(5), pp.790-801.

Mishra, U.K. (1983). Palaeontological studies of Disang and Barail sediments in a part of Manipur East district. *Geological Survey of India Unpublished Progress Report.*

Mishra, D. and Tiwari, R.N. (2005). Provenance study of siliciclastic sediments, Jhura Dome, Kachchh, Gujarat. *Jour. Geol. Soc. India*, v.65 (6), pp.703-714.

Moiola, R.J. and Weiser, D. (1968). Textural parameter – an evaluation, *Jour. Sediment. Petrol*. 38. pp.45-53.

Moiya, J.N., Luirei, K., Longkumer, L., Kothyari, G.C., and Thong, G.T. (2019). Late Quaternary deformation in parts of the Belt of Schuppen of Dimapur and Peren districts, Nagaland, *NE India. Geol. J.*

Moore G. F. (1979) Petrography of subduction zone sandstones from Nias Island. Indonesia. *Journal of Sedimentary Petrology* 49, pp.71-84

Morad, S., Bergan, M., Knarud, R., and Nystuen, J.P. (1990). Albitization of detrital plagioclase in Triassic reservoir sandstones from the Snorre Field, Norwegian North Sea, *J. Sediment. Petrol.* 60. pp.411-425.

Moss, A.J. (1972). Bed load sediments, *Sedimentology*. 18. pp.159-219.

Müller, A., Breiter, K., Seltmann, R., and Pécskay, Z. (2005). Quartz and feldspar zoning in the eastern Erzgebirge volcano-plutonic complex (Germany, Czech Republic). Evidence of multiple magma mixing. *Lithos, 80*(1-4), pp.201-227.

Myrow, P.M. (1995). *Thalassinoides* and the enigma of Early Palaeozoic open-framework burrow systems. *Palaios*, v.10, pp.58–74.

Naik, G.C. (1994). Subsurface geology and tectono-sedimentary evolution of pre-Miocene sediments of Upper Assam, India, *PhD thesis submitted to ISM, Dhanbad*.

Naik, G.C. (1998). Tectonostratigraphic Evolution and Paleogeographic Reconstruction of NE India, *Proc. Indo-German Workshop on Border Strandlogy Magnetostratigraphy Pilot Project Calcutta.*

Nandy, D.R. (1976). The Assam Syntaxis of the Himalaya. a re-evaluation. *Geol. Surv. India, Misc. Publ*., v. 24, pp.363-368.

Nandy, D.R. and Dasgupta, S. (1989) Seismotectonics of north eastern India and adjacent parts. *20th International Geological Congress, Abstract* volume, 2, 494p.

Nandy, D.R. (2017). Geodynamics of Northeastern India and the Adjoining Region, Guwahati, India, *Scientific Book Centre*. 272p.

Nazarkin, L. A. (1979). Vliyanie tempa sedimentatsii i erozionnykh srezov na neftegazonosnost'osadochnykh basseinov.

Nechaev, V. P. and Isohording, W. C. (1993). Heavy mineral assemblages of continental margins as indicators of plate tectonic environment. *Journal of Sedimentary Petrology., 63*, pp.1110–1117.

Nesbitt, H. W., Young, and G. M. (1982). Early Proterozoic climates and plate motions inferred from major element chemistry of lutites. *Nature,* 299, pp.715-717.

Nesbitt, H. W., Young. G. M., McLennan, S.M., and Keays, R. R. (1996). Effect of geochemical weathering and sorting on the petrogenesis of siliciclastic sediments, with implications for provenance studies. *The Journal of Geology*, 104, pp.525-542.

Nichols, G. (2009) Sedimentology and stratigraphy. *Blackwell Science Ltd., London,* 335p.

Oldham, R.D. (1883) Report on the geology of parts of Manipur and naga hills. Mem. Geol. Surv. India, v.19(4), pp.216-226.

Ozukum, A., Srivastava, S. K., and Desai, B. (2022). Ichnological study of the Palaeogene sedimentary succession of Botsa, Kohima District, Nagaland, India. *Geological Journal*, *57*(12), pp.5239-5249.

Pandey, N. and Srivastava, S.K. (1998). A preliminary report on Disang-Barail Transition, NW of Kohima, Nagaland (Abst.), *Workshop on Geodynamics and Natural Resources of NE India, Dibrugarh,* 24p.

Pascoe, E.H. (1912). Coal in Namchik Valley, Upper Assam. *Geological Survey of India Records,* v.41, No. 3, pp.214-216.

Passega, R. (1957). Textures as characteristics of clastic deposition, *Bull. Am. Assoc. Petrol. Geol.* 41. pp.1952-1984.

Passega, R. (1964). Grain size representation by CM patterns as a geological tool, *Jour. Sediment. Petrol*. 34. pp.830-847.

Pemberton, S.G., Frey, R.W., Ranger, M.J., and MacEachern, J.A. (1992). The conceptual framework of ichnology. In. Applications of Ichnology to Petroleum Exploration, a Core Workshop (SEPM Core Workshop) (Ed. S.G. Pemberton), *Society for Sedimentary Geology*, v.17, pp.1–28.

Pettijohn, F.J. (1941). Persistence of heavy minerals and geological age. *Jour. Geol.*, V. 49, pp.610-625

Pettijohn, F.J., Potter, P.E. and Siever, R. (1972). Sand and Sandstones, *Springer-Verlag*, New York, 617p.

Pettijohn, F.J. (1975). Sedimentary Rocks, 3rd Edition, *Harper and Row*, 614p.

Pettijohn, F.J. (1984). Sedimentary Rocks, 3rd edition. *CBS Publishers and Distributors, New Delhi*, 628p.

Pitman, E.D. (1972). Diagenesis of quartz in sandstone as revealed by SEM. *Jour. Sed. Petrol.*, v.42, pp.507-519.

Potter, P.E. and Pettijohn, F.J. (1977). Palaeocurrents and Basin Analysis, *Springer-Verlag, New York*. 425p.

Potter, P.E. (1978). Petrology and chemistry of modern big rivers. *Jour. Geol.*, v.86, pp.423-449.

Prothero, R.D. and Schwab, F. (2004). Sedimentary Geology. An Introduction to Sedimentary Rocks and Stratigraphy, 2nd edition, *W.H. Freeman and Company, New York*. 557p.

Quatrefages, M. D. (1849). Note Sur la *Scolicia prisca* (A. Deq.), annelid fossil de la craie. Ann. Sci. Nat. Ser. 3 Zoologie., v.12, pp. 265-266.

Quenstedt, F. A. (1879). Petrefactenkunde Deutschlands. I. Abt. v. 6. Korallen. Die Röhrenund Steinkorallen. L.F. Fues, Leipzig, Germany

RangaRao, A. (1983). Geology and hydrocarbon potential of a part of Assam-Arakan Basin and its adjacent region. *Petroleum Asia Jour.*, pp.127-158.

Rangarao, A. and Samanta, M. K. (1987). Structural style of the Naga overthrust belt and its implication on exploration. *Bull. ONGC, 24*, pp.69-109.

Reading, H.G. (1978). Sedimentary Environment and Facies, *Elsevier, North Holland, New York*, 464p.

Reading, H.G. (1986). Sedimentary Environment and Facies, *Elsevier, North Holland, New York*. 464p.

Reading, H. G. (1991). The classification of deep-sea depositional systems by sediment calibre and feeder systems. *Quarterly Jour. of the Geological Soc. of London*, v.148, pp.427-430.

Reading H.G. and Levell, B. K. (1996). Controls on the sedimentary record. Sedimentary Environments. Processes, Facies and Stratigraphy. 3rd edition. *Blackwell Science Oxford*, pp.5-35

Reineck, H.E. and Singh, I.B. (1980). Depositional Sedimentary Environments. *Springer- Verlag, New York*, 547p.

Richa, H. O. and Srivastava, S. K. (2024). Petrography and tectono-provenance of the Barail Group of rocks, Belt of Schuppen, India. *Journal of Sedimentary Environments, 9*(3), pp.597-613.

Rindsberg, A. K. (1994). Ichnology of the Upper Mississippian Hartselle Sandstone of Alabama, with notes on other Carboniferous formations (No. 158). *Geological Survey of Alabama, Economic Geology Division*.

Roser, B. P. and Korsch, R. J. (1986). Determination of tectonic setting of sandstone mudstone suites using SiO2 content and K2O/Na2O ratio. *The Journal of Geology,* 94, pp.635-650.

Sagoe, K.O. and Visher, G.S. (1977). Population breaks in grain size distribution of sand – a theoretical model, *Jour, Sediment. Petrol*. 47. pp.285-310.

Sahu, B.K. (1964). Depositional mechanism from size analysis of clastic sediments, *Jour. Sediment. Petrol*. 34. pp.73-83.

Sahu, B.K. (1983). Multigroup discrimination of depositional environments using size discrimination statistics, *Ind. Jour. Earth Sci.* 10. pp.20-29.

Sarma, H. (1985). Systematic geological mapping around Pukha-Lungwa-Chenwent-Hyou-Champang areas of Mon district, *Unpublished. Prog. Rep. GSI* (Field Season 1984-85).

Seilacher, A. (1967). Bathymetry of trace fossils. *Marine Geology*, v.5, pp.413-428.

Selley, R.C. (1968). A classification of palaeocurrent models, *Jour. Geol*. 76. pp.349-368.

Selley, R.C. (1970). Ancient Sedimentary Environments, *Chapman and Hall, London*, 273p.

Selley, R.C. (1976). Subsurface environmental analysis of North Sea sediments, *Bull. Am. Assoc. Petrol. Geol.* 60. pp.184-195.

Sengupta, S.M. (1982). Interpretation of log probability graphs of grain sizes in the light of experimental studies (Abst.), *11th International Congress on Sedimentology, Hamilton,* 81p.

Sengupta, S. M. (1994). Introduction to Sedimentology. 1st Edition. *CRC Press*, 325p. ISBN. 978-9054102304

Severin, K.P. (2005). Energy Dispersive Spectrometry of common rock forming minerals. Springer Science and Business Media. *Kluwer Academic Publishers*. 225p.

Singh, R.N. and Adiga K.S. (1977). Systematic Geological mapping in parts of flysch and mollassic sediments around Kiphire, Tuensang district, Nagaland. *Geol. Surv. of India Progress Report for (Field Season 1976-77) (Unpublished),* 16p.

Singh, B.E and Singh, H. (1994). Diagenetic influence and porosity pattern in the sandstones of Murree Group, Jammu Himalaya. *Himalayan Geology*, 15, pp.205-217.

Singh, B.P., Pawar, J.S., and Karlupia, S.K. (2004). Dense mineral data from the north western Himalayas foreland sedimentary rocks and recent sediments- evaluation of the hinderland. *Jour. Asian Earth Sci.*, v.23, pp.23-25.

Singh, R.H., Rodriguez-Tovar, F.J., and Ibotombi, S. (2008). Trace fossils of the Upper Eocene- Lower Oligocene Transition of the Manipur, Indo-Myanmar ranges (North-east India). *Turkish Journal of Earth Sciences*, v.17, pp.821–834.

Singh, B. P. (2012). How deep was the early Himalayan foredeep?. *Journal of Asian Earth Sciences*, *56*, pp.24-32.

Singh, Y. R., Singh, B. P., Murthy, S., Kom, K. B., Singh, K. A., and Guruaribam, V. (2016). Reworked early permian palynomorphs and tertiary palynomorphs from the upper Bhuban Formation (Miocene), Nagaland, India. *Himalayan Geology*, *37*(1), pp.35-41.

Sinha, R. N. and Khan, K. N. (1965). Heavy mineral investigations in Nahan Series near Nahan, Himachal Pradesh. Current Science, 34(11), pp.340-342.

Smith, R. (1966). Grain size measurement in thin section and in grain mount, *Jour. Sediment. Petrol.*, v.36, pp.841-843.

Srivastava, S.K. (2002). Facies Architecture and Depositional Model for Palaeogene Disang-Barail Transition, North West of Kohima, Nagaland, *Ph.D. thesis submitted to Nagaland University, Kohima (Unpublished).*

Srivastava, S.K., Pandey, N., and Srivastava, V. (2004). Tectono-sedimentary evolution of Disang- Barail Transition, NW of Kohima, Nagaland, India. *Himalayan Geology*, v.25(2), pp.121-128.

Srivastava, S.K. and Pandey, N. (2005). Depositional mechanism of Palaeogene sediments at Disang-Barail Transition, NW of Kohima, Nagaland, India. *Jour. Pal. Soc. India*, v.50(1), pp.135-140.

Srivastava, S.K. and Pandey, N. (2008). Palaeoenvironmental reconstruction of Disang- Barail Transition using grain size parameters in Nagaland, *Nagaland Univ. Res. Jour.* 5. pp.164-176.

Srivastava, S.K. and Pandey, N. (2011). Search for provenance of Oligocene Barail sandstones in and around Jotsoma, Kohima, Nagaland. *Jour. Geol. Soc. India*, v.77, pp.433-442.

Srivastava, S.K. and Kesen, K. (2018). Tectonic-sedimentary evolution of Laisong sandstones exposed in and around pherima, Dimapur, Nagaland, *Journal of Applied Geochemistry*. 19(4). pp.471-479.

Srivastava, S.K. and Kichu, A.M. (2021). Mineral assemblages and tectono-provenance of the Oligocene Barail sandstones in parts of Naga Hills of the Assam-Arakan Orogenic Belt, Northeast India. *Geol. Jour.*, v.57 (2), pp.801-817.

Srivastava, S. K. and Kikon, F. (2021). Petrography of Upper Bhuban Surma sandstones in and around Patkai Bridge, Chumukedima, Dimapur, Nagaland. *Recent advances in Earth Science research in northeast India*, pp.101-115.

Srivastava, S. K., Humtsoe, Z. M., Laskar, J. J., and Richa, H. O. (2024). Provenance of the Oligocene Barail Sandstones Exposed in and Around LongsaVillage, Wokha District, Nagaland. Reflections from Petrography and Heavy Minerals. *Journal of Geosciences Research*, 9, pp.23-29.

Stauffer, P.H. (1966). Thin section size analysis – a further note. *Sedimentology*, v.7, pp.261- 263.

Stewert, H.B. Jr. (1958). Sedimentary reflections of depositional environments in San Miguel Lagoon, Baja California, Mexico, *Am. Assoc. Petrol. Geol. Bull*. 2. pp.2567-2618.

Stonecipher, S. A. (2000). Applied sandstone diagenesis Practical petrographic solutions for a variety of common exploration, development, and production problems. SEPM Short Course Notes 50, *SEPM, Tulsa, Okla*., 143p.

Suczek, C.A. and Ingersoll, R.V. (1985). Petrology and provenance of Cenozoic sandform in the Indus Cone and Arabian Basin (DSDP sites 221, 222, 224). *Jour. Sed. Petrol.*, v.55, pp.340-346.

Sudan, C.S., Singh, B.P., and Sharma, U.K. (2002). Ichnofacies of the Murree Group in Jammu area and their ecological implications during late Palaeogene in the NW Himalaya. *Jour. Geol. Soc. India*, v.60, pp.547–557.

Suess, E. (1904). The Face of the Earth. *Oxford University Press*.

Surdam, R.C. and Boles, R.J. (1979). Diagenesis of Volcanic Sandstones (*Eds*. P.A. Scholle and P.R. Schluger).

Surdam, R.C., Crosse, L.J., Hagen, E.S., and Heasler, H.P. (1989). Organic inorganic interactions and sandstone diagenesis, *Amer.Asso. Petrol. Geol. Bull.* 73. pp.1-23.

Suttner, L.J. (1974). Sedimentary petrographic provinces. In. *Paleogeographic Provinces and Provinciality* (*Ed*. C.A. Ross), *Society for Sedimentary Geology, Tulsa*, pp.75-84.

Suttner, L.J., Basu, A., and Mack, G.H. (1981). Climate and the origin of quartz arenites. *Jour. Sed. Petrol.*, v.51, pp.1235-1246.

Suttner, L.J. and Dutta, P.K. (1986). Alluvial sandstone composition and palaeoclimate framework mineralogy. *Jour. Sed. Petrol.*, v.56, pp.329-345.

Swift, D.J.P. (1969). Inner shelf sedimentation. processes and products. In. *The New Concepts of Continental Margin Sedimentation - Application to the Geological Records* (Ed. D.J. Stanley), *Am. Geol. Instt., Washington*, pp.DS.5-1.

Swift, D.J.P., Stanley, D.J., and Curray, J.R. (1971). Relict sediments on continental shelf – A reconsideration. *Jour. Geol.,* v.79, pp.322-346.

Tanner, W.F. (1964). Modification of sediment size distributions, *Jour. Sediment. Petrol*. 34. pp.156-164.

Teichert, C. (1958). Concepts of facies. *AAPG Bulletin*, *42*(11), pp.2718-2744.

Textoris, D.A. (1971). Grain size measurement in thin section. In. Procedures in Sedimentary Petrology (*Ed*. R.E. Craver), *Wiley, New York*, pp.95-108.

Tiwari, R.P., Rajkonwar, C., Lalchawimawii, Malsawma, P.L.J., Ralte, V.Z., and Patel, S.J. (2011). Trace fossils from Bhuban Formation, Surma Group (Lower to Middle Miocene) of Mizoram, India and their palaeoenvironmental significance. *Jour. Earth Syst. Sci.*, v.120, pp.1127–1143.

Torell, O.M. (1870). Suecana Formations, Cambridge. *Lunds University Arsskr.*, v.2, pp.1–14.

Tortosa, A., Palomares, M., and Arribas, J. (1991). Quartz grain types in Holocene deposits from the Spanish central system - some problems in provenance and analysis. In. *Developments in Sedimentary Studies* (*Eds*. A.C. Morton, S.P. Todd and P.D.W. Haughton), *Geol. Soc. Amer. Special Pub., Bath, UK*, v.57, pp.447-454.

Towe, K.M. (1962). Clay mineral diagenesis as a possible source of silica cement in sedimentary rocks. *Jour. Sediment. Petrol.*, v.32, pp.26-28.

Tucker, R.W. (1989). Techniques in Sedimentology. *Blackwell Scientific Publications, Oxford, London*.

Tucker, R.W. (1993). Carbonate diagenesis and sequence stratigraphy. In. *Sedimentology Review* (*Ed*. W.P. Wright), v.1, pp.51-72.

Uchman, A. (1995). Taxonomy and palaeoecology of flysch trace fossils. The Marnoso-arenacea Formation and associated facies (Miocene, Northern Apennines, Italy). *Beringeria, 15*, 3p.

Uddin, A. and Lundberg, N. (1998a). Unroofing history of the Eastern Himalayas and the Indo-Burman Ranges. heavy mineral study of the Cenozoic sediments from the Bengal Basin, Bangladesh. *Jour. Sediment. Research*, v.68 (3), pp.465-472.

Uddin, A. and Lundberg, N. (1998b). Cenozoic history of Himalayan-Bengal system. Bangladesh. *Bull. Geol. Soc. Amer.*, v.110 (4), pp.497-511.

Vadlamani, R., Wu, F. Y., and Ji, W. Q. (2015). Detrital zircon U–Pb age and Hf isotopic composition from foreland sediments of the Assam Basin, NE India. Constraints on sediment provenance and tectonics of the Eastern Himalaya. *Journal of Asian Earth Sciences, 111*, pp.254-267.

Verma, K.P. and Yedekar, D. (1983). Systematic Geological mapping in Unger-Dikhu-Mangmetong-Chungtiya- Longchang area, district Mokokchung, Nagaland. *Geol. Surv. of Ind. (Field Season 1980-81), (Unpublished*).

Vernon, R.H. (2000). Granites Really Are Magmatic. Using Microstructural Evidence to Refute Some Obstinate Hypotheses. *Journal of the Virtual Explorer,* 35(1). pp.1-36.

Visher, G.S. (1969). Grain size distribution and depositional processes, *Jour. Sed. Pet*. 39(3). pp.1074-1106.

Visher, G.S. (1970). Fluvial processes as interpreted from ancient and recent fluvial deposits, *Soc. Econ. Palaeont. Mineralogy*, Sp. Pub. 12. pp.116-132.

Walderhaug, O. (1990). A fluid inclusion study of quartz-cemented sandstones from offshore mid-Norway, possible evidence for continued quartz cementation during oil emplacement. *Journal of Sedimentary Research*, *60*(2), pp.203-210.

Walker, T.R. (1974). Formation of red beds in moist tropical climate - a hypothesis. *Geol. Soc. Amer. Bull.*, v.85, pp.633-638.

Walker, R. and James, N. (1992). Facies Models. Response to Sea Level Change. *Geol. Asso. Canada*. 407p.

Walther, J. (1894). Einleitung in die Geologie als historische Wissenschaft, Bd. 3, Lithogenesis der Gegenwart. *G. Fischer, Jena*, pp.535-1055.

Walton, E.K., Stephens, W.E. and Shawa, M.S. (1980). Reading segmented grain – size curves, *Geol. Mag*. 117. pp. 517-524.

Weller, S. (1899). Kinderhook faunal studies. the fauna of the vermicular sandstone of the Northview, Webster County, Missouri, *Transactions of the Academy of Science of St. Louis*, v.9, pp.9–51.

Wenger, F. D., Buatois, L. A., Mángano, M. G., Muñoz, D. F., and Rustán, J. J. (2025). An anomalous shallow-marine ichnofacies gradient from the Lower Devonian Talacasto Formation of the Argentine Precordillera. *Palaeogeography, Palaeoclimatology, Palaeoecology*, 112747.

Wentworth, C.K. (1922). A scale of grade and class terms for sediments, *Jour. Geol*. 30. pp.377-392.

Worden, R. H. and Utley, J. E. (2022). Automated mineralogy (SEM-EDS) approach to sandstone reservoir quality and diagenesis. *Frontiers in Earth Science*, *10*, 794266.

Yan, Y., Xia, B., Lin, G., Cui, X., Hu, X., Yan, P., and Zhang, F. (2007). Geochemistry of the sedimentary rocks from the Nanxiong Basin, South China and implications for provenance, paleoenvironment and paleoclimate at the K/T boundary. *Sedimentary Geology*, *197*(1-2), pp.127-140.

Yedekar, D.B. and Ray, B. (1984). Systematic Geological mapping in Changpang Mirinokpo area, Wokha and Mokokchung districts, Nagaland. *Geol. Surv. Ind., (Field Season 1983-84), (Unpublished*).